

# POLITECNICO DI TORINO

Collegio di Ingegneria Energetica  
**Corso di Laurea magistrale  
in Ingegneria Energetica e Nucleare**

Tesi di Laurea Magistrale  
**Simulation based optimization of cogeneration and  
trigeneration systems coupled to thermal energy  
storage for prototype hospital facilities**



**Relatore**

Professor Marco Masoero  
Professor William Ryan

**Candidato**  
Carolina Pizzutto

Anno Accademico 2019/2020

# Table of Contents

<b>1 Health Care Infrastructures.....</b>	<b>1</b>
1.1 The Hospital Prototype.....	1
1.2 eQuest® Base Model.....	2
<b>2 Microturbines .....</b>	<b>6</b>
2.1 Thermodynamic cycle .....	6
2.2 Components .....	7
2.3 eQuest® microturbine model.....	8
2.3.1 Partial Load.....	9
2.3.2 Recoverable heat.....	11
2.3.3 Ambient Conditions.....	12
2.3.4 Check of the model.....	14
<b>3 Combined Heat and Power (CHP) .....</b>	<b>16</b>
3.1 Advantages .....	16
3.2 Current situation .....	17
3.3 Components and general operation of the process .....	18
3.4 eQuest® CHP Model.....	20
<b>4 Combined Cooling, Heat and Power (CCHP) .....</b>	<b>22</b>
4.1 Absorption chillers.....	23
4.1.1 eQuest® absorption chiller model.....	25
4.2 eQuest® CCHP model.....	29
<b>5 Thermal Energy Storage .....</b>	<b>32</b>
5.1 Basic thermodynamics of sensible energy storage.....	33
5.2 Technical parameters.....	35
5.3 Methodology.....	36
5.3.1 TES-CHP model.....	36
5.3.2 TES-CCHP model .....	37
<b>6 eQuest® simulations and Energy analysis .....</b>	<b>42</b>
6.1 Base hospital model.....	43
6.1.1 Electric demand .....	43
6.1.2 Heat and fuel demand .....	46
6.2 CHP system .....	49
6.2.1 Electric demand .....	49
6.2.2 Heat demand .....	52

6.2.3 Fuel demand.....	54
6.3 CHP system coupled with TES.....	56
6.4 CCHP and TES systems .....	63
<b>7 Emissions.....</b>	<b>71</b>
7.1 Average vs Marginal Carbon.....	72
7.2 AVERT system.....	75
7.3 Emissions evaluation method .....	76
7.4 Results.....	78
<b>8 Conclusions .....</b>	<b>88</b>
<b>Appendix A .....</b>	<b>90</b>
<b>Cited Literature.....</b>	<b>91</b>

## List of Figures

Figure 1: Hospital prototype 3D model.....	2
Figure 2: Hospital prototype layout.....	3
Figure 3: Plant layout, water side .....	4
Figure 4: HVAC system layout, air side.....	5
Figure 5: Microturbine components and Brayton cycle .....	6
Figure 6: Scheme of microturbine components.....	8
Figure 7: Capstone parameters per 200 kW module .....	9
Figure 8: Capstone C1000 ISO partial load efficiency vs output power.....	10
Figure 9: HIR vs PLR - normalized curve.....	11
Figure 10: Recoverable heat vs. PLR – normalized curve .....	12
Figure 11: Capstone C200 Elevation vs. Ambient Temperature.....	13
Figure 12: Efficiency vs. Ambient temperature .....	13
Figure 13: Net power vs. Ambient temperature – normalized curve .....	14
Figure 14: Capstone fuel consumption vs output power .....	15
Figure 15: Comparison between the eQuest® fuel consumption and the one calculated .....	15
Figure 16: Consumption and losses of a CHP system versus SHP .....	17
Figure 17: CHP served hospitals in U.S. ....	18
Figure 18: CHP Topping cycle .....	19
Figure 19: Operation of a trigeneration system .....	22
Figure 20: Schematic representation of an absorption cycle .....	24
Figure 21: Chiller capacity percentage vs Chilled water temperature.....	26
Figure 22: Percentage COP and COP vs Chilled water temperature.....	27
Figure 23: Percentage COP and COP vs Condenser temperature .....	28
Figure 24: Percentage Capacity vs Condenser temperature .....	28
Figure 25: COP vs Partial Load Ratio .....	29
Figure 26: CCHP plant layout .....	30
Figure 27: Annual fuel consumption, Base model vs CHP and CCHP.....	31
Figure 28: Complete storage cycle .....	33
Figure 29: Climate regions in US .....	43
Figure 30: Base model annual electric demand, Chicago.....	44
Figure 31: Base model annual electric demand, Atlanta .....	44
Figure 32: Base model annual electric demand, Duluth.....	45
Figure 33: Base model annual electric demand, Miami .....	45
Figure 34: Base model electric duration curve .....	46
Figure 35: Base model annual heat and fuel demand, Chicago.....	47
Figure 36: Base model annual heat and fuel demand, Atlanta .....	48
Figure 37: Base model annual heat and fuel demand, Duluth.....	48
Figure 38: Base model annual heat and fuel demand, Miami .....	48
Figure 39: Base model thermal duration curve.....	49
Figure 40: Base model fuel duration curve.....	49
Figure 41: Hospital electric demand vs Electricity produced by the turbine .....	50
Figure 42: Hospital electric duration curve vs Electricity produced by the turbine.....	51
Figure 43: Hospital heat demand and comparison between recoverable, recovered and wasted heat, Chicago .....	53

Figure 44: Hospital heat demand and comparison between recoverable, recovered and wasted heat, Atlanta.....	53
Figure 45: Hospital heat demand and comparison between recoverable, recovered and wasted heat, Duluth .....	53
Figure 46: Hospital heat demand and comparison between recoverable, recovered and wasted heat, Miami.....	54
Figure 47: Base model fuel consumption vs CHP fuel consumption.....	55
Figure 48: Annual fuel consumption, Base model vs CHP.....	56
Figure 49: Storage operation, 20,000 [gal], Chicago.....	57
Figure 50: Storage operation, 20,000 [gal], Atlanta .....	58
Figure 51: Storage operation, 20,000 [gal], Duluth.....	58
Figure 52: Storage operation, 20,000 [gal], Miami .....	58
Figure 53: Boiler demand, 60,000 [gal], Chicago .....	59
Figure 54: Recovered heat, 60,000 [gal], Chicago .....	59
Figure 55: Boiler demand, 60,000 [gal], Atlanta.....	60
Figure 56: Recovered heat, 60,000 [gal], Atlanta.....	60
Figure 57: Boiler demand, 60,000 [gal], Duluth .....	60
Figure 58: Recovered heat, 60,000 [gal], Duluth .....	61
Figure 59: Boiler demand, 60,000 [gal], Miami.....	61
Figure 60: Recovered heat, 60,000 [gal], Miami.....	61
Figure 61: Comparison between Recovered Heat ratio for different TES volume .....	62
Figure 62: Recovered heat ratio for different chiller cooling capacity, Chicago .....	64
Figure 63: Recovered heat ratio for different TES volume, Chicago.....	64
Figure 64: Recovered heat ratio for different chiller cooling capacity, Atlanta.....	64
Figure 65: Recovered heat ratio for different TES volume, Atlanta .....	65
Figure 66: Recovered heat ratio for different chiller cooling capacity, Duluth.....	65
Figure 67: Recovered heat ratio for different TES volume, Duluth.....	65
Figure 68: Recovered heat ratio for different chiller cooling capacity, Miami.....	66
Figure 69: Recovered heat ratio for different TES volume, Miami .....	66
Figure 70: Comparison between recovered heat ratio without TES.....	67
Figure 71: Storage operation and cooling demand covered by the absorption chiller, Chicago .....	68
Figure 72: Storage operation and cooling demand covered by the absorption chiller, Atlanta.....	68
Figure 73: Storage operation and cooling demand covered by the absorption chiller, Duluth .....	69
Figure 74: Storage operation and cooling demand covered by the absorption chiller, Miami.....	69
Figure 75: CO2 emissions for SHP vs CHP .....	71
Figure 76: Bid Stack and marginal plants.....	72
Figure 77: Mid-Atlantic grid generation and emissions.....	73
Figure 78: Southeast grid generation and emissions .....	74
Figure 79: Midwest grid generation and emissions.....	74
Figure 80: Florida grid generation and emissions .....	74
Figure 81: Bid Stack in term of carbon .....	75
Figure 82: AVERT electricity market regions .....	76
Figure 83: Marginal carbon due to electric production, Chicago.....	79
Figure 84: Average carbon due to electric production, Chicago.....	79
Figure 85: Total marginal emissions, Chicago.....	79
Figure 86: Total average emissions, Chicago.....	79
Figure 87: Marginal carbon due to electric production, Atlanta .....	80
Figure 88: Average carbon due to electric production, Atlanta.....	80

Figure 89: Total marginal emissions, Atlanta.....	80
Figure 90: Total average emissions, Atlanta .....	80
Figure 91: Marginal carbon due to electric production, Duluth .....	81
Figure 92: Average carbon due to electric production, Duluth .....	81
Figure 93: Total marginal emissions, Duluth .....	81
Figure 94: Total average emissions, Duluth .....	81
Figure 95: Marginal carbon due to electric production, Miami.....	82
Figure 96: Average carbon due to electric production, Miami.....	82
Figure 97: Total marginal emissions, Miami.....	82
Figure 98: Total average emissions, Miami .....	82
Figure 99: Total emissions comparison, Chicago.....	83
Figure 100: Total emissions comparison, Atlanta .....	84
Figure 101: Total emissions comparison, Duluth.....	84
Figure 102: Total emissions comparison, Miami .....	85
Figure 103: Map of generation and emission changes, Mid-Atlantic region (Chicago) .....	86
Figure 104: Map of generation and emission changes, Southeast region (Atlanta) .....	86
Figure 105: Map of generation and emission changes, Midwest region (Duluth) .....	86
Figure 106: Map of generation and emission changes, Florida (Miami) .....	87

## List of Tables

Table 1: Typical materials used in sensible heat TES .....	34
Table 2: Different volumes and capacity of TES .....	35
Table 3: Electric demands .....	46
Table 4: Turbine electric production vs Electric demand.....	51
Table 5: Amount of recovered heat in comparison with recoverable heat and facility demand .....	52
Table 6: Reduction in boilers fuel consumption in CHP systems .....	55
Table 7: Comparison between the CHP system and the coupling between CHP and a 20,000 [gal] TES .....	62
Table 8: Maximum hospital cooling demand .....	63
Table 9: Best TES and Absorption Chiller sizes .....	67
Table 10: Comparison between the CCHP system and the coupling between CCHP and TES, Chicago .....	68
Table 11: Comparison between the CCHP system and the coupling between CCHP and TES, Atlanta .....	69
Table 12: Comparison between the CCHP system and the coupling between CCHP and TES, Duluth .....	69
Table 13: Comparison between the CCHP system and the coupling between CCHP and TES, Miami	70
Table 14: Average emission factor for analyzed regions .....	77
Table 15: Reduction in emissions, Chicago .....	83
Table 16: Reduction in emissions, Atlanta .....	84
Table 17: Reduction in emissions, Duluth.....	84
Table 18: Reduction in emissions, Miami .....	85
Table 19: Recovered heat vs Recoverable heat .....	88

## Summary

During the past decades, combined heat and power (CHP) and combined cooling, heating and power (CCHP) plants have become increasingly interesting in the market as they provide electricity, useful heat and cooling, in the latter case, to the user, offering higher thermal efficiencies, lower operational costs and reduced carbon dioxide emissions compared to separate heat and power production. Ideally suitable for these systems are health care facilities, which needs to be characterized by a high reliability and require a constant electric and thermal production over the whole year.

The main goal of this thesis is to simulate and study different plant layouts for the fulfillment of the energy needs of a hospital facility. The analysis performed is based on a prototype located in four different climates zones of U.S.: Chicago IL in zone 5A, Atlanta GA in zone 3A, Miami FL in zone 1A and Duluth MN in zone 7A. At first, both a cogeneration and trigeneration plant, driven by a 1000 [kW] gas microturbine, are modeled using eQuest<sup>®</sup>, a free open source software provided and developed by the US Department of Energy (DOE). The thermal needs are satisfied by the recovery of the heat coming from the prime mover and, in the second case, the cooling loads are partially fulfilled by an absorption chiller driven by the microturbine exhaust; in this way the heat recovered and stored in the warmer months is better exploited and, at the same time, the electric need required for the electric chillers is reduced. Using the software, it has been possible to analyze and compare the electric and heat profiles of the building and the fuel consumption for the different scenarios. To provide a further improvement in the systems, a High Temperature Thermal Energy Storage has been introduced in both types of plants' layout. The model developed is a fully mixed water tank where no stratification effect takes place. Various volumes are studied, ranging from 0 [gal] to 60,000 [gal], in order to study the impact of a TES on a large health care facility.

The results obtained show how, due to inner constrains of eQuest<sup>®</sup>, the CCHP system and the Thermal Storage were not working properly so, in order to simulate a correct operation, an Excel model has been implemented, starting from the CHP data provided by the software, which were reliable. The model was developed in such a way that it is possible to change the TES volume and the absorption chiller capacity. By setting the chiller capacity to 0, the trigeneration plant will work as a cogeneration plant. With a single model it was possible to summarize all the different configurations analyzed and to compare the different solutions, evaluating the best equipment sizes to optimize the systems operation.

Finally, the work focus on the evaluation of carbon dioxide emissions and especially on the reduction due to applying CHP, CCHP and TES systems on the hospital facilities. In particular, is explained how electricity markets work “on the margin” and is provided a comparison between two different emissions evaluation methodologies suggested by U.S. Environmental Protection Agency (EPA). It is proposed how, for determining the impact of a new generation unit, is fundamental using marginal carbon emissions, which have been studied with the AVERT system Excel Main Module, instead of average carbon emission factors. In fact, with average factors it is assumed that each decrease in the grid is evenly distributed over all the facilities and that the emissions are constant over time, which does not reflect the real operation of electricity markets.

# 1 Health Care Infrastructures

Health care facilities make use of different thermal products and they're characterized by a significant energy consumption, about 2.5 times larger than an average commercial building, since they function 365 days a year, 24 hours a day [1]. Moreover, hospitals are classified as Critical Infrastructures (CI) [2], those networks that, if incapacitated, would cause a tremendous impact on national security, economy or public health and safety: in order to prevent the occurrence of tragic scenarios, hospitals must perform their functions even when the supply from the utility grid is interrupted and their demand have to be satisfied promptly at any time.

The continuous, simultaneous and great need for electricity, heat and cold, make hospitals ideally suitable for cogeneration and trigeneration systems; in this way, thanks to on-site production, they will be able to operate during emergencies without being affected by the grid uncoupling and to restore power without relying on external energy sources.

Not only the energy reliability will increase, but also the costs will be reduced, through the operation of a system characterized by a higher efficiency and also lower emissions compared to a traditional energy production system. In addition, the investment payback time is always shorter compared to other types of facilities, due to the continuous energy demand [3].

## 1.1 The Hospital Prototype

The analysis of the Health Care facilities sector has been conducted by studying a prototype, representative of the average US hospital. The model was developed by the National Renewable Energy Laboratory (NREL) [4] and implemented on eQuest<sup>®</sup>, a simulation software developed by the US Department of Energy (DOE). The guidelines for the definition of the prototype were provided by the DOE support to the development of energy codes and standards for commercial buildings. The aim of the US Department of Energy Building Technologies Program was to document the analysis performed and the resulting design guidance that will enable the building to achieve energy savings up to 50% over the ASHRAE Standard 90.1-2004 [5] (Energy Standard for Buildings Except Low-Rise Residential Buildings), a US standard providing the minimum accepted requirements for the design of energy efficient buildings. The first release of ASHRAE Standard 90 was in 1975 and after that different upgrades and review have been developed in 2004, 2007, 2010, 2013 and 2016, as a consequence of legislative changes due to always newer and more efficient technologies.

The information for the correct simulation of the prototype facility include:

- Building internal layout description
- Building shell description
- Internal loads
- Occupation and equipment schedules
- Lighting schedules
- Heating, ventilating and air conditioning information
- Service water heating

Starting from the hospital prototype developed, which throughout the study will be referred as base model, different improvements to the facility have been implemented and compared.

## 1.2 eQuest<sup>®</sup> Base Model

The base model is characterized by a total surface of 527,000 [ft<sup>2</sup>], split in two main buildings: the hospital area of 427,000 [ft<sup>2</sup>], which is divided into seven stories, and the five stories medical office building (MOB) of 10,000 [ft<sup>2</sup>].

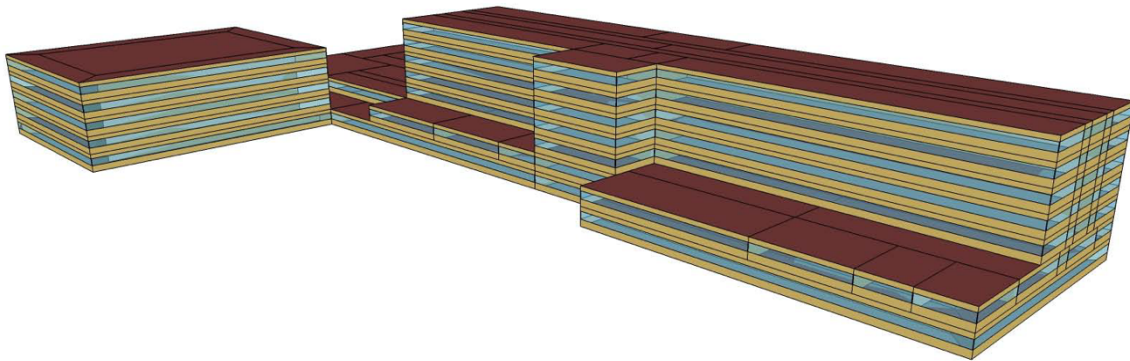


Figure 1: Hospital prototype 3D model

The structure is made of a steel frame construction and an arrangement of the roof with insulation above the deck. The fenestration area is not directly defined but it has been estimated by knowing the floor-to-floor height, 10 [ft], and the heights from the floor to the bottom of the window and from the top of the window to the ceiling, respectively 3.6 [ft] and 2.4 [ft];

moreover the windows follow the whole perimeter of the building without any interruption. The ratio between glazed and opaque surface is therefore 40%.

In order to simulate the building performance on the software the building has been divided in different spaces, defined as one or more rooms characterized by the same required thermal condition. The hospital has been divided in nine main spaces:

- Medical Office Building - MOB, five stories
- Patient Tower - PT, five stories (from third to seventh floor)
- Building 3 and Building 4, both two stories
- Building 5, one story
- Building 6, two stories
- Building 7, three stories
- Building 8, one story
- Building 9, two stories

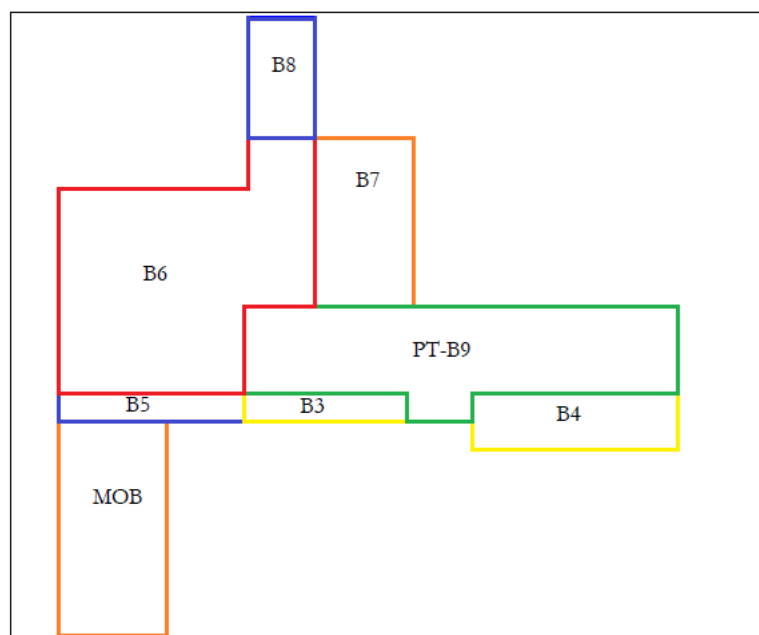


Figure 2: Hospital prototype layout

All the spaces defined are considered to operate with the same schedule:

- Hospital Space 24/7
- MOB from 7:00 am to 5:00 pm
- Extended hours from 5:00 am to midnight

The prototype has been developed to achieve the target of 50% reduction in energy consumption, independently on the climatic zone: some of these Energy Design Measures (EDM) consisted in reducing the power density of the lighting system and introducing daylighting control and occupancy sensors in suitable spaces. In addition, the insulation layer is increased, the envelope is tighter in order to reduce infiltrations and free gains are handled by putting overhangs on the windows facing south.

The heating, ventilation and air conditioning system (HVAC) consists of central air handling units (AHU), boiler, chillers, chilled and hot water air handling unit coils and terminal units with hot water reheat coils. Each space is managed by the same HVAC system. The base model is not provided with any type of power generator, thus the electric demand is satisfied from the grid. The heating demand is fulfilled by three fired boilers, connected to the *Space Heating Hot Water loop*, and the *Domestic Hot Water loop* is connected to a water heater, also driven by natural gas; the cooling needs are satisfied by three electric chillers, connected to the *Chilled Water loop*. Hence, the need of a *Condenser Water loop*, to properly operate the chillers. This configuration will be implemented by installing new equipment to enable the heat recovery for hot water and chilled water production.

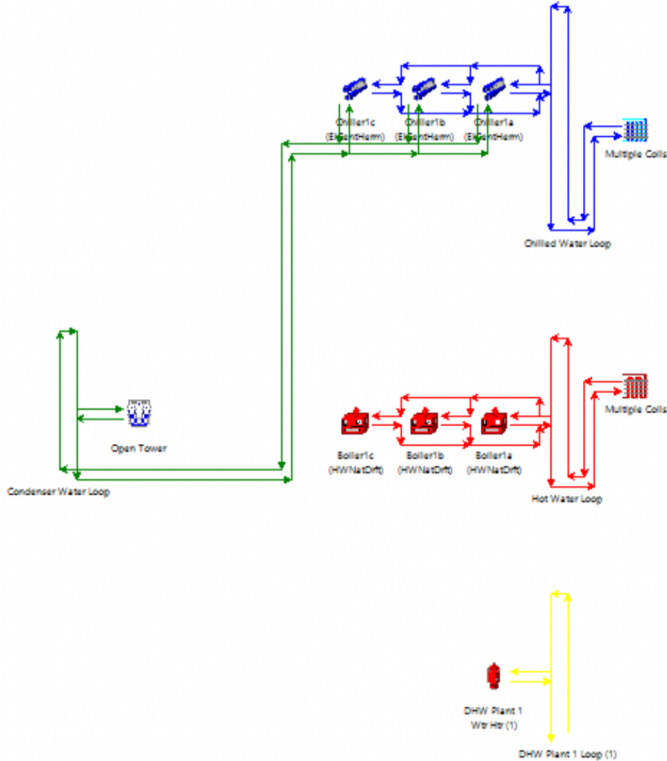


Figure 3: Plant layout, water side

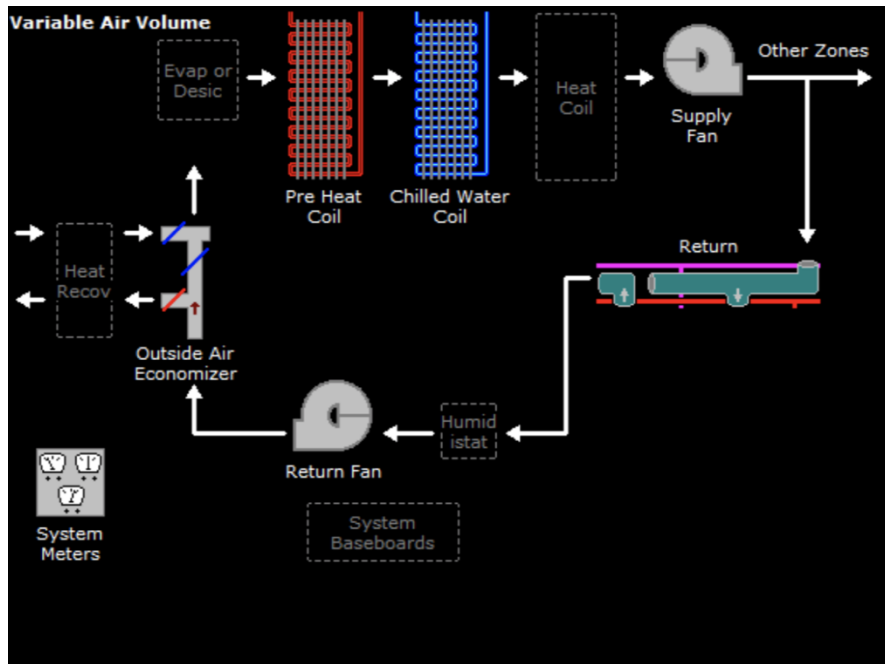


Figure 4: HVAC system layout, air side

The model implemented on eQuest<sup>®</sup> has been tested in previous works and further improved by fixing some irregularities found through the analysis of the output records [6] [7]. In fact, in some spaces, the data measured by the thermostats, revealed that the temperature was below the set-point for a considerable number of hours throughout the year. This issue was linked to the interaction of the thermal load with some default parameters in the HVAC system. As a result, to achieve in each space a temperature equal to the design one, three main improvements were introduced:

- The introduction of pre-heat coils in each of the variable air volume (VAV) HVAC systems, extremely important especially in winter months when the air temperature may drop below the water freezing point, avoiding in this way the risk of damaging the coils themselves.
- The increase of the eQuest<sup>®</sup> parameter *Reheat Delta T*, the maximum temperature increase that the supply air undergoes while crossing the reheat coils; it was increased from 30 [°F], in the default layout, to 50 [°F] to ensure that air is supplied at the correct temperature.
- The increment of the *Sizing Ratio*, a multiplier for the coil size and air flow rate values calculated by the software. The parameter, used to undersize or oversize the equipment, was modified from 1 to 1.15, where an under heating was showed.

## 2 Microturbines

Microturbines are small combustion turbines that burn gaseous or liquid fuels to drive an electrical generator. Their size ranges from 30 to 330 [kW]; integrated packages consisting of multiple generators up to 1,000 [kW] are also available if larger power outputs are required [9]. Many are the advantages over the modern internal combustion engine, not only the compact size, but also the high-power density, the small number of moving parts and the extremely low emissions. Since the exhaust temperatures vary between 500 and 600 [°F], microturbines are well suited to be used both in CHP and in CCHP applications, with an absorption cooling equipment driven either by low pressure steam or by the exhaust heat directly [9].

There were a large number of competing systems under development throughout the 1990s, but today in the U.S. remain two main manufacturers of stationary microturbines, Capstone Turbine Corporation and FlexEnergy [9].

### 2.1 Thermodynamic cycle

Microturbines operate on the same thermodynamic cycle as larger gas turbines, the Brayton Cycle. As shown in Figure 5, it consists of four processes:

- a-b Adiabatic, quasi-static compression of atmospheric air in the inlet and compressor
- b-c Fuel combustion at constant pressure
- c-d Adiabatic, quasi-static expansion of the hot gases in the turbine and exhaust nozzle, which drives both the inlet compressor and a generator.
- d-a Cool of the air at constant pressure back to its initial condition

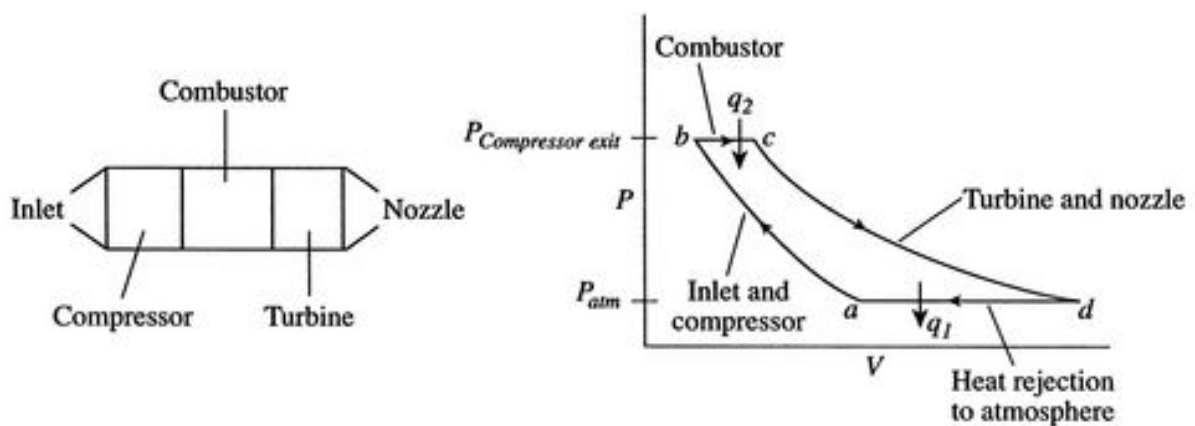


Figure 5: Microturbine components and Brayton cycle

Based on the thermodynamic cycle described, the efficiency of a turbine can be defined as:

$$\eta = 1 - (r_p)^{\frac{1-k}{k}} \quad (1)$$

Where  $r_p$  is the compression ratio between the pressure at the exit of the compressor ( $P_b=P_c$ ) and the pressure of the air at the inlet, usually equal to the atmospheric pressure ( $P_a=P_d$ ). Compared to larger gas turbines, microturbines are characterized by lower pressure ratios and lower combustion temperatures, as a consequence also the efficiencies are lower. To increase the energy of the gases entering the expansion turbine and therefore the efficiency, a portion of the exhaust heat can be recovered in a recuperator, even though such system elevates the construction costs. The efficiency ranges from 15% to 20% for a simple cycle and 20% to 30% for the regenerative turbines [10].

## 2.2 Components

To better understand the basic operation of a microturbine a brief description of the main components is provided.

- **Turbine and Compressor.** The core of the system is mounted on a single shaft along with the electric generator. Unlike larger turbines, based on multi-stage axial flow turbocompressors, microturbines use single-stage radial flow systems [9].
- **Generator.** The electrical power is produced by the high-speed generator which turn on the turbocompressor shaft. This high frequency AC output, around 1,600 [Hz] for a 30 [kW] machine, is converted to a constant 60 [Hz] power output in a power conditioning unit with an efficiency penalty of approximately 5% [9]. During the start-up, the generator acts as a motor by turning the single shaft until sufficient rpm is reached to start the combustor. In case of black starting, when the system is independent of the grid, a power storage unit is necessary to power the generator.
- **Recuperator and combustor.** In the combustor the fuel is combined with high pressure air and burned. The resulting high temperature exhaust gases are used to turn the power turbine. The recuperator is a heat exchanger fed by the exhaust gas, usually around 1,200

[°F], which preheat the compressed air going into the combustor. In this way is reduced the amount of fuel needed for the air to reach the turbine inlet temperature and the system efficiency can increase more than double. However, this means also an increase in the pressure drop both on the compressed air and the turbine exhaust side of the recuperator, causing a decrease of 10-15% in power output [9].

- **CHP Heat Exchanger.** This additional component is integrated in CHP systems in order to extract part of the remaining energy in the turbine exhaust exiting the recuperator at 500-600 [°F]. Since microturbine exhausts are clean and high in oxygen, this heat can be directly used for process applications as driving a double effect absorption chiller, providing preheat combustion air for boiler or process heat applications [9].

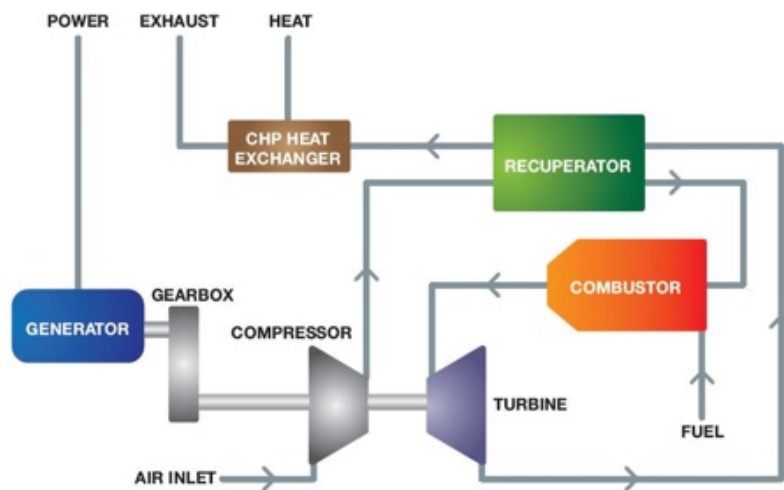


Figure 6: Scheme of microturbine components

### 2.3 eQuest<sup>®</sup> microturbine model

In order to run the energy simulation properly, a microturbine model has been implemented on eQuest<sup>®</sup>. All the information required are provided by Capstone and the model is based on the Capstone C1000 Microturbine, a modular system composed of five 200 [kW] power modules [11]. Combustion turbines are typically rated at International Organization for Standardization (ISO) conditions, which are 59 [°F] at sea level and 1 [atm] [11].

The data necessary for the model can be found in the Capstone Technical references; the parameters are provided both as a function of the power generated and as a function of the ambient temperature.

Net Power per 200 kW module (kW / N)	Net Efficiency (%)	Exhaust Temp (°F)	Exhaust Mass Flow Rate per module (lbm/s / N)	Exhaust Energy Rate per module (kW / N LHV)	Fuel Flow Energy Rate per module (Btu/hr / N LHV)	Net Heat Rate (Btu/kWh LHV)
--------------------------------------	--------------------	-------------------	---	---	---	-----------------------------

Figure 7: Capstone parameters per 200 kW module

The information required to implement the microturbine module on eQuest® are:

- Microturbine capacity [kW]
- Partial load ratio (PLR) vs Heat input ratio (HIR) curve
- Ambient temperature vs Electric power curve
- PLR vs Exhaust heat recovery curve

All the functions required by the software have to be normalized, meaning that each parameter should be divided by the same parameter at full load.

**2.3.1 Partial Load**

In applications that require electric load following, microturbines may operate during some periods at part load. The output power can be satisfied either by running on each module at the same power or by turning on a number of microturbines at full power and the remaining modules at partial load or off, optimizing the efficiency. When the Maximum efficiency mode is applied, the overall electrical efficiency will be a weighted average of the efficiencies and power outputs of the running modules [11].

In Figure 8 is shown the behavior of the C1000 system operating in the two different possible way. With the maximum efficiency mode, the peak is already reached at a power output of 200 kW, just 1/5 of the package maximum output. Each time a new module starts to work, the efficiency has a drop since at first the new microturbine is working at low load and, as a consequence, its efficiency will be very poor, affecting the overall performance. More are the modules running, more stable will be the efficiency curve, reaching 32-33%.

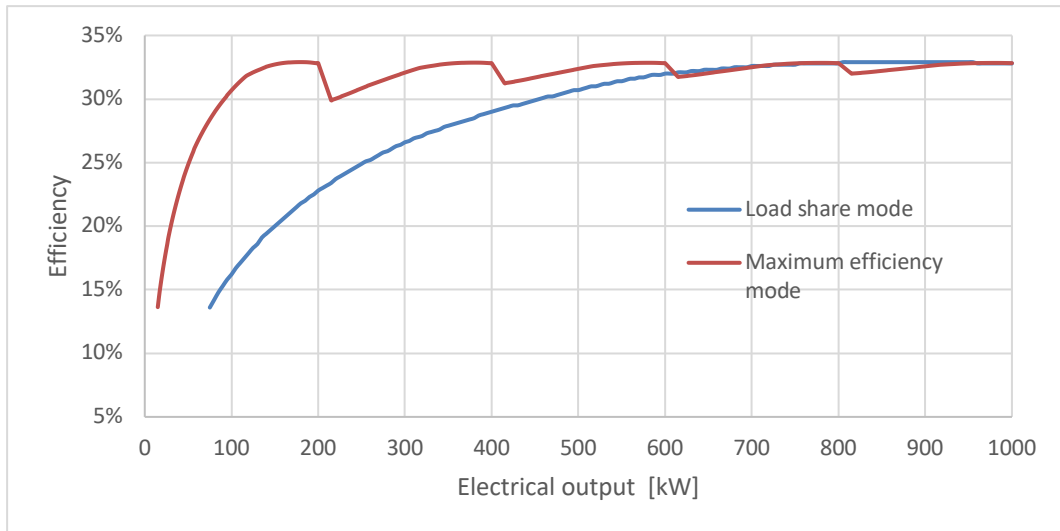


Figure 8: Capstone C1000 ISO partial load efficiency vs output power

It is necessary to have a simulation model able to predict the efficiency, the quality of exhaust gas and the consumption of the turbine for different outputs. In order to control the output power, the quantity of fuel burnt inside the combustor is varied; in this way less heat is developed and the power generation is lowered.

The Partial load ratio vs Heat input ratio curve gives information about the behavior of the modules during partial load and about the fuel/heat demand for any output.

PLR is the ratio between the power generated at any instant and the full load power of the microturbine.

$$PLR = \frac{\text{Actual output power}}{\text{Full load power}} = \% \text{Full load} \quad (2)$$

HIR is the ratio between the heat currently supplied by the fuel and the heat supplied in full load conditions.

$$HIR = \frac{\text{Heat currently supplied}}{\text{Heat supplied in full load condition}} \quad (3)$$

eQuest® requires a quadratic curve where the heat input ratio is a function of the partial load ratio:

$$HIR = a + bx + cx^2 \quad (4)$$

where  $x=PLR$

The three coefficients were obtained through an interpolation between the experimental points, represented in the following Excel graph.

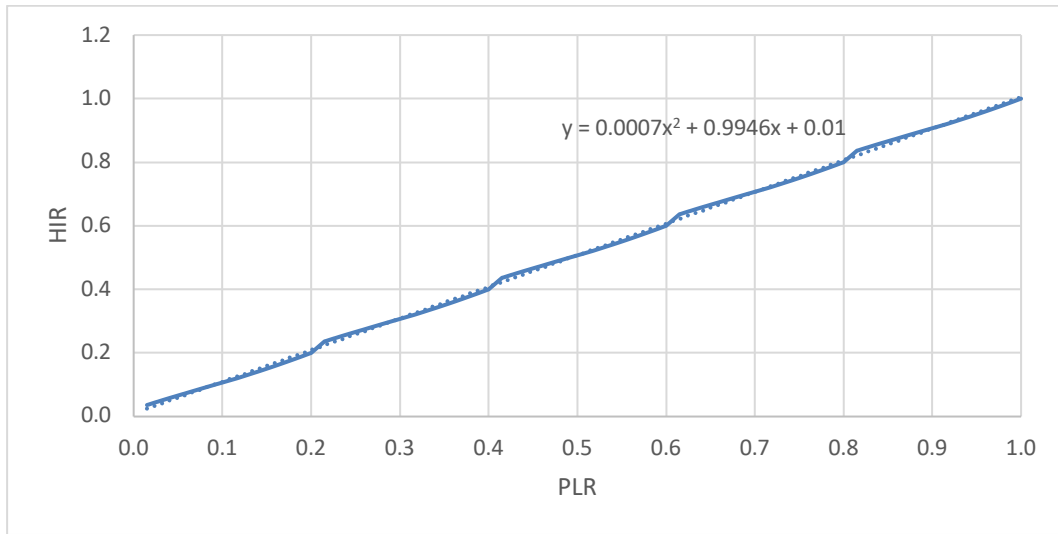


Figure 9: HIR vs PLR - normalized curve

### 2.3.2 Recoverable heat

eQuest<sup>®</sup> also requires a correlation between the partial load ratio at which the turbine is operating and the recoverable heat from the exhaust gases.

Starting from the parameter provided by Capstone, listed in Figure 7, and knowing the effectiveness of the heat exchanger in the model and the incoming water temperature in the loop, it was possible to compute the maximum recoverable heat coming from the exhaust for each operating point:

$$\text{Maximum recoverable heat} = \eta \cdot \dot{m} \cdot c_p \cdot (T_{\text{exh}} - T_w) \quad (5)$$

Where:

- $\eta$  is the effectiveness of the heat exchanger, equal to 0.8
- $\dot{m}$  is the mass flow rate of the exhaust gases, in [lbm/s]
- $C_p$  is the exhaust gas specific heat, equal to 1.1 [kJ/kgK]
- $T_{\text{exh}}$  is the exhaust gases temperature
- $T_w$  is the water temperature, set to 180 [°F]

The maximum recoverable heat was then normalized, plotted in the following graph and the coefficients, obtained through a quadratic approximation, implemented in eQuest®.

The software already provides a curve for the turbine model but, since we are dealing with a much smaller microturbine, the quantity of heat would have been too high for the system examined.

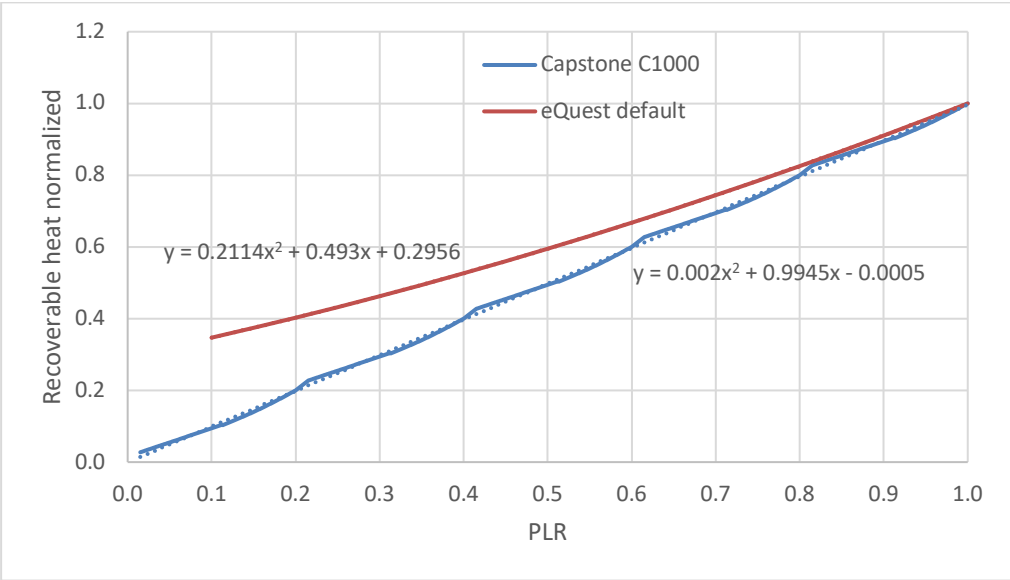


Figure 10: Recoverable heat vs. PLR – normalized curve

### 2.3.3 Ambient Conditions

The ambient condition under which a microturbine operates have a noticeable effect on both the power output and efficiency. With high inlet air temperatures and, as a consequence, lower air density, the power decreases due to the reduced mass flow rate and also the efficiency decreases, since the compressor requires more power to compress less dense air. Given a fixed compression ratio the power required by the compressor increases with higher inlet temperature. Another condition affecting the air density is the altitude: the density decreases at altitudes above sea level and consequently the power output decreases, as illustrated in the following Figure [11].

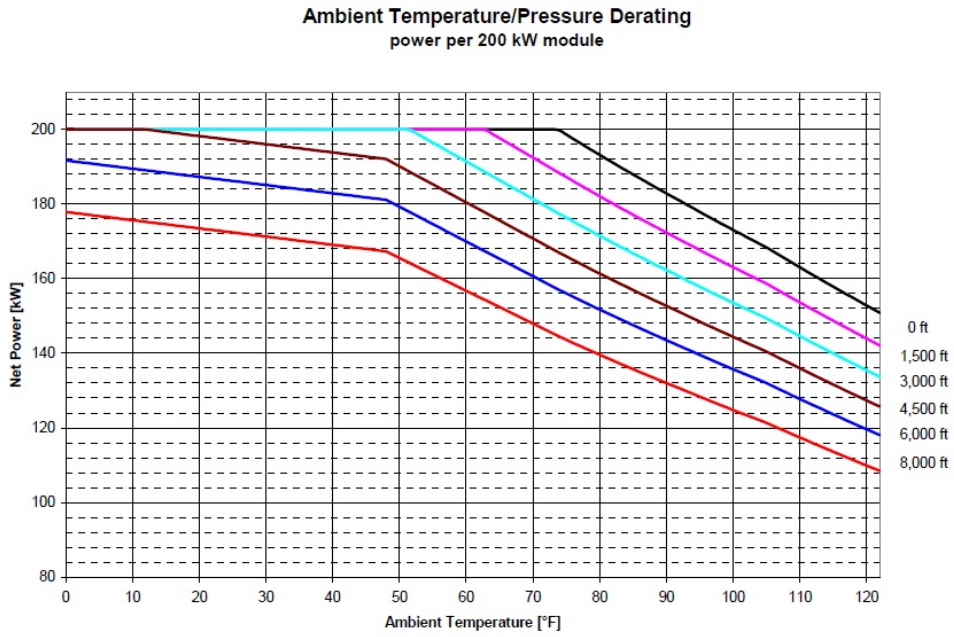


Figure 11: Capstone C200 Elevation vs. Ambient Temperature

As already mentioned, microturbines are designed in order to produce the maximum power at ISO conditions (59 °F). Starting from this point, a reduction of temperature will cause an increase in the efficiency, while the output power keeps constant. Since it's interesting to look at this behavior, also the efficiency curve is provided, even if it's not directly required by the software.

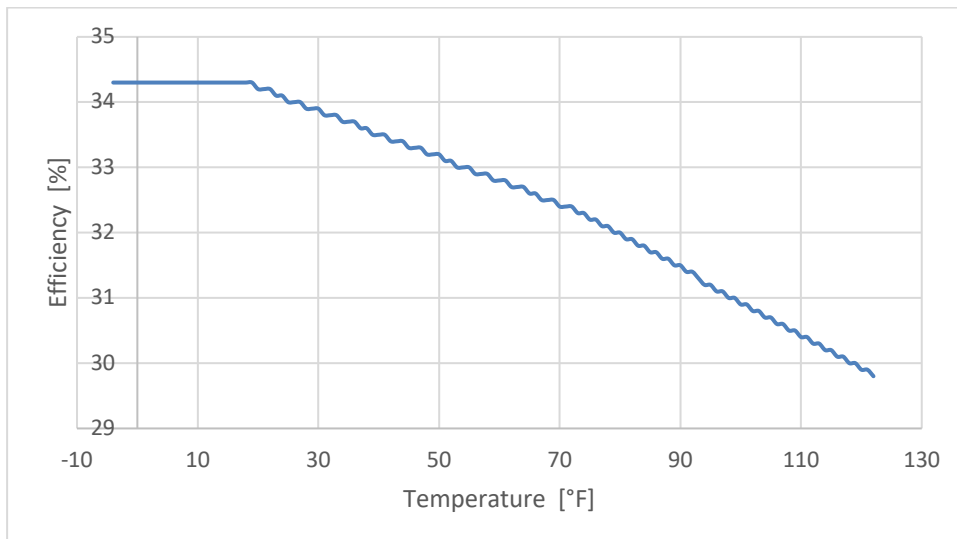


Figure 12: Efficiency vs. Ambient temperature

Regarding the electric power curve, by looking at its trend, a quadratic approximation would not be correct. The power, in fact, remain constant until the external temperature reaches 74 [°F]. Fortunately, eQuest® allows to set a limit below which the variable is constant and equal to a value specified and, since the curve required have to be normalized, this value is equal to 1. In the range of 73-122 [°F], instead, a linear curve describes the net power behavior.

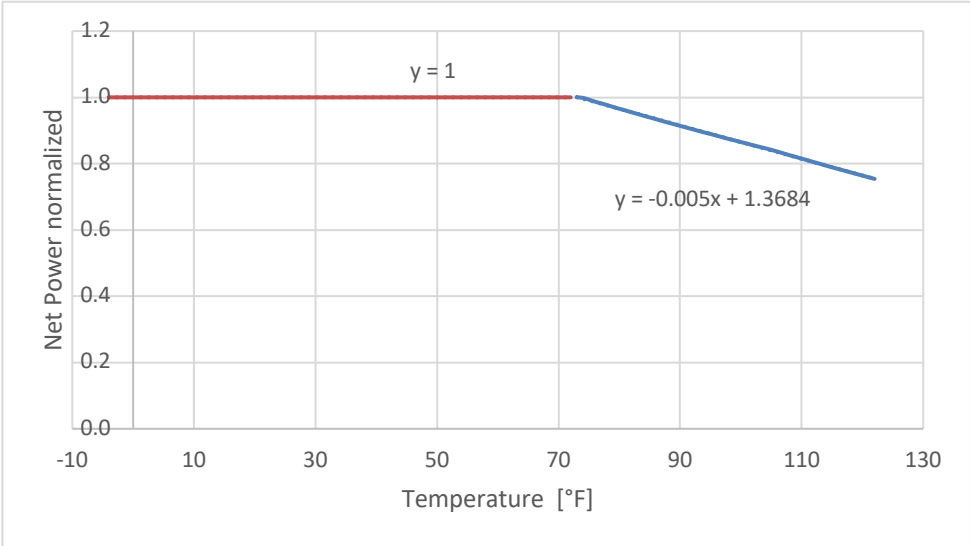


Figure 13: Net power vs. Ambient temperature – normalized curve

**2.3.4 Check of the model**

Once the microturbine Capstone model was set in the software, it’s important to verify if it’s working in a proper way. One method to check whether the turbine model is correct, which was already applied in previous works [12] [13], is to look at the fuel consumption. In the Capstone’s specification table [11] is provided the fuel consumption in [Btu/h] for each power output, so it was possible to obtain a quadratic correlation between the two parameters, plotted in Figure 14.

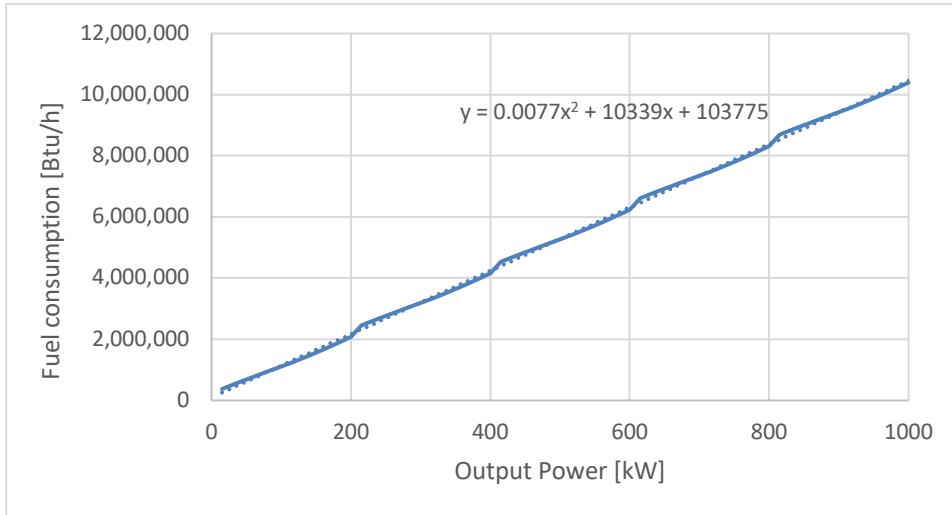


Figure 14: Capstone fuel consumption vs output power

For each simulation, eQuest<sup>®</sup> provides the hourly information about the power produced and the fuel consumed by the microturbine. Using the equation previously obtained, it was possible to calculate for each hour of the year the theoretic fuel consumption based on the power produced. Lastly, the fuel consumption provided by the software and the one computed thanks to Capstone data were compared. In Figure 15 is provided the model check regarding Chicago, but the same result was obtained in all the other locations. It can be noticed from the graph how the two curves overlap almost totally, with a correlation of 99.97%, confirming that the model developed is correct.

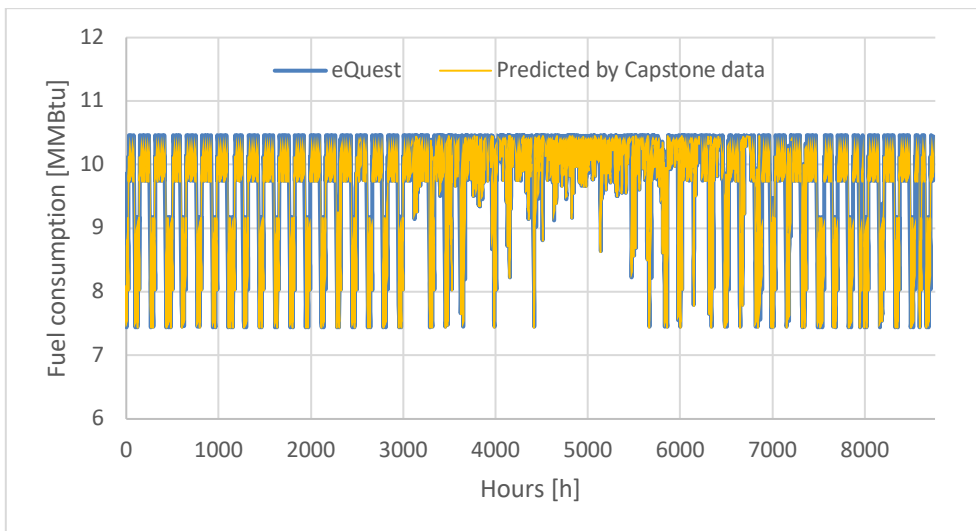


Figure 15: Comparison between the eQuest<sup>®</sup> fuel consumption and the one calculated

### **3 Combined Heat and Power (CHP)**

Because of the need to reduce costs and emission of pollutants in the atmosphere, in the energy field there is a constant search for more efficient solutions; one definitely is Combined Heat and Power production. CHP consists in the simultaneous production of electric power and useful thermal energy in an integrated system, starting from a single fuel source; in addition, the production takes place at or near the end-user's site, in this way the energy and heating demand of the facility can be directly satisfied. In cogeneration systems the heat that otherwise would be wasted during the electric production, is recovered; in this way it can be delivered in form of steam or hot water for space heating or domestic hot water use [14]. Any unused electricity can be sold back to the national electricity grid and heat can be sold to neighboring buildings, or, when existing, saved into a thermal hot storage that will be discussed in the following chapters.

#### **3.1 Advantages**

Thanks to heat recover and on-site production, which reduces losses due to transmission over long distances and distribution, CHP plants are much more efficient with respect to traditional separate heat and power production (SHP), where almost two third of the energy used is wasted in form of heat rejected. Cogeneration systems efficiency varies between 65-85% [15] while, when electricity and thermal energy are provided separately, in traditional fossil fuel-powered plants the efficiency ranges from 30% to 45% [9], getting an overall efficiency around 50%. As a result, CHP systems require up to 40% less fuel while producing the same amount of energy, as shown in Figure 16 [16]. By exploiting the same type of primary energy in a more efficient way, the pollutant emissions, such as greenhouse gases (GHG), carbon oxides, nitrogen oxides and sulfur dioxide, can be reduced by 30% [14], for the same output power.

The on-site production allows the facility to keep running even during catastrophic events or grid outages: this allow cogeneration systems to be more reliable than traditional plants. During recent extreme storm events, such as Hurricane Sandy [17], it has been noticed how several facilities with CHP systems were able to maintain both power and heat, as opposed to traditional emergency backup generators that weren't able to operate as expected over the full duration of the outage.

All these combined factors make these power production plants advantageous investments, which will be less exposed to the electricity rate increase. Since the energy related costs are reduced, providing direct savings, the economic competitiveness of the business is increased.

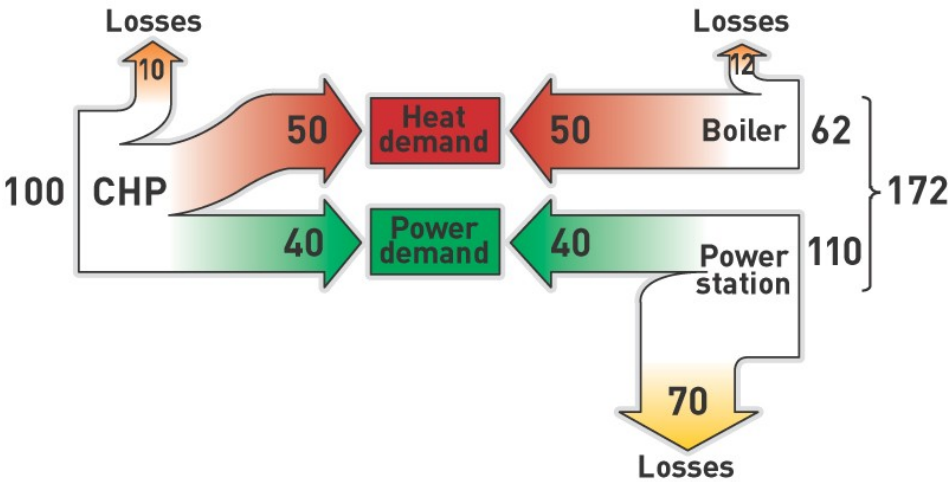


Figure 16: Consumption and losses of a CHP system versus SHP

### 3.2 Current situation

Despite the several advantages, CHP remains an under-utilized resource today: back in 2006 it represents approximately 8% of U.S. generating capacity, compared to over 30% in countries such as Denmark, Finland and the Netherlands [17]. Its deployment has been limited by some barriers, such as market uncertainties and local permitting and siting issues.

Cogeneration plants require a significant capital investment and, despite the equipment has a long life, around 20 years, the uncertainties of an unstable and rapidly changing economic environment, such as fuel and electricity prices, market sector growth and regulation, environmental policies, have affected their development. As regards the siting concern, a CHP installation must take into account a series of environmental, health and safety requirements at the site. These includes rules on air and water quality, fuel storage, fire prevention, hazardous waste disposal, worker safety and building construction standards [17].

Fortunately, in the last years have been recognized the potential benefits that this technology could play in producing clean, reliable and convenient energy. That’s why the U.S. DOE established seven regional Technical Assistance Partnerships (TAPs) and a number of federal

policies and financial incentives were introduced to help promote the CHP market; currently there is a 10% investment tax credit for installation [17].

In addition, recently were introduced some environmental regulations which creates opportunities for combined heat and power production [17]:

- EPA Clean Power Plan (CPP), which establishes state-specific targets for reducing carbon emissions from existing power plants.
- Boiler MACT: the national emissions standard for hazardous air pollutants requires industrial and commercial boilers to meet new emissions limits, for example by converting them to natural gas CHP.

According to the U.S. Department of Energy, there are more than 4,500 sites around the United States with a capacity of almost 81 GW installed, with a reduction of 241 million metric tons of CO<sub>2</sub> emissions per year. Of these installations 217 are health care facilities, producing 722 MW [18].

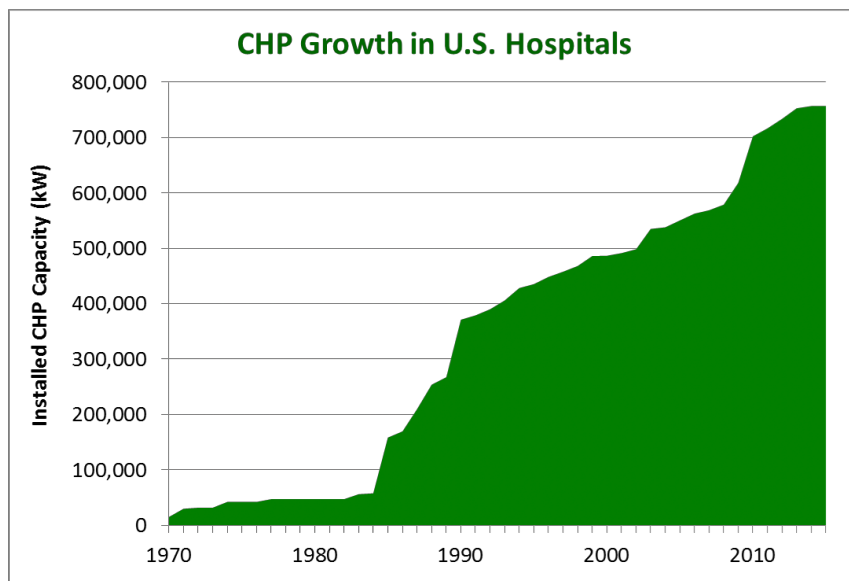


Figure 17: CHP served hospitals in U.S.

### 3.3 Components and general operation of the process

The main element of a CHP system is the *prime mover*, whose purpose is to convert the fuel chemical energy into mechanical energy required by the *generator*, which in turn converts it into electricity. The most common prime mover in hospitals are reciprocating engines, combustion turbines and microturbines, on which focuses this study, and steam turbines, mostly

fueled by natural gas. The main difference in comparison with traditional plants is the *waste heat recovery system*: since during the electric production operation some thermal energy is released by the exhaust gases, the WHRS recovers the waste heat by transferring it to a fluid, and converts it into useful thermal energy to satisfy the user’s heat demand.

The prime mover chosen will affect the performance and configuration of the whole system, resulting into two different types of plants: topping and bottoming cycle [19]. Figure 18 illustrates the typical topping cycle, that of interest in microturbines case, where the fuel is directly burnt in the prime mover. In the second configuration, common for steam turbines, the fuel feeds a boiler for the production of high-pressure steam.

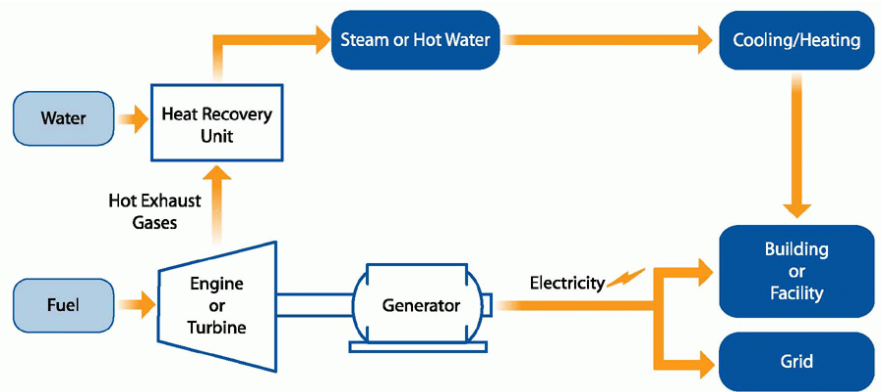


Figure 18: CHP Topping cycle

The Figure shows also the energy fluxes involved in the cycle. As explained, the combustion process generates hot exhaust gases. During the expansion a fraction of the heat content, defined Wasted Heat, is inevitably lost due to the inefficiencies of the plant; the remaining amount of heat potentially usable is the Recoverable Heat. Only a percentage of this heat meets the constrains of the system, both in terms of temperature and pressure, both on the basis of the thermal demand of the facility: the amount that actually reaches the final user is the Recovered Heat, the remainder, the Wasted Recoverable Heat, will assume a key role during the implementation of a TES device.

An important factor in the design of a CHP system is the choice of the proper operation strategy. Depending on the load the user would like to satisfy, two different options are available: following the thermal load (FTL) or following the electrical load (FEL). In the first case the system is sized to cover the thermal demand of the facility and the electricity is considered a

secondary product. In the other solution, instead, the heat produced is the secondary output, only meant to reduce the gas consumption by the boilers; the system is designed to satisfy the user electrical demand, meaning that when it's smaller than the prime mover capacity, that is totally covered, otherwise, the prime mover runs full load and the difference is purchased from the grid.

The choice of the most suitable option is based on the evaluation of the Heat to Power Ratio (HPR) defined as:

$$\text{HPR} = \frac{\text{Heat Demand [MWh]}}{\text{Electric Demand [MWh]}} \quad (6)$$

When the electric demand is much higher than the heat demand and the HPR is less than 1, which is the case of most health care facilities, especially during the warmer months, a FEL strategy is more convenient. In this way the plant will work in full load conditions as long as possible while, if we had chosen the FTL strategy, the result would have been a continuous fluctuation in the microturbine operation and, as a consequence, a partial load ratio operation for a large amount of hours. To avoid a drastic decrease of the technology efficiency, the only solution is to undersize the equipment. In addition, this strategy increases the reliability of the system in case of power outages.

Anyway, nowadays, as opposed to the past, the most common management strategy is to track the electric load mainly because of economic reasons, since the electricity is much more expensive than natural gas.

### **3.4 eQuest® CHP Model**

The CHP model was developed starting from the base model of the facility. In the new layout the microturbine is introduced as an electric generator and implemented in eQuest® as described in the previous chapter. The exhaust gases feed a recovery heat exchanger in order to satisfy the thermal request of the hot water loop. The fired boilers have not been removed since they will provide heat if the recovered amount isn't enough to cover the demand. For now, the wasted recoverable heat is lost, later on a TES will be introduced to recover that portion, reducing even more the number of hours the boilers run. The plant layout remains the same already shown in Figure 3, since the software doesn't show both the prime mover and the heat recovery loop.

Due to a restriction of eQuest<sup>®</sup>, it is not allowed to attach multiple loops to the heat recovery loop of the electric generator. To solve this the hot water loop and the domestic hot water loop are considered as one by setting manually to zero the water heater capacity of the DHW loop and by adding the DHW loop to the hot water loop as a miscellaneous load. Thanks to this approximation we are able to make the CHP system work on the software without affecting the thermal demand. In order to incorporate the domestic hot water into the space heating load two parameters are required: the domestic hot water process flow  $G$ , a specific characteristic of the building, and the process load  $Q$ , the equivalent hot water load of the two loops. The equation used to evaluate this last is:

$$Q = G \cdot \rho \cdot c \cdot \Delta T \quad (7)$$

Where  $\rho$  is the water density,  $c$  is the water specific heat capacity, and  $\Delta T$  is the difference of water temperature between inlet and outlet.

All the value required were provided by the software in the DHW specification:  $G$  is equal to 37.807 [gpm] and the difference in water temperature is 80 [°F]. The facility ends up with a process load equal to 2.717 [MBtu per hour].

## 4 Combined Cooling, Heat and Power (CCHP)

Although cogeneration systems are a big improvement in the energy field, by looking at the different heat fluxes involved a significant waste is still existing. While the winter months provide a good exploitation of the exhaust gases for space heating and domestic hot water production, in the rest of the year most of the heat is irremediably lost, since there is lower demand from the facility. The solution is to use this amount of wasted heat to generate chilled water for air conditioning or refrigeration, improving even more the cost-effectiveness and the efficiency of the system, in the order of 85% [20]. The better exploitation of the primary energy source allows to further reduce the amount of pollutants discharged into the environment, especially greenhouse gas emissions. It is shown that there is more than 200  $[\frac{\text{kg}}{\text{MWh}}]$  reduction in CO<sub>2</sub> emissions when trigeneration is used compared to the case where a power cycle is only used [20].

By producing cold water, hot thermal energy and electricity, each type of energy demand can be partially satisfied. The suitable facilities for installing a CCHP system are the same previously described in the cogeneration chapter, with the additional feature of cooling demand. Recalling that we are dealing with a CI infrastructure, this asset represents a profitable way to increase the reliability of the energy supply.

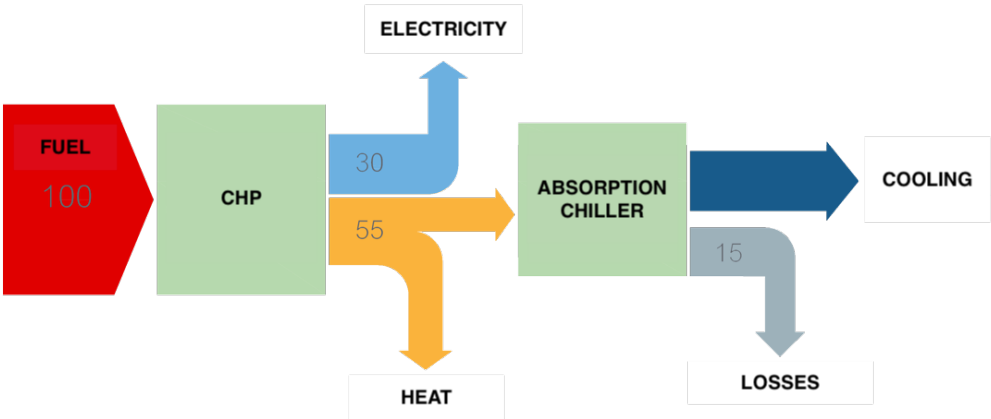


Figure 19: Operation of a trigeneration system [21]

A trigeneration or CCHP system works similarly to a combined heat and power system; the main difference is the new benefit provided by the introduction of a chilling technology. Through an inverse thermodynamic cycle, chillers remove heat from a system, thus decreasing

its temperature, and transfer it to another one at a higher temperature. According to the cycle performed, two main technologies can be identified: vapor compression chillers, based on the Clausius-Rankine cycle, and absorption chillers, which are the one on which this study will focus.

#### **4.1 Absorption chillers**

The main difference between vapor compression chillers and absorption chillers is that the second one, instead of using an electric compressor, exploits a high temperature source to cause the refrigerant evaporation and condensation. The principle behind this technology is to separate and recombine two different fluids, defined refrigerant and absorbent, that needs to show a strong chemical affinity, meaning that one of them has to be highly soluble in the other one [22]. Usually, the mixture is either  $\text{NH}_3\text{-H}_2\text{O}$ , where ammonia is used as refrigerant and water as absorbent, or  $\text{H}_2\text{O-LiBr}$ , where instead the refrigerant is the water and the lithium bromide is the absorbent. Lithium bromide is a salt in liquid form which is able to attract vapor water molecules; higher is the percentage of  $\text{H}_2\text{O}$  dissolved in the mixture, lower will be the absorption capacity of the absorbent. When they are mixed together, by applying a certain amount of heat, the water easily evaporates and separates from the LiBr salt particles, even at the low pressure and low temperature condition that characterize an absorption chamber, usually around 840 [Pa] and 40 [°F].

As mentioned above, this is the technology considered and, in particular, the study will deal with a  $\text{H}_2\text{O-LiBr}$  single-stage absorption chiller. Double-stage chillers are more complex, since additional steps are required to complete the process, and, despite they are characterized by higher performances, they have not been considered in this study because of the higher investment costs and the higher temperature required by the hot thermal source connected to the generator.

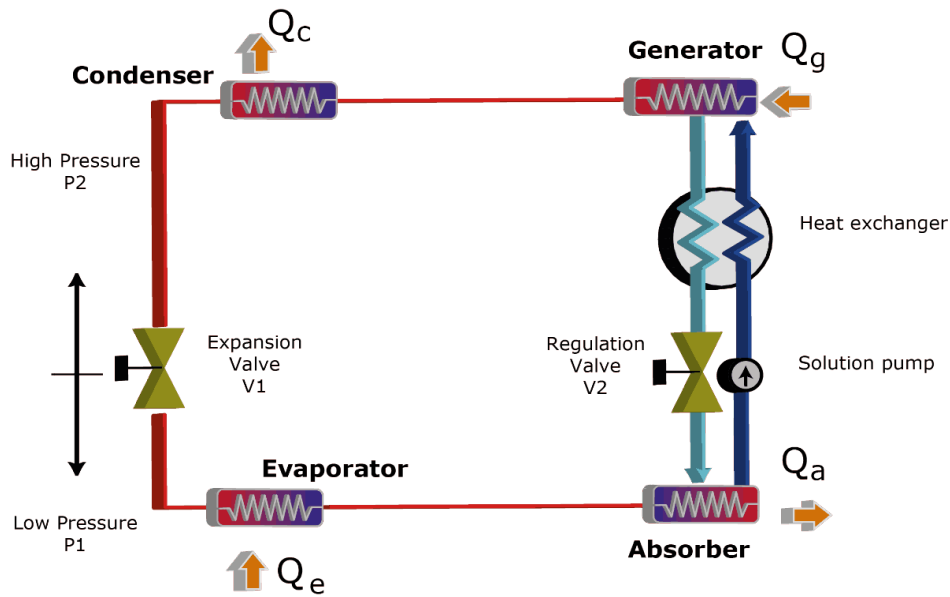


Figure 20: Schematic representation of an absorption cycle [23]

In Figure 20 is illustrated the operation of a single stage absorption chiller. The *generator* is connected to the high temperature source, in our case the waste heat coming from the prime mover. Here the heated operating fluid evaporates, separating the water vapor from the lithium bromide particles. The vapor enters the *condenser*, where is converted back into a liquid by the cooler heat exchanger. In fact, the condenser is linked to an intermediate heat reservoir at a lower temperature, e.g. a cooling tower or the outdoor environment. The liquid then has to pass through an expansion valve, so that temperature and pressure are reduced; in this way the liquid can enter the *evaporator*, whose purpose is to chill. The water enters this section at a very low-pressure and it is sprayed on the chilled water coils that cause it to evaporate. The evaporation is going to subtract thermal energy from the chilled water that, in this way, is cooled down. The last step is the *absorber* where the original concentration of the refrigerant and absorbent in the mixture is restored. As the water vapor enters this component, it is absorbed by the high concentration LiBr solution and, thanks to the high attraction between the two substances, the low-pressure condition is maintained. The resulting heat from the process is discarded to the atmosphere via the cooling water. The pump directs the new solution back to the generator through a heat exchanger where heat is exchanged with a parallel loop, which brings the high concentration LiBr fluid from the generator to the absorber to enable the regeneration process.

The efficiency of an absorption chiller is evaluated through the Coefficient of Performance (COP) defined as the ratio between the heat removed from the low temperature source and the heat transferred from the hot source to the generator.

$$\text{COP}_T = \frac{Q_e}{Q_g} \quad (7)$$

In the case of electric chillers, instead, the heat transferred from the hot source is replaced by the amount of work needed to perform the cycle.

$$\text{COP}_E = \frac{Q_e}{W} \quad (8)$$

In order to distinguish the two different parameters, they are usually referred to respectively as thermal COP and electrical COP.

Typical values of  $\text{COP}_T$  vary between 0.6 and 0.8 for a single-stage absorption chiller and between 1.0 and 1.2 for a double-stage one [22]. Electric chillers, instead, are characterized by a much higher performance, with a  $\text{COP}_E$  that range from 4.0 to 8.0, but is important to point out that they run on electricity, a valuable source, while absorption chillers exploit waste heat.

#### ***4.1.1 eQuest<sup>®</sup> absorption chiller model***

As it has been done for the microturbine, also in this case a proper chiller model is required for the energy simulation in eQuest<sup>®</sup>. The model provided by the software was too outdated compared to the modern technologies available in the market, so a new one was developed in previous studies [7][24], based on the MILLENIUM YIA<sup>™</sup> single-effect absorption chiller produced by YORK<sup>®</sup> [25]. Since the implementation of a new model is not part of this research, a brief summary is provided just to have an overview on the operation process of the equipment.

- **Chilled water temperature effect**

The chilled water temperature is the temperature of the cold water inside the cooling coils, which is set according to the user. Even a small reduction of this temperature is going to affect negatively the evaporation capacity and, as a consequence, the chiller performance since it will be harder to let the fluid evaporate because the evaporation temperature decreases.

eQuest® requires two curves as a function of this parameter. The first one is the behavior of the *capacity percentage*, which is the ratio between the cooling capacity in a specific condition and the design capacity. The design capacity, which correspond to the 100% percentage, is reached at 44 [°F] CWT with a constant condensed water temperature of 85 [°F], as imposed by the ARI 550/590 standard to evaluate the chillers performance [26]. In Figure 21 the default curve provided by the software is compared to the experimental one obtained by the interpolation of the manufacturer data, that, being less steep, is less affected by the CWT variation.

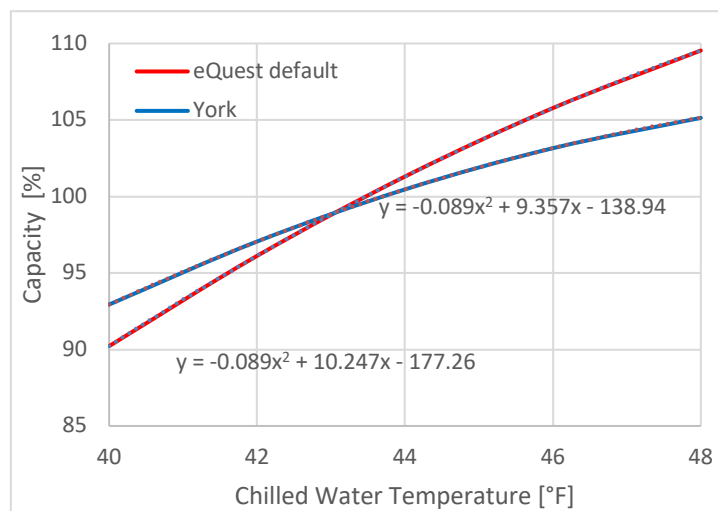


Figure 21: Chiller capacity percentage vs Chilled water temperature

The second curve required is the trend of the ratio of the COP in a particular condition and the design one, defined *percentage COP*. Even though the manufacturer does not provide direct information regarding this dependence, through some algebra it can be evaluated as the ratio of the capacity percentage and the percentage variation in fuel consumption, provided by YORK® again as a function of CWT.

$$\begin{aligned}
COP\% &= \frac{COP}{COP_{design}} = \frac{\frac{Cooling\ Cap.}{Fuel\ Cons.}}{COP_{design}} = \frac{\frac{(Cooling\ Cap.)_{design} \cdot Capacity\ \%}{(Fuel\ Cons.)_{design} \cdot Fuel\ Cons.\ \%}}{COP_{design}} \\
&= \frac{COP_{design} \frac{Capacity\ \%}{Fuel\ Cons.\ \%}}{COP_{design}} = \frac{Capacity\ \%}{Fuel\ Cons.\ \%}
\end{aligned} \tag{8}$$

The old eQuest<sup>®</sup> model, which did not take into account the effect of the chilled water temperature on the COP was replaced by the following curve where COP=100% correspond to 44 [°F]. In the second graph are compared the actual COP values relating to the variation of the CWT: in the default model the COP was constantly equal to 0.65, the YORK<sup>®</sup> chiller, instead, in the design condition is characterized by a COP=0.75. Once all the curves were defined, a basic assumption was made: the CWT imposed by the user is assumed constant at 44 [°F]. In this way the curves were normalized assuming 100% of cooling capacity and COP, as the standard requires.

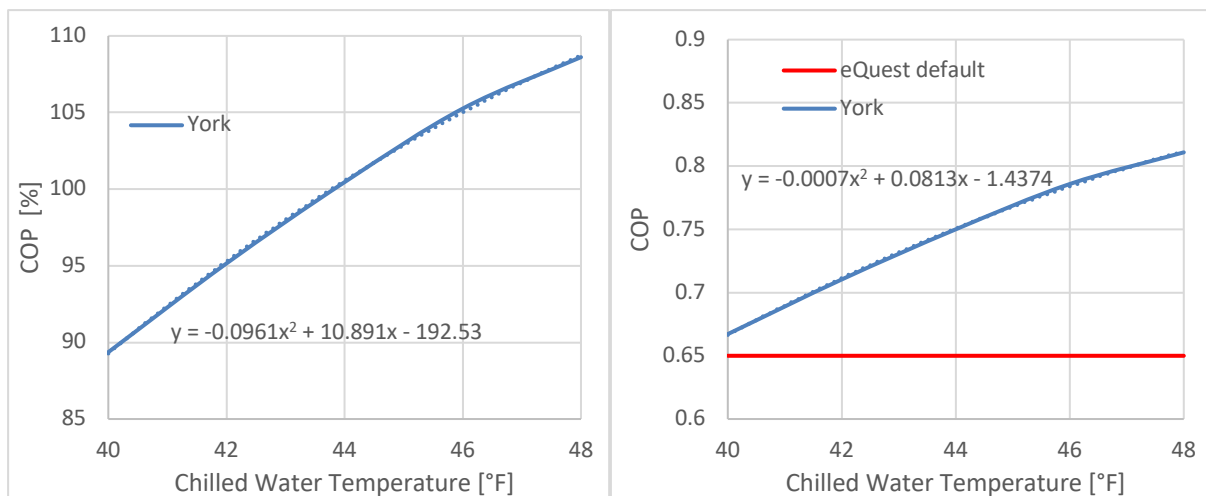


Figure 22: Percentage COP and COP vs Chilled water temperature, comparison between eQuest<sup>®</sup> default model and YORK<sup>®</sup> model

- **Condenser temperature effect**

The condenser temperature depends on the outdoor condition, under the assumption of constant rejected thermal energy operated by the cooling tower. Increasing the condenser temperature

produces deleterious effects on both the thermal COP and the cooling capacity of the absorption chiller.

In order to evaluate the performance changes due to the effect of this parameter, Cicciarella F. in his study [7], obtained the curves which describe the trend of the percentage COP and the percentage cooling capacity, starting from the relation between the energy input requested by the equipment and the cooling capacity produced at several condenser temperatures, provided by YORK® [25]. The implied assumption is a constant chilled water temperature equal to 44 [°F]. The curves are reported in Figure 23, where are shown both the percentage COP and the comparison between YORK® and eQuest® COP values, and Figure 24. The design capacity is reached at full load condition for a temperature of 85 [°F], according to ARI standard [26].

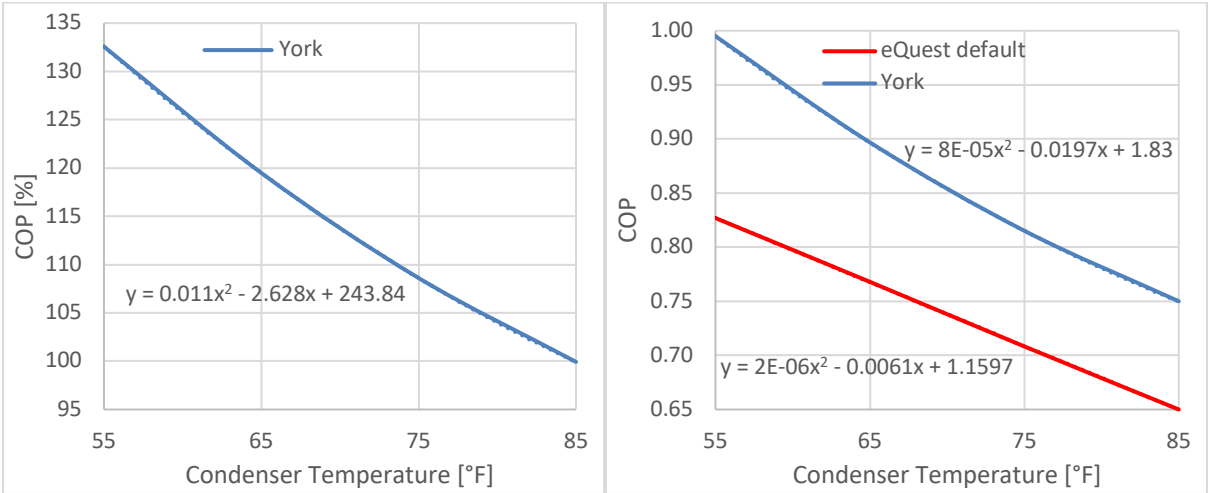


Figure 23: Percentage COP and COP vs Condenser temperature, comparison between eQuest® default model and YORK® model

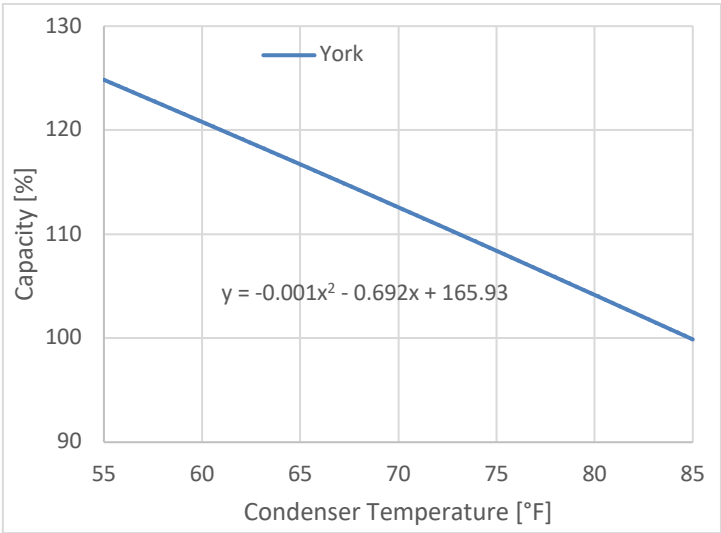


Figure 24: Percentage Capacity vs Condenser temperature

- **Partial Load Ratio**

As happens for the microturbines, also the chillers are not always running at full load. The sizing of a chiller is based on the maximum amount of recoverable heat produced, but the amount of thermal energy available change throughout the year and it's not always granted, since the chiller is fed by the wasted recovered heat. In addition, the facility cooling demand is variable as well. As a consequence, in some period of the year the chiller is oversized with respect to the real needs, so it's essential that the chiller shows good performance even at very low partial load ratio.

The model developed describing the COP in function of the PLR, is provided in the following figure. The drastic improvement of the YORK® model is probably due to the fact that eQuest® one was developed a long time ago, resulting in a very obsolete and inefficient component.

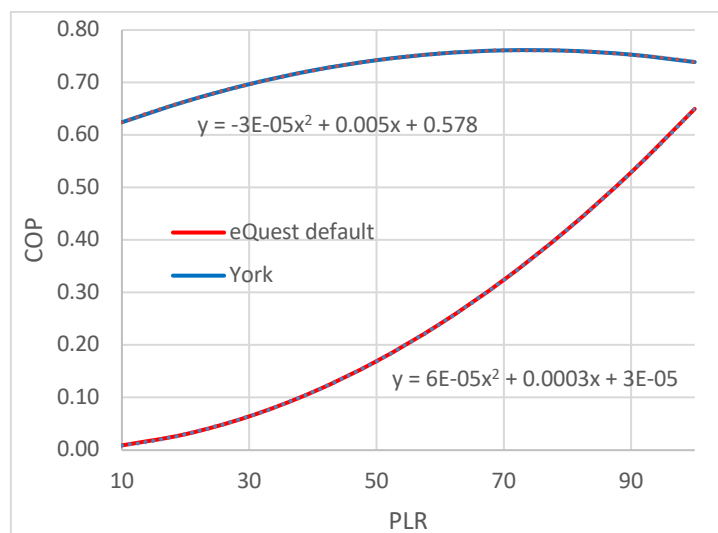


Figure 25: COP vs Partial Load Ratio, comparison between eQuest® default model and YORK® model

## 4.2 eQuest® CCHP model

The trigeneration plant was developed starting from the cogeneration system previously described. Figure 26 shows the main modification in the layout, which consists in the introduction of the single-stage absorption chiller, connected to the *Hot Water Loop*. Here is where the recovered heat is discharged and, from this loop, the chiller gets the high-temperature thermal energy to run. Then, it is obviously connected to the *Chilled Water Loop* to provide the

cooling effect, and, through the *Condenser Water Loop*, to a cooling tower for the discharge of the heat produced during the process. The electric chillers are kept as a backup in case the absorption chiller is not able to satisfy the entire cooling demand. To prioritize the exploitation of the absorption chiller instead of the electric ones, a control system was implemented.

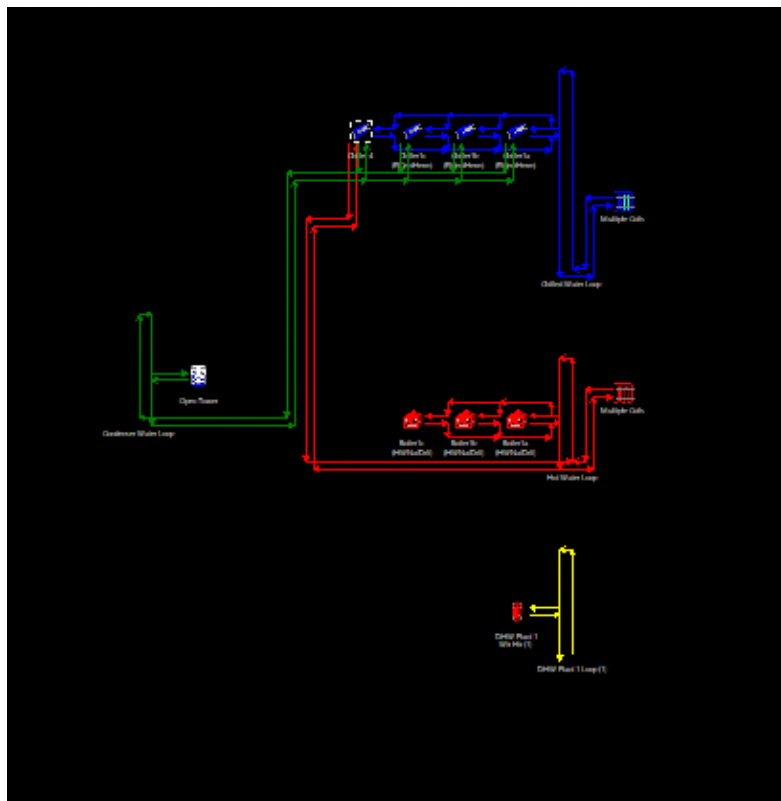


Figure 26: CCHP plant layout

After the implementation of the trigeneration plant, the simulation results were collected. However, the fuel consumption analysis showed how the system was not working properly. What is meant to happen, in a correct operation, is that the absorption chiller runs with the wasted recoverable heat and, when it's not provided, the electric chillers have the priority. In this way the boiler consumption should not increase. Instead, despite the equipment control implemented, when the heat for the absorption chiller was not enough, the boilers start to run in order to make it work, causing a significant rise in the fuel consumption from the boilers. Ciccirella F., in his work, [7] also developed a method to ensure the proper operation of the system. The absorption chiller was sized on the basis of the amount of recoverable heat available and, in this way, the chiller runs until the heat is fully exploited and then, the electric

chillers start to work. However, even by applying this method, the increase in the consumption was too high to be acceptable, as shown above.

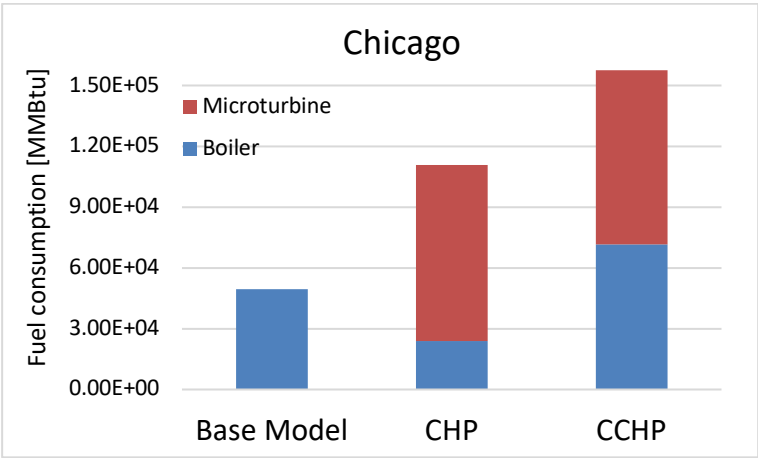


Figure 27: Annual fuel consumption, Base model vs CHP and CCHP

For simplicity, the only chart provided is the Chicago one, but the same problem was noticed in all the other locations, so, in order to simulate a correct trigeneration system, a more specific Excel model was implemented. Since the cogeneration system has proved to be effective and the results collected reliable, the CCHP model is based on the CHP data provided by eQuest®. In fact, as above mentioned above, during the normal operation of a trigeneration system, the boilers shouldn't run more frequently, since the chiller works just with the wasted heat coming from the microturbine. A single model has been developed for the CCHP system and the CCHP- TES coupled system, with the possibility to set the tank volume to 0; for this reason, all the methodology is explained in detail in the next chapter.

## 5 Thermal Energy Storage

One major concern regarding cogeneration and trigeneration systems is the mismatch between energy generation and energy demand [27]. A solution to this problem is the implementation of a Thermal energy storage (TES). It refers to a system which can store thermal energy at high or low temperature when it's not being used, and then deliver it at a later time, when the CHP or CCHP system cannot provide it. In this way the waste heat from the electricity production can be captured and stored for future retrieval. Therefore, the whole system performance and reliability is going to be increased and it will operate for longer periods [27]. Previous studies [28][29] showed how the introduction of a TES can reduce the amount of additional heat required from the boiler and, also through a better exploitation of the energy, the result is a reduction in carbon dioxide emissions and a reduction in primary energy consumption. All these features allow to reduce the capital and operational costs, also because the storage of energy could be a useful strategy in order to shift the energy purchase to a more convenient period and use the stored energy when prices are higher.

There are three main type of thermal energy storage systems. The first one is *sensible thermal energy storage*, the most traditional technique based on warming up or cooling down a certain quantity of mass, commonly water. Another common solution is *latent thermal energy storage*, where is exploited the internal energy difference associated to each of the states in a phase change process. The main advantages of these systems are the higher storage density and that the storage cycle take place with low temperature variations [27]. The last one, still in R&D phase, is the *thermochemical energy storage*, based on the energy storing or releasing that occurs with the formation or split of molecular bonds during reversible chemical transformations. The type of TES is chosen on the basis of the temperature operating range, storage duration and type of application. The most common configuration, which is also the one selected for this research, is to employ a vertical cylindrical hot water tank as the storage medium.

Despite the type of technique, the way a TES system works is always the same, involving three steps. The energy is supplied to the storage during the charging process, then it is stored inside the tank, although, for a hot TES, a certain percentage is usually lost towards the environment and finally, during the discharge process, the heat is transferred to the user [27].

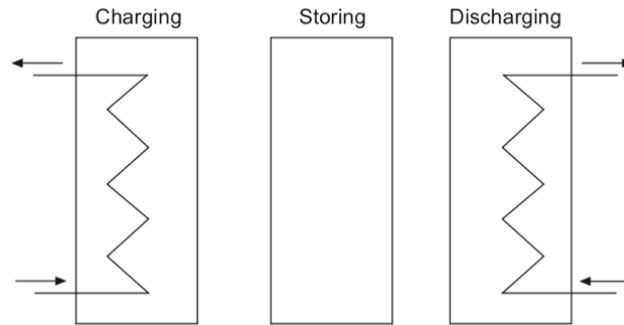


Figure 28: Complete storage cycle

Different CHP/CCHP-TES interaction levels can be found in any applications:

- There is no demand and the system runs charging the storage
- The demand is lower than the thermal power generated and while the system runs, the heat surplus is stored in the TES system
- The demand is higher than the thermal power generated. The system runs and the remainder of heat needed is released from the TES if available
- The demand is satisfied only by the heat released from the storage

## 5.1 Basic thermodynamics of sensible energy storage

Most of hot water sensible thermal energy storage systems exploit the stratification effect, caused by the temperature difference and occurring between the inlet and outlet water. As a consequence of the density difference, the hot water flows to the top and the cold water lays on the bottom, resulting in two thermal zone with an intermediate region in between, called thermocline. This phenomenon makes it possible to have higher temperature to satisfy the demand and, by reducing the mixing of the fluid between the thermal zones, tends to improve the global performance of the plant [27]. However, since the analysis starts from eQuest<sup>®</sup> data and the software does not support the dynamic of stratified tank, the storage implemented is based on the fully mixed model, the limiting case where it is supposed that all the water stored remains at the same temperature and therefore, no stratification effect takes place [30].

The basic principle to explain the operation of a TES system is that every substance is characterized by an energy content proportional to its temperature. The amount of heat stored

in the material is, in fact, determined by the product of the difference between the initial and final temperature of the tank ( $T_2-T_1$ ), the mass of the storage medium and its heat capacity [27]:

$$Q = m \cdot c_p \cdot (T_2 - T_1) = \rho \cdot V \cdot c_p \cdot (T_2 - T_1) \quad (9)$$

The quality of the energy, crucial during the design of a system, is strictly linked to the amount of water heated and on the  $\Delta T$  it undergoes. It suffices to think that the same amount of thermal energy can be stored by heating up to a higher temperature a smaller quantity of water. A high temperature range is much more useful for a cogeneration or trigeneration plant.

In order to achieve a high heat content per volume, the heat storage material is chosen for its high specific capacity and high density. From Table 1 it appears that water has a very high heat storage density both per weight and per volume compared to other potential materials and, since it's also relatively inexpensive and easy to work with, it's the most suitable to operate in the temperature range required for the analyzed plants.

<b>Material</b>	<b>Density [kg/m<sup>3</sup>]</b>	<b>Specific heat [J/kgK]</b>	<b>Volumetric thermal capacity [10<sup>6</sup> J/m<sup>3</sup>K]</b>
Clay	1,458	879	1.28
Brick	1,800	837	1.51
Sandstone	2,200	712	1.57
Wood	700	2,390	1.67
Concrete	2,000	880	1.76
Glass	2,710	837	2.27
Aluminum	2,710	896	2.43
Iron	7,900	452	3.57
Steel	7,840	465	3.68
Gravelly earth	2,050	1,840	3.77
Magnetite	5,177	752	3.89
Water	988	4,182	4.17

Table 1: Typical materials used in sensible heat TES [27]

## 5.2 Technical parameters

After having defined the type of TES system and the storage medium, the operating temperature must be defined. As already explained, the storage is charged by the wasted exhaust gases through the *Heat Recovery Loop* and the heat is discharged into the *Space Heating Hot Water Loop*, whose operating temperature is set to 170 [°F]. This same temperature has been chosen as the minimum operating temperature of the storage. In order to work with a higher storage capacity, the tank is working with pressurized water. In these systems the minimum temperature differential recommended is 100 [°F] and usually they are designed to operate at export temperatures of 350 to 420 [°F]. The system pressure must be at least 25 [psi] above the saturation pressure of the maximum temperature to prevent pump cavitation and flashing of superheated water to steam [31]. The maximum operating temperature of the storage tank was set to 350 [°F], requiring at least a pressure of 160 [psi]. Considering the average temperature equal to 260 [°F], water is characterized by a density equal to 7.82 [lb/gal] and a specific heat of 1.02 [Btu/lb°F].

The last parameter required to define the capacity of the storage is its volume. Since one of the goals of this analysis is to study the impact of a thermal energy storage system on a large health care facility, the volume has been varied in a range between 0 [gal] and 60,000 [gal]. These dimensions were chosen on the basis of the tank catalog of Highland Tank manufacturer, among the “HigDRO® Vertical Water Tanks” [32]. In this way is possible to determine if the introduction of a thermal storage is useful in this kind of applications and whether a much larger tank is actually more convenient than a smaller one. The various dimension and capacity considered, calculated using the Equation 9, are listed in the table below.

Volume [gal]	0	1,000	2,000	5,000	10,000	20,000	30,000	40,000	50,000	60,000
Capacity [MMBtu]	0.00	1.44	2.87	7.18	14.36	28.73	43.09	57.46	71.82	86.19

Table 2: Different volumes and capacity of TES

Since eQuest® has some inner strong limitations regarding the integration between a hot thermal storage and a CHP or CCHP system and the results are usually unrealistic, the TES model has been developed on Excel, starting from the hour-by-hour data provided by the software for the CHP system. Starting from these data it was possible to model also the trigeneration plant, as

mentioned in the previous chapter. In the following paragraphs is explained in detail how the TES Excel model has been developed and integrated in both systems.

### 5.3 Methodology

The wasted heat available for the charge of the storage has been evaluated by comparing the amount of recoverable heat provided by the microturbine ( $Q_{\text{recoverable}}$ ) and the heat demand of the facility ( $Q_{\text{demand}}$ ). In this way it was possible to compute how much was the actual heat recovered ( $Q_{\text{recovered}}$ ) and the waste per hour ( $Q_{\text{wasted}}$ ). In addition to understand how much heat the boilers are required to provide, it is sufficient to subtract the recovered heat from the thermal load of the hospital ( $Q_{\text{boiler}}$ ).

$$\text{If } Q_{\text{recoverable}} - Q_{\text{demand}} > 0$$

$$Q_{\text{recoverable}} - Q_{\text{demand}} = Q_{\text{wasted}}$$

$$\text{Otherwise } Q_{\text{recoverable}} - Q_{\text{demand}} = Q_{\text{recovered}} \quad (10)$$

$$Q_{\text{boiler}} = Q_{\text{demand}} - Q_{\text{recovered}} \quad (11)$$

In the Excel spreadsheet developed, which includes all the data provided by eQuest<sup>®</sup> and the ones calculated, the storage capacity can be varied by varying the volume of the tank. In this way it is possible to determine the profiles of the total recovered heat and the impact of the different sizes on the system.

#### 5.3.1 TES-CHP model

Having evaluated the energy fluxes involved in the system, all measured in [MMBtu], it was possible to model the thermal storage model and combine it with the cogeneration plant. Starting from a hypothetical empty tank ( $Q_{\text{old\_storage}} = 0$ ), at each hour the available heat charges the storage adding up to the amount already in the tank. At the same time this energy is compared with the demand that the boilers must still cover. When the available energy is smaller or equal to the amount required, the whole quantity of heat is recovered

( $Q_{\text{recovered\_TES}}$ ) and the storage empties. Otherwise, just a portion of heat, equal to the boilers demand, is recovered and the remainder is stored. This amount cannot exceed the maximum thermal capacity of the TES ( $\text{TES}_{\text{cap}}$ ); once it is reached the remaining energy is irremediably lost.

$$\text{If } (Q_{\text{old\_storage}} + Q_{\text{wasted}}) > Q_{\text{boiler}}$$

$$\{Q_{\text{recovered\_TES}} = Q_{\text{boiler}}$$

$$\text{If } Q_{\text{old\_storage}} + Q_{\text{wasted}} - Q_{\text{boiler}} < \text{TES}_{\text{cap}}$$

$$Q_{\text{new\_storage}} = Q_{\text{old\_storage}} + Q_{\text{wasted}} - Q_{\text{boiler}}$$

$$\text{Otherwise } Q_{\text{new\_storage}} = \text{TES}_{\text{cap}} \}$$

$$\text{Otherwise } \{Q_{\text{recovered\_TES}} = Q_{\text{old\_storage}} + Q_{\text{wasted}}$$

$$Q_{\text{new\_storage}} = 0 \} \quad (12)$$

$$Q_{\text{old\_storage}} = Q_{\text{new\_storage}} \quad (13)$$

The additional heat required beyond the total amount of heat recovered from the plant and the TES will be satisfied by the boilers ( $Q_{\text{final\_boiler}}$ ):

$$Q_{\text{tot\_recovered}} = Q_{\text{recovered}} + Q_{\text{recovered\_TES}} \quad (14)$$

$$Q_{\text{final\_boiler}} = Q_{\text{demand}} - Q_{\text{tot\_recovered}} \quad (15)$$

### 5.3.2 TES-CCHP model

As already mentioned, the trigeneration system was modeled on the basis of the CHP system implemented on eQuest<sup>®</sup>. The energy fluxes considered remain unchanged; in fact, the operation condition of the microturbine should be almost the same and so also the boilers consumption, since the absorption chiller runs just with the wasted heat coming from the microturbine and no additional work is required from the boilers. The additional flux necessary

to model a CCHP system is the facility cooling demand ( $Q_{\text{cooling\_demand}}$ ), provided by the software.

In a cogeneration plant not coupled with a TES system, all the heat not recovered is lost, instead, in a trigeneration system, when there is exhaust heat available and the cooling demand is not 0 the absorption chiller runs directly and satisfy the demand exploiting that heat. Therefore, in this case, a certain amount of wasted heat is recovered anyway; the addition of a thermal storage should decrease even more the loss of available thermal energy, avoiding the use of the electric chillers. Similar to what was done in the CHP system, an Excel spreadsheet was implemented to describe the charge and discharge dynamics of the tank. The model was developed in such a way that it is possible to change the TES volume and the absorption chiller capacity. Thus, by varying the tank volume, both a CCHP-TES coupled system and a CCHP without storage system can be simulated, just by setting the volume to 0. In addition, a chiller with capacity equal to 0, means that the system is working like a cogeneration plant. With a single model it was possible to summarize all the different condition analyzed and to compare the different solution. Supposedly, in the trigeneration case, the introduction of a thermal storage should be even more convenient since most of the waste occurs in the warmer months, due to the excess of recoverable heat compared to the thermal demand.

At each hour the storage cycle is divided in two separated steps to better control the equipment and the recovered heat. The boilers operation is prioritized, so at first the wasted heat is used to satisfy the thermal demand; then, the remainder is available for the absorption chiller if needed. As a consequence, the first step follows exactly the TES operation described previously in Equation 12. The only difference is that the heat recovered thanks to the thermal storage is renamed  $Q_{\text{boiler\_recovered\_TES}}$ , in fact in this phase we are just dealing with the boiler operation and, to distinguish the two different steps, the updated storage is defined  $Q_{\text{new\_storage\_1}}$ .

In the second step is fundamental to determine the thermal energy needed by the absorption chiller to satisfy the cooling demand; this is obtained through the  $\text{COP}_T$  equation, by dividing the cooling demand by the COP of the chiller, which in the design condition is equal to 0.75:

$$Q_{\text{heat\_req\_chiller}} = \frac{Q_{\text{cooling\_demand}}}{\text{COP}} \quad (16)$$

Another crucial concept is the absorption chiller cooling capacity ( $\text{CHILLER}_{\text{cap}}$ ). When this last is greater than or equal to the heat requested to cover the cooling demand, the previous condition

representing the available energy in storage ( $Q_{\text{new\_storage}_1}$ ), if sufficient, can cover the request. Otherwise, at most the thermal storage can provide an amount of energy corresponding to the chiller capacity. Of course, since we are dealing with heat fluxes, in order to make a comparison with the heat required, also the capacity should be divided by the COP; in this way we obtain the amount of thermal energy equivalent to a certain cooling capacity. The second step, regarding the absorption chiller operation, is described in the following equations:

$$\begin{aligned}
& \text{If } \frac{\text{CHILLER}_{\text{cap}}}{\text{COP}} \geq Q_{\text{heat\_req\_chiller}} \\
& \quad \left\{ \text{If } Q_{\text{new\_storage}_1} \leq Q_{\text{heat\_req\_chiller}} \right. \\
& \quad \quad Q_{\text{new\_storage}_2} = 0 \\
& \quad \left. \text{Otherwise } Q_{\text{new\_storage}_2} = Q_{\text{new\_storage}_1} - Q_{\text{heat\_req\_chiller}} \right\} \\
& \quad \left\{ \text{If } Q_{\text{new\_storage}_1} \leq \frac{\text{CHILLER}_{\text{cap}}}{\text{COP}} \right. \\
& \quad \quad Q_{\text{new\_storage}_2} = 0 \\
& \quad \left. \text{Otherwise } Q_{\text{new\_storage}_2} = Q_{\text{new\_storage}_1} - \frac{\text{CHILLER}_{\text{cap}}}{\text{COP}} \right\} \tag{17}
\end{aligned}$$

$$Q_{\text{old\_storage}} = Q_{\text{new\_storage}_2} \tag{18}$$

The heat recovered for the absorption chiller is evaluated in a different way with respect to the boilers. In fact, if we use the same approach as before, in the case of no storage, that amount would be incorrectly equal to zero, since the TES charging cycle would stop. Instead, without the TES system, the wasted heat available at each moment should feed the chiller anyway. Therefore, the recoverable heat available for the absorption chiller is evaluated by looking at the thermal energy in the storage and at the amount of heat recovered for the boilers. Then, the recovered heat is obtained by finding first the minimum between the thermal energy needed by the absorption chiller and the chiller capacity, and then by computing again the minimum between the value just found and the recoverable heat. In this way, we are taking into account the wasted heat available for the chiller even in absence of thermal storage.

$$Q_{\text{chiller\_recoverable}} = Q_{\text{old\_storage}} + Q_{\text{wasted}} - Q_{\text{boiler\_recovered\_TES}} \quad (19)$$

$$Q_{\text{chiller\_recovered}} = \min [Q_{\text{chiller\_recoverable}}, \min (\frac{\text{CHILLER}_{\text{cap}}}{\text{COP}}, Q_{\text{heat\_req\_chiller}})] \quad (20)$$

The heat recovered thanks to the introduction of the TES system is the sum of the amount recovered for the boilers ( $Q_{\text{boiler\_recovered\_TES}}$ ) and the amount recovered for the absorption chiller ( $Q_{\text{chiller\_recovered\_TES}}$ ) calculated separately:

$$Q_{\text{recovered\_TES}} = Q_{\text{boiler\_recovered\_TES}} + Q_{\text{chiller\_recovered}} \quad (21)$$

$$Q_{\text{tot\_recovered}} = Q_{\text{recovered}} + Q_{\text{recovered\_TES}} \quad (22)$$

At this point, knowing all the different recovered thermal energy fluxes, it is possible to compute how much of the cooling demand will be covered by the absorption chiller ( $Q_{\text{abs\_cooling}}$ ) and how much by the electric chillers ( $Q_{\text{electric\_cooling}}$ ):

$$Q_{\text{abs\_cooling}} = \text{COP} \cdot Q_{\text{chiller\_recovered\_TES}} \quad (23)$$

$$Q_{\text{electric\_cooling}} = Q_{\text{cooling\_demand}} - Q_{\text{abs\_cooling}} \quad (24)$$

The last step is to estimate the electric savings thanks to the implementation of the CCHP-TES coupled system. The electric input required by the electric chillers to run is obtained through the  $\text{COP}_E$  equation and then converted from [MMBtu/h] in [kW]. The coefficient of performance considered is equal to 5, as they are modeled in eQuest<sup>®</sup>. Equations 25 and 26 refer respectively to the input required by the chillers in the CHP plant, where all the cooling demand is satisfied

by the electric chillers, and in the CCHP plant after the introduction of the thermal storage and of the absorption chiller. In this way it is possible to compare the electric building demand for the two different plants studied.

$$E_{\text{electric\_chiller\_before}} = 293.071 \cdot \frac{Q_{\text{cooling\_demand}}}{\text{COP}_E} \quad (25)$$

$$E_{\text{electric\_chiller\_after}} = 293.071 \cdot \frac{Q_{\text{electric\_cooling}}}{\text{COP}_E} \quad (26)$$

$$E_{\text{demand\_CCHP}} = E_{\text{demand\_CHP}} - E_{\text{electric\_chiller\_before}} + E_{\text{electric\_chiller\_after}} \quad (27)$$

## 6 eQuest<sup>®</sup> simulations and Energy analysis

In each work meant to modify and improve a pre-existing energy supply layout, the first step is always to examine all the information about the energy demand of the facility.

The base model performance was evaluated with eQuest<sup>®</sup>, which, for each simulation, provides hour-by-hour the energy loads and consumption profiles throughout the whole year. The hourly data concerning the electric demand, heat demand and fuel consumption were extrapolated by the reports provided by the software and post processed on an Excel spreadsheet in order to obtain a graphic representation of the hospital profiles throughout the 8760 hours of the year. In addition, for each demand, the data were rearranged in descendent order in order to obtain the duration curve. A load duration curve represents the time duration of the magnitude of a load: on the y-axis is reported the load size, while the x-axis shows the number of hours for which that load persists. As a consequence, the curve will always have a decreasing behavior starting from the peak load, usually for a negligible number of hours, to the minimum value, which is the base load that persists for the whole year, meaning that the load is always at least equal to this number.

After the analysis of the energy demand of the hospital facility, a cogeneration and a trigeneration system will be studied. The development of both eQuest<sup>®</sup> models has been explained in the previous chapters. Lastly the systems were implemented introducing a hot thermal storage, in order to try to improve the wasted heat exploitation.

Regarding the power generator, as explained previously, in case of a high electric demand, the microturbines are available in packages of multiple generators up to 1000 [kW]. Considering the peak electric demand of the different locations, around 2000 kW, this output power seems suitable for satisfying the demand and, at the same time, working at partial load non for too long, since this would affect negatively the efficiency of the system. So, in each of the simulations the generator is the Capstone C1000 microturbine.

One of the aims of this study is to compare the profiles of locations characterized by different weather for understanding how precipitation and heating degree days, defined as the difference in temperature between the average outdoor temperature over a 24-hour period and a given base temperature for a building space, typically 65 [°F], are going to affect the facilities.

In ASHRAE 169-2006 [8] each region is defined by a number, which range from 1 (hot) to 8 (subarctic), and a letter to describe the moisture regimes, humid climate (A), dry climate (B) and marine subzones (C).

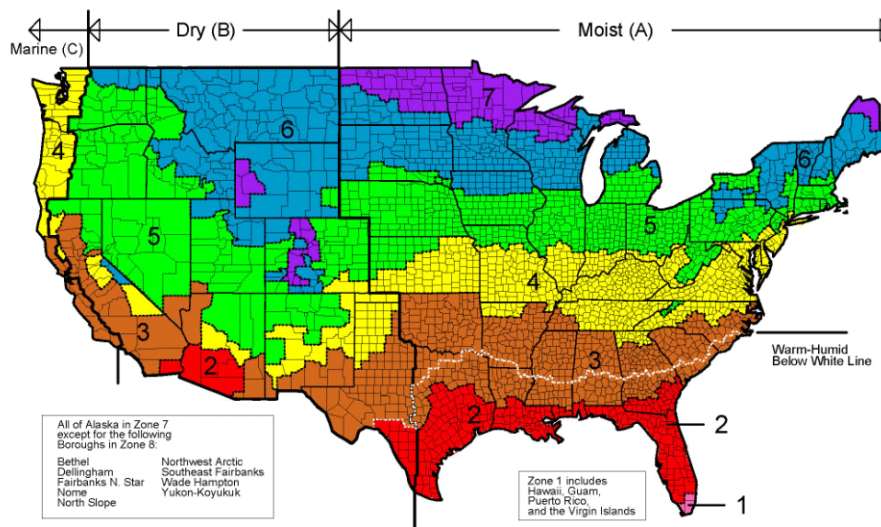


Figure 29: Climate regions in US

Starting from Chicago IL (climate zone 5A), three more were the locations chosen to cover the variable US climate range: Atlanta GA (climate zone 3A), Miami FL (climate zone 1A) and Duluth MN (climate zone 7A). In order to obtain comparable results, all the locations are characterized by the same humid climate.

## 6.1 Base hospital model

### 6.1.1 Electric demand

In the following graphs are provided the hourly electric load in [kW] for each of the city chosen. As expected, the demand never decreases to zero, since the hospital is characterized by an almost continuous need for electricity, as already mentioned. Overall the profiles show an increase during warmer months because of the cooling demand, which is satisfied with the electric chillers, while in the heating season the fluctuations are more regular by varying between two limit bands, since the heat demand is related with boilers that use natural gas as fuel. The daily fluctuations are due to the occupancy of the structure and the periodical usage of electrical equipment, not only space cooling, but also lights, ventilations fans, heat rejection system, miscellaneous equipment, pumps and other auxiliaries.

On closer examination, it can be noticed as the climate is going to influence the facility demand. A warmer climate will correspond to higher electric peaks in the cooling season, while in the

rest of the year the electric demand will remain unchanged, because of the other electrical equipment. In fact, by comparing Chicago and Atlanta, in the latter case the electric profile in the warm season is shifted upward towards higher peaks, while Duluth, characterized by a very cold climate, is quite cool also in the summer, so the cooling demand and, as a consequence the electric demand, is obviously going to be lower.

Different is the situation regarding Miami: it remains true the fact that the demand is a little higher in the cooling season, but in this case the electric consumption is almost constant during the whole year. This is due to the lower change in temperature between winter and summer, in fact the difference is usually around 15 [°F]; therefore, a warm climate, which decrease just slightly during the cold season, similar to an equatorial climate, reflects in an almost continuous operation of the electric cooling chillers.

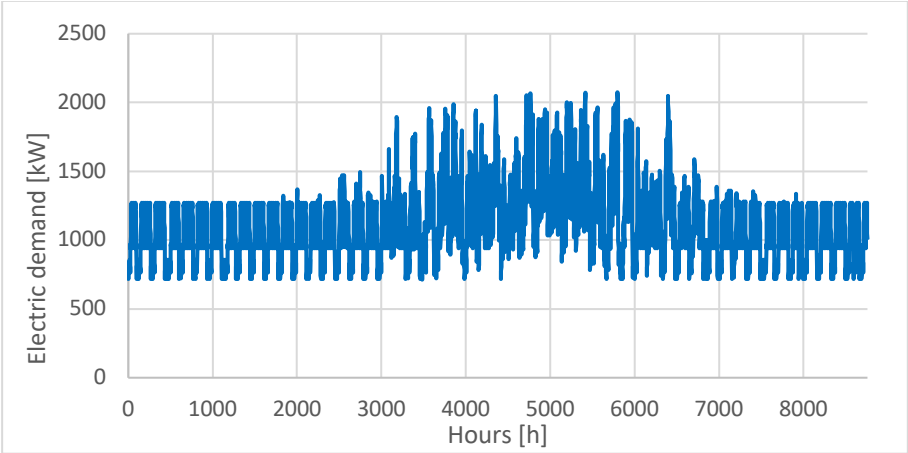


Figure 30: Base model annual electric demand, *Chicago*

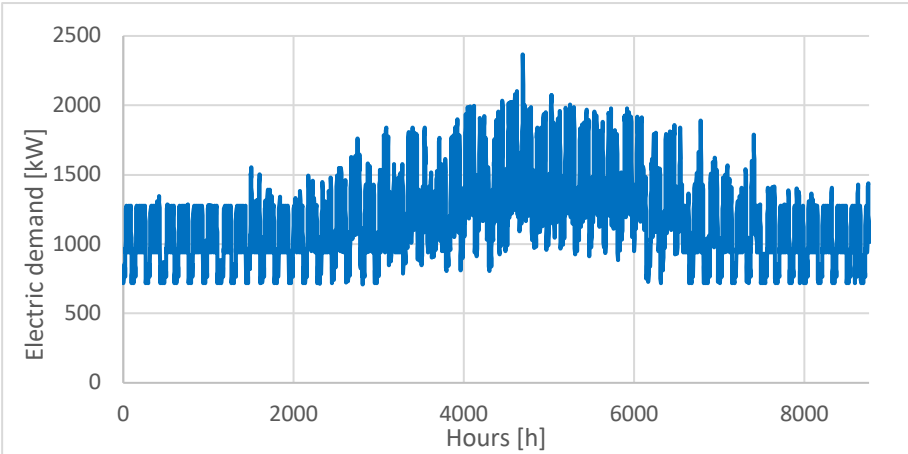


Figure 31: Base model annual electric demand, *Atlanta*

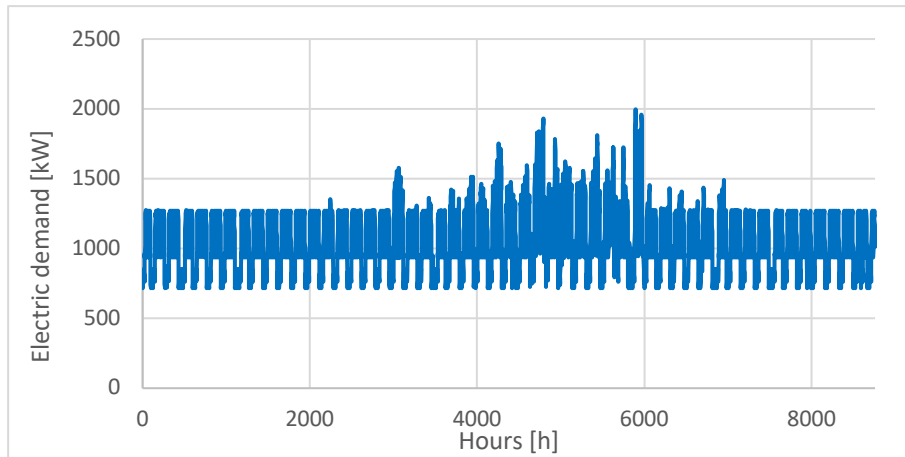


Figure 32: Base model annual electric demand, *Duluth*

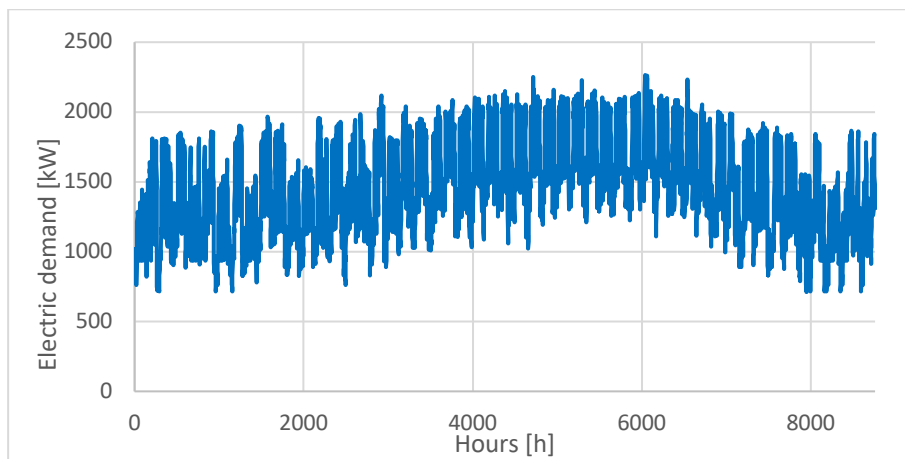


Figure 33: Base model annual electric demand, *Miami*

Although the previous profiles give an overall view on the facility needs throughout the year, they don't provide any type of information regarding the generator sizing. The electric duration curve is useful for this purpose, in fact, looking at its trend, is possible to check the maximum electric demand for the building and to choose the optimal size of the prime mover, as the curve provides information about the number of hours the generator would run full load. This number is found by projecting on the x-axis the intersection between the curve and the capacity of the prime mover. As regards the choice of the prime mover size, a component that produces a power close to the maximum demand, will work at full load just for a few hours and at partial load ratio (PLR) for the remaining time, resulting in an oversized system. Instead, a smaller size generator will run steadily and at full load for a larger number of hours. Each time the demand is higher than the power produced by the prime mover, it is necessary to buy the electricity from

the grid. The choice will mainly depend of the efficiency of the component chosen: if working at PLR implies a reduction in efficiency or vice versa.

In Figure 34 the four different duration curves are compared. As expected from the previous graphs provided, the base load is almost the same among all the locations. Chicago, Atlanta and Duluth curves have a similar behavior, where a warmer climate, means a higher maximum load and a higher demand, while Miami is characterized by a peak which is not higher compared to the other ones, actually lower than the Atlanta one, but during the whole time the demand is higher due to the continuous running of the electric chillers. In fact, in the cooling period Miami is not warmer than Atlanta, but it is in the rest of the year and, during this time, the change in temperature is quite small compared to the other cities.

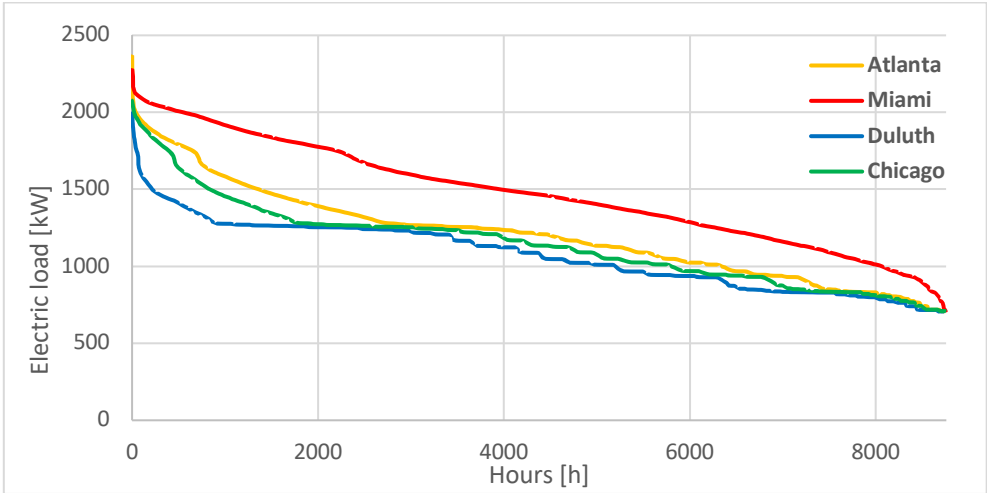


Figure 34: Base model electric duration curve

	<b>Chicago</b>	<b>Atlanta</b>	<b>Duluth</b>	<b>Miami</b>
<b>Total demand [MW]</b>	10015	10539	9400	12874
<b>Max demand [kW]</b>	2074	2367	1997	2279
<b>Min demand [kW]</b>	709	708	687	707

Table 3: Electric demands

**6.1.2 Heat and fuel demand**

It was decided to study together the heat demand and fuel consumption of the facility since there is a strong correlation between them. The heating demand of the hospital takes into account both the hot water requested by the *Domestic Hot Water Loop* and by the *Space Heating*

*Loop*; in either case the demand is satisfied by the fired boilers and the fuel consumption increases. Most of the fuel is used to feed the heating system, but it also supplies other miscellaneous equipment in the hospital, such as kitchens and laundries. As a result, the two profiles follow the same trend, but they will just differ in terms of magnitude. It is also important to mention that the fuel consumption is affected not only by the demand, but also by the efficiency of the equipment installed, in this case boilers; this is of primary importance in the comparison of different technical solutions.

The annual profile is presented in the following graphs. The trend is exactly the opposite compared to the electric one, since, as already mentioned, the heat demand is satisfied by boilers that use natural gas as fuel; therefore both the thermal and fuel demand reach their maximum during the colder months, when the heating system works at full load in order to satisfy the needs of the facility. During the middle months of the year, instead, the demand is lower and almost constant since there is just request for domestic hot water and, regarding the fuel, also for miscellaneous equipment; this is also noticeable in the thermal duration curves comparison. Duluth, the coldest of the city studied, is characterized by higher peaks and it requires space heating for a longer amount of time compared to Chicago and to Atlanta, whose demand for space heating, instead, lasts for a shorter period. Regarding Miami, the thermal demand is almost just for domestic hot water production, beside a few peaks during the colder months.

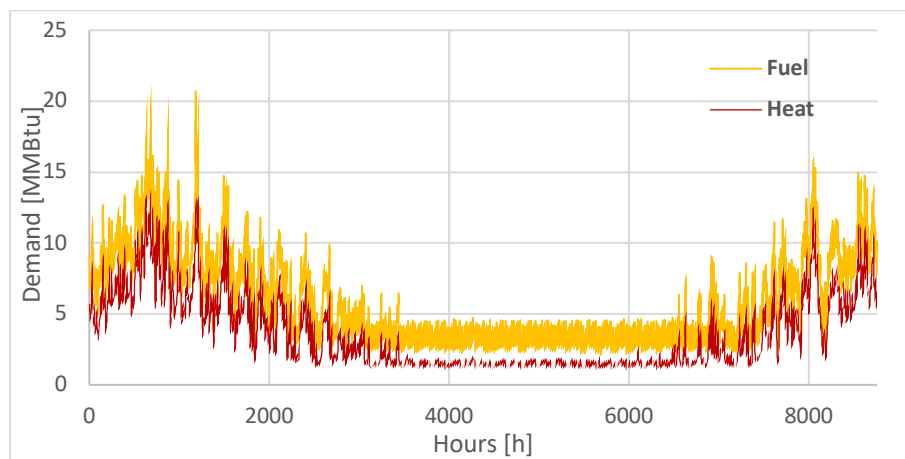


Figure 35: Base model annual heat and fuel demand, *Chicago*

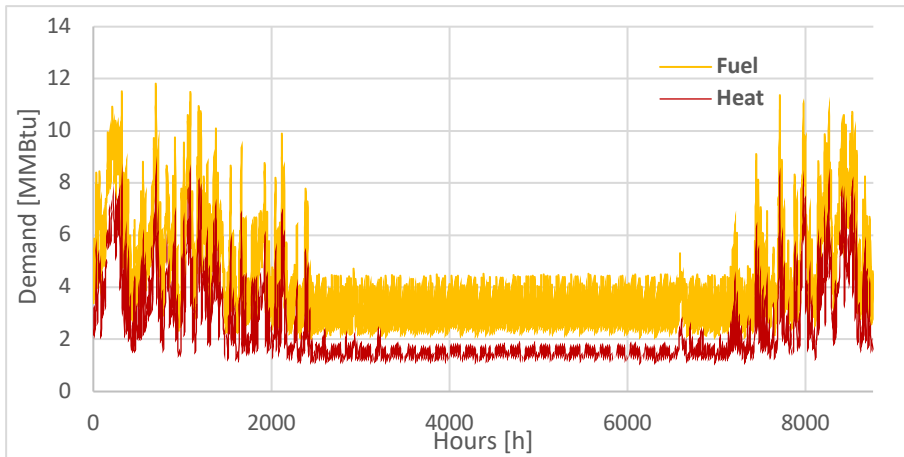


Figure 36: Base model annual heat and fuel demand, *Atlanta*

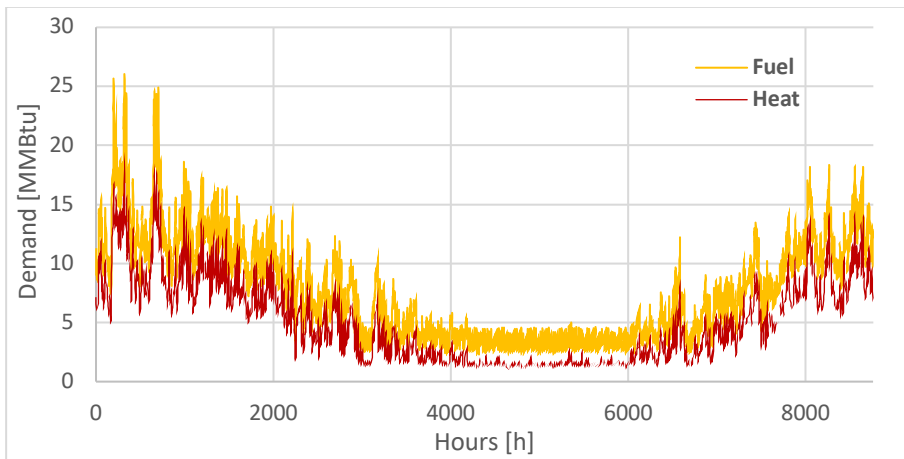


Figure 37: Base model annual heat and fuel demand, *Duluth*

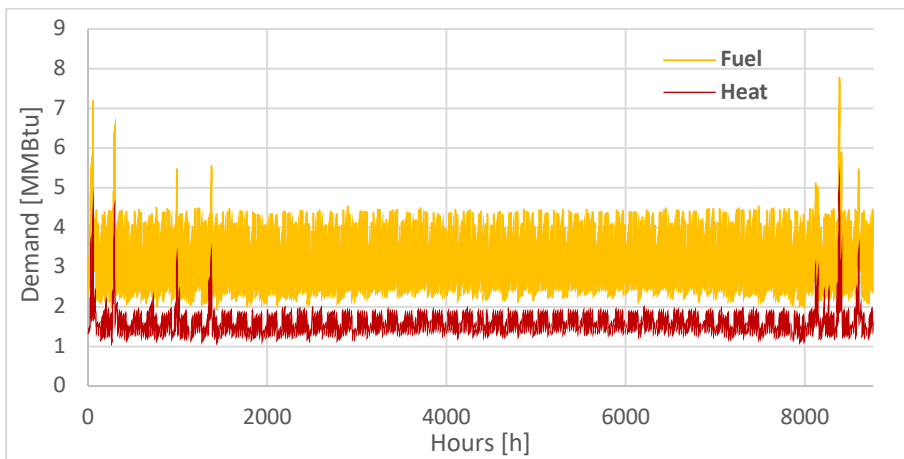


Figure 38: Base model annual heat and fuel demand, *Miami*

Certainly, also the trend of the duration curves is similar. What can be noticed regard the locations with a lower space heating demand, Atlanta and especially Miami, is that their peaks

in the fuel duration curve increase less with respect to the heat curve; instead when we look at Chicago and Duluth, the maximum value of the fuel demand is greater than more than 5 [MMBtu] compared to the maximum of the heat demand. In fact, even if the fuel is requested for different final uses, most of it is always used to satisfy the heating system.

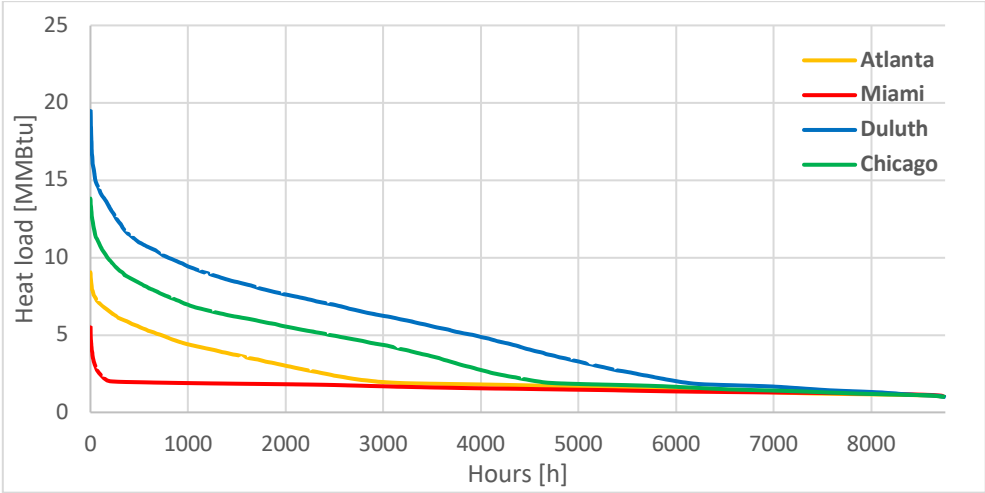


Figure 39: Base model thermal duration curve

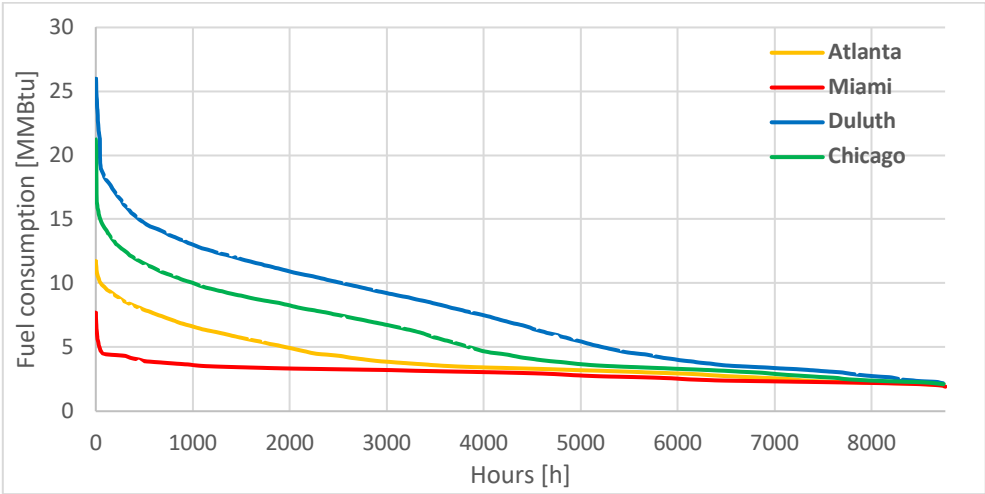


Figure 40: Base model fuel duration curve

## 6.2 CHP system

### 6.2.1 Electric demand

The first effect produced by the new microturbine installed, is the reduction in the amount of electricity purchased from the grid. The prime mover is going to provide a big part of the electric

demand during the year. The results of the simulations are compared in Figure 41 and Figure 42, where the red line represents the hospital electric demand and the blue line the amount of electricity the microturbine was able to produce. From the chronological electric demand, it can be seen how the facility request is satisfied during the night, instead during the day it is too high to supply. In addition, the demand is covered for the most part of each month, except for the summer period when the demand is too high, due to the electric chillers running.

As explained in the base model simulations, Miami is the exception among the locations since the electric demand is constantly higher so the electric demand will not be satisfied for a large part of the year.

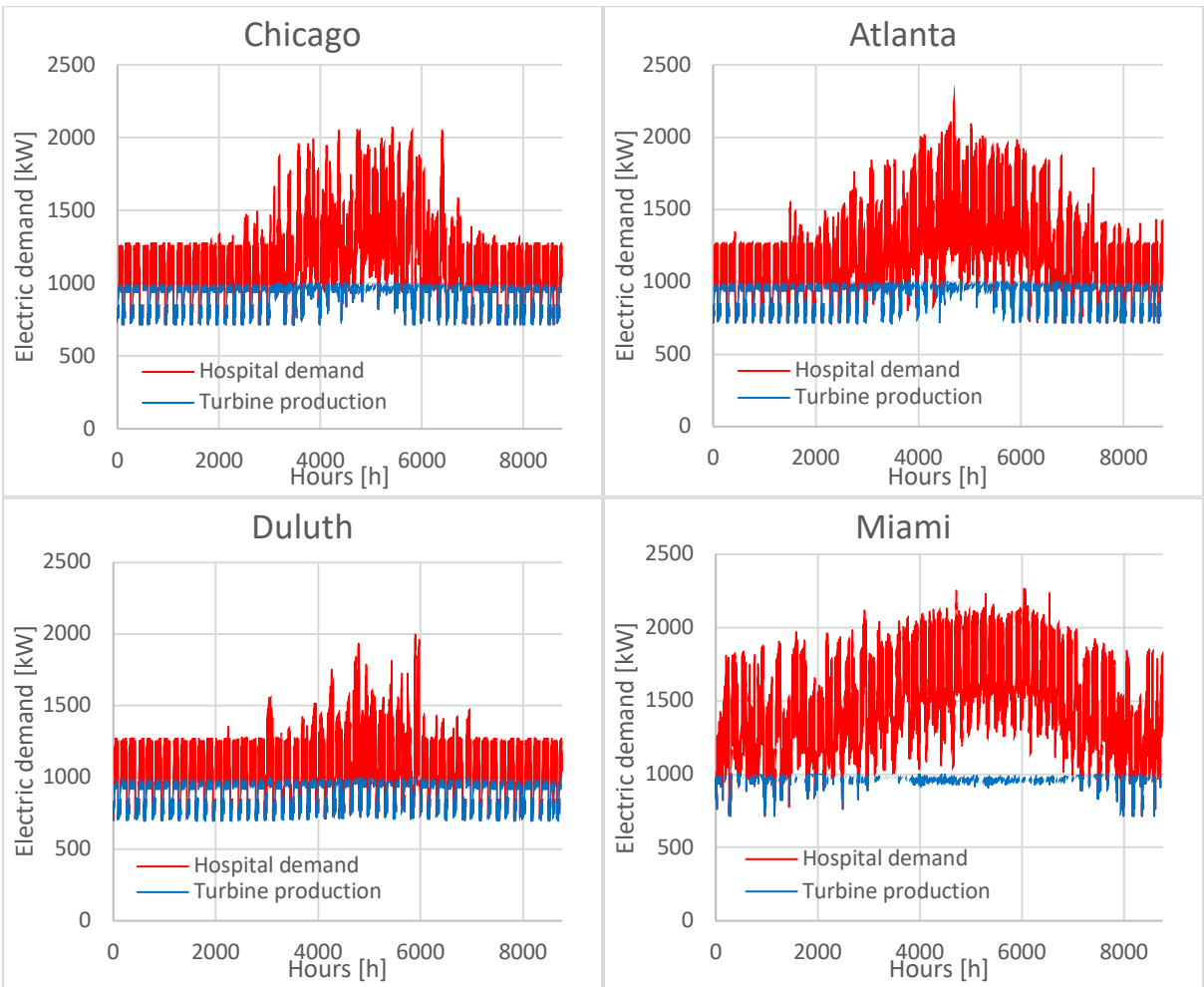


Figure 41: Hospital electric demand vs Electricity produced by the turbine

From the electric duration curves is even clearer how in Miami it will be necessary to buy more electricity from the grid, while the microturbine remains at full load for more time in comparison with the other locations.

By looking at the percentage of electricity covered by the turbine, just the 66.1% of the electric demand is satisfied in Miami: since we are dealing with a warmer, almost tropical, climate, it's interesting to look at the amount of recoverable heat and, especially in this case, a trigeneration system will be fundamental to exploit the microturbine and all the heat that otherwise would be wasted. In Duluth the amount of turbine production reaches the 86.7% since the demand is constantly lower.

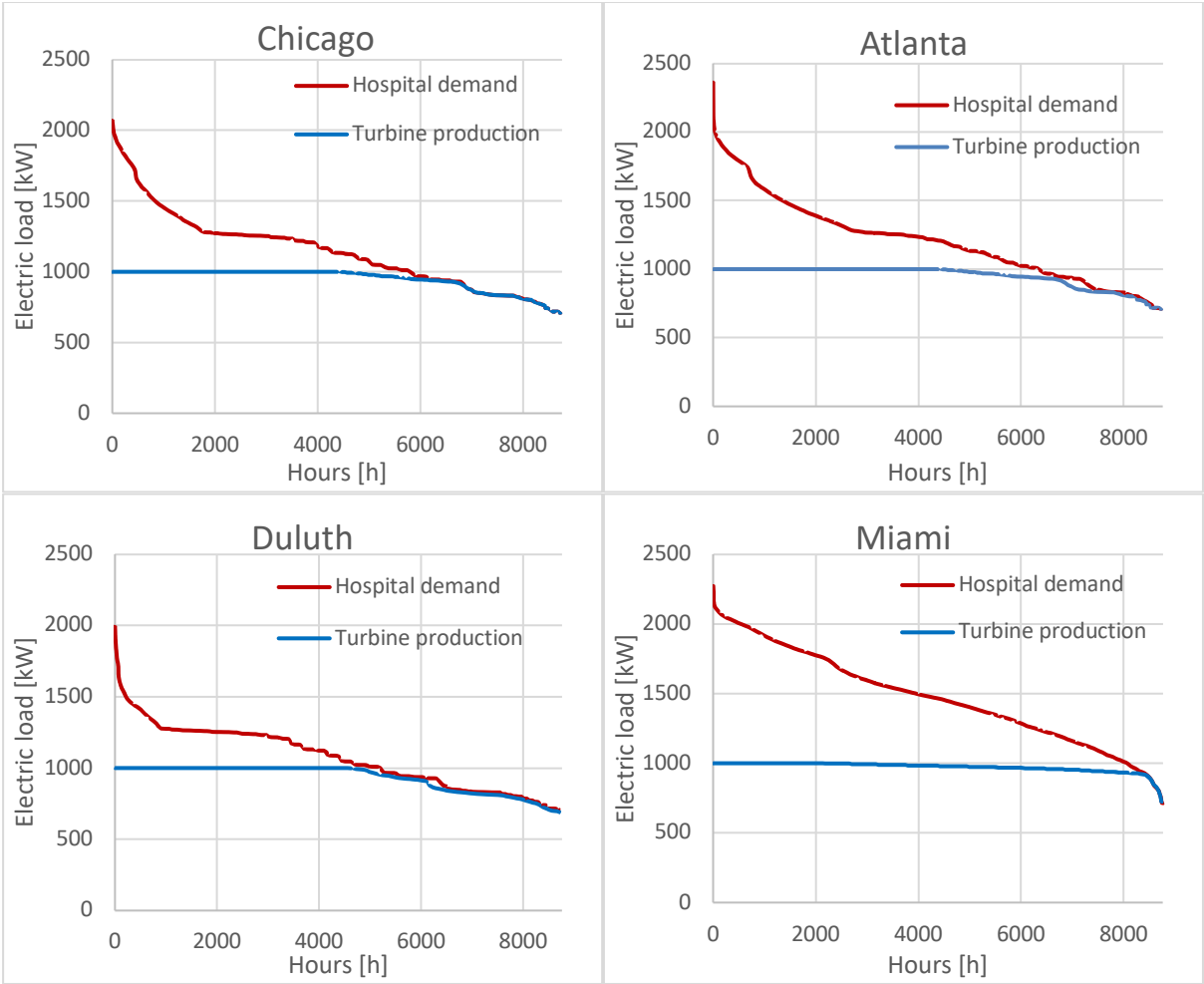


Figure 42: Hospital electric duration curve vs Electricity produced by the turbine

	<b>Chicago</b>	<b>Atlanta</b>	<b>Duluth</b>	<b>Miami</b>
<b>Turbine electric production</b>	82.8%	79.3%	86.7%	66.1%

Table 4: Turbine electric production vs Electric demand

**6.2.2 Heat demand**

The other product obtained by the cogeneration plant is the recoverable heat available from the microturbine. Starting from the heat load of the facility and the amount of total recoverable heat, the actual recovered heat was post processed on an Excel spreadsheet in order to obtain a graphic representation of the profiles.

For each location two graph are provided: in the first one is compared the heat demand of the facility with the recoverable heat available; in the second one is shown how much heat is actually recovered and how much would be lost. During the warmer months the exhaust gases are sufficient to satisfy the demand, while during the winter the fired boilers are necessary to cover the higher peaks. To better understand the exploitation of the available heat in each location, the amount of recovered heat in comparison with recoverable heat and facility demand are provided in Table 5. It is clear that even if the heat demand is not totally satisfied but there is still a certain percentage of recoverable heat not exploited, this may be wasted because in that particular moment, the heat required by the facility is lower than the one produced. The only way to be able to use also this amount of wasted heat is to introduce a storage: in this way the excess heat can be collected and exploited when needed.

With the climatic variation, the two rates calculated have the opposite trend. As already explained, a cooler climate means higher thermal peaks and a longer period where the space heating is required; vice versa in a warm climate the demand for space heating lasts for a shorter period, for example in Miami the thermal demand is really small and almost constant since it's mainly for domestic hot water production. Having said that, what happens in the first situation is that the recoverable heat is quite low compared to the high thermal demand, so almost all of that can be exploited but it will satisfy poorly the hospital demand. For example, if we take a look at Duluth just the 16.4% of recoverable heat is wasted, but only slightly more than half of the total demand is satisfied. Instead in a very warm climate, as Miami, the recoverable heat is always higher than the thermal demand, which can be almost totally satisfied; of course, in this case there will be a lot of wasted heat.

	<b>Chicago</b>	<b>Atlanta</b>	<b>Duluth</b>	<b>Miami</b>
<b>Recovered heat vs Heat demand</b>	69.5%	87.7%	56.5%	99.9%
<b>Recovered heat vs Recoverable heat</b>	75.1%	65.8%	83.6%	53.6%

Table 5: Amount of recovered heat in comparison with recoverable heat and facility demand

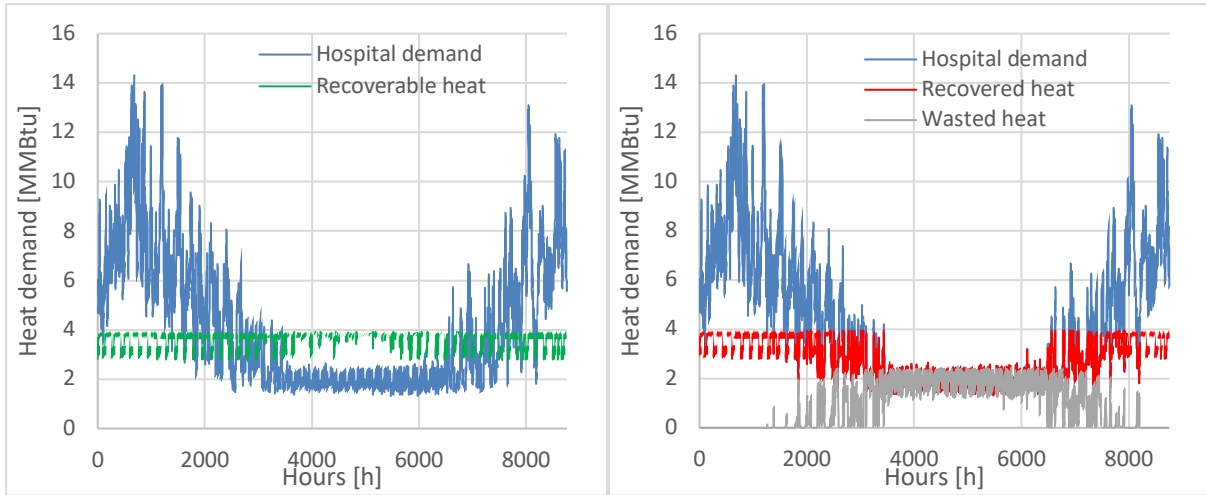


Figure 43: Hospital heat demand and comparison between recoverable, recovered and wasted heat, *Chicago*

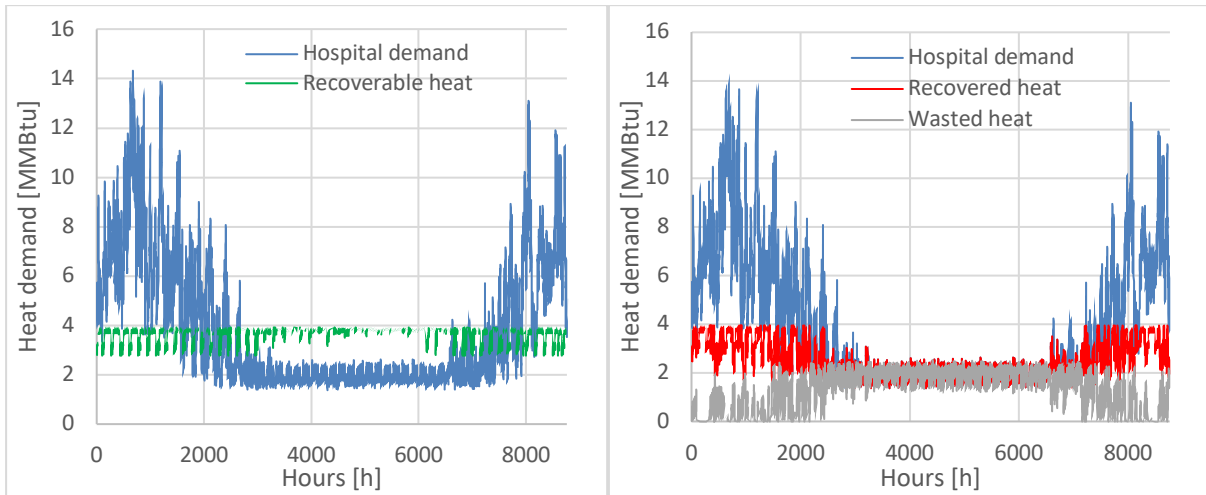


Figure 44: Hospital heat demand and comparison between recoverable, recovered and wasted heat, *Atlanta*

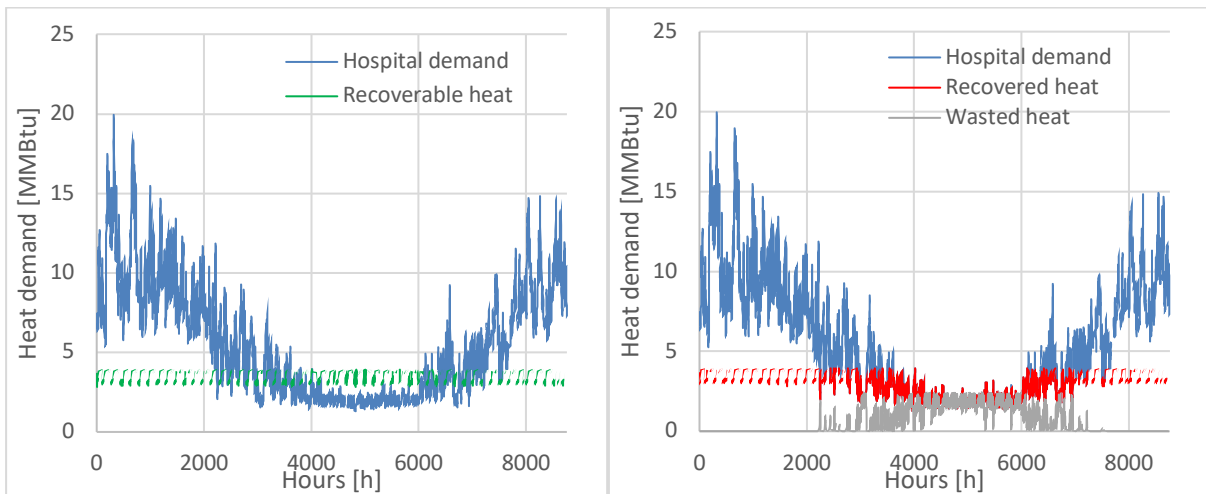


Figure 45: Hospital heat demand and comparison between recoverable, recovered and wasted heat, *Duluth*

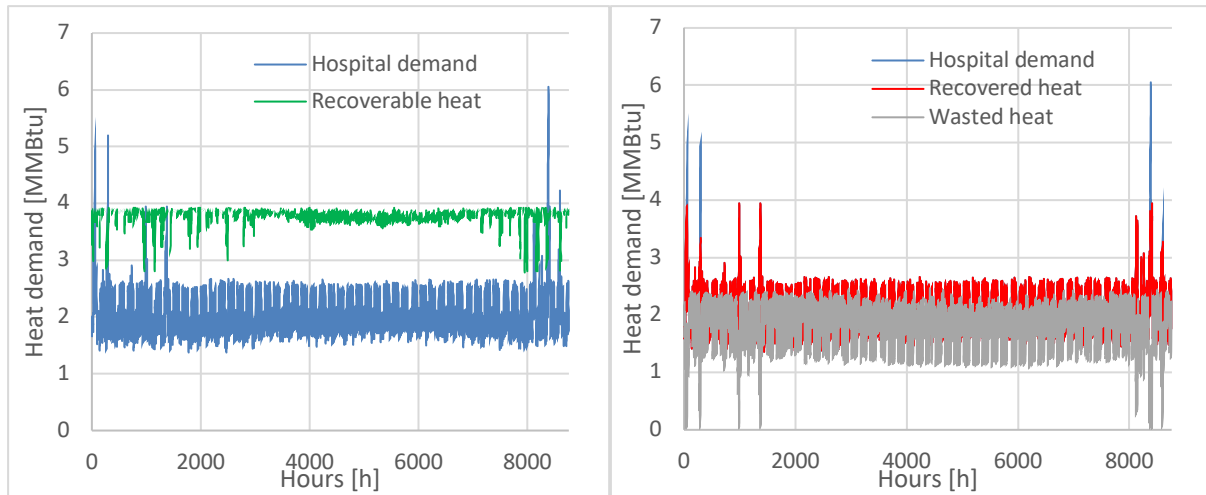


Figure 46: Hospital heat demand and comparison between recoverable, recovered and wasted heat, *Miami*

### 6.2.3 Fuel demand

By introducing the new prime mover, the overall fuel consumption increases in comparison with the base model, since fuel is used to feed the microturbine, as shown in Figure 47. Before the installation of the turbine the fuel consumption was strictly connected to the boilers, with a higher demand in the cold season. Now, the fuel consumption is more uniform during the year since most of it is required by the prime mover. This behavior of course does not apply to Miami since the fuel consumption trend was already almost constant before, but it's very clear in the other locations, especially Atlanta, where almost 90% of the heat demand was satisfied by recovered heat. This means that the boiler will start to run much more rarely.

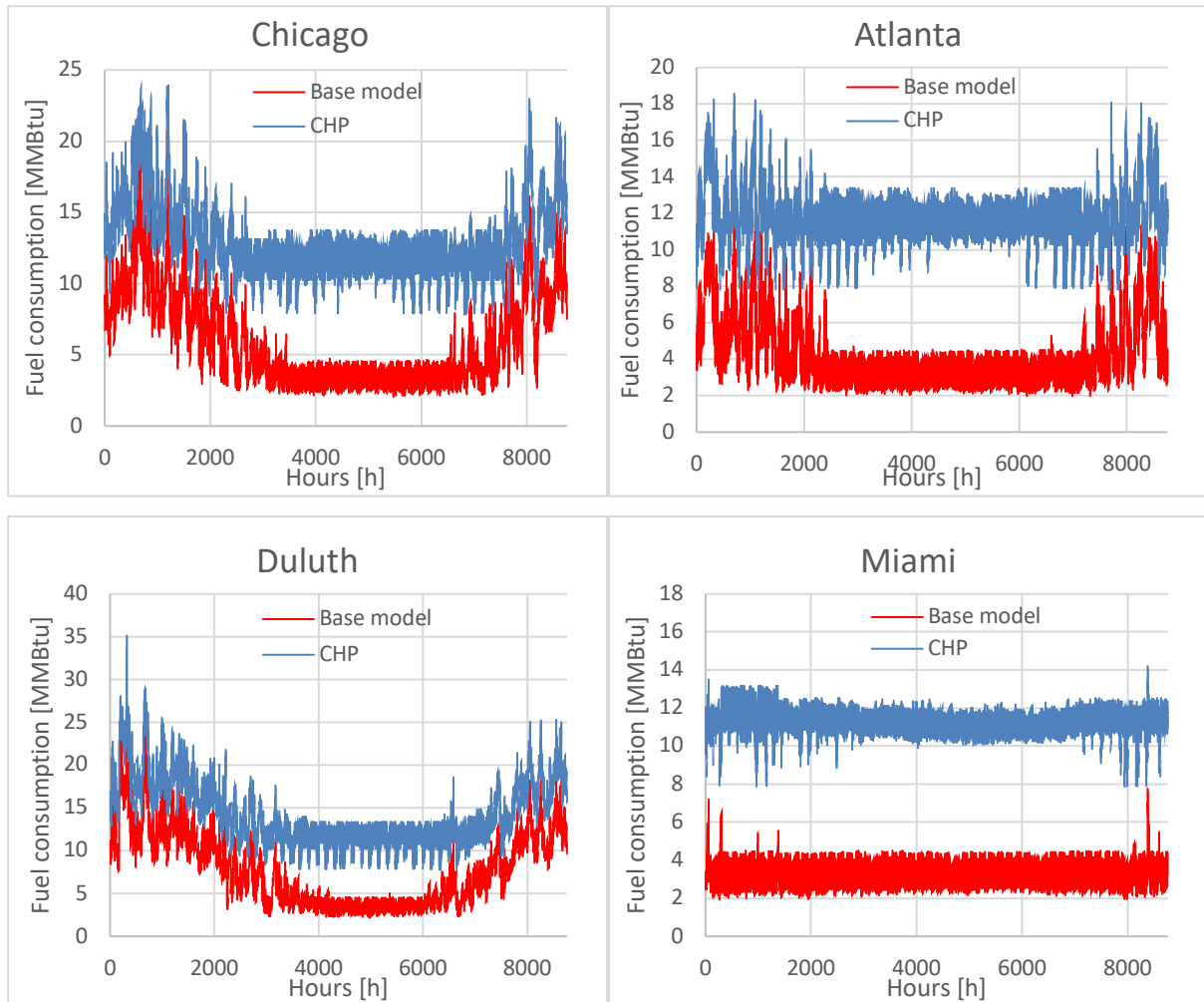


Figure 47: Base model fuel consumption vs CHP fuel consumption

The effect of the CHP system is also shown through the variation of the annual fuel consumption: the boiler consumption is lower than in the base model because, thanks to the heat recovered from the exhaust gases, it is possible to reduce the heat production from the boilers, proving that the system was modeled in a correct way. Obviously, higher is the percentage of heat demand satisfied by recovered heat, lower will be time the boilers need to run and, as a consequence, also their fuel consumption, and vice versa, as displayed in Table 6.

	<b>Chicago</b>	<b>Atlanta</b>	<b>Duluth</b>	<b>Miami</b>
<b>Reduction in boilers fuel consumption</b>	-63.8%	-80.3%	-52.4%	-91.1%

Table 6: Reduction in boilers fuel consumption in CHP systems

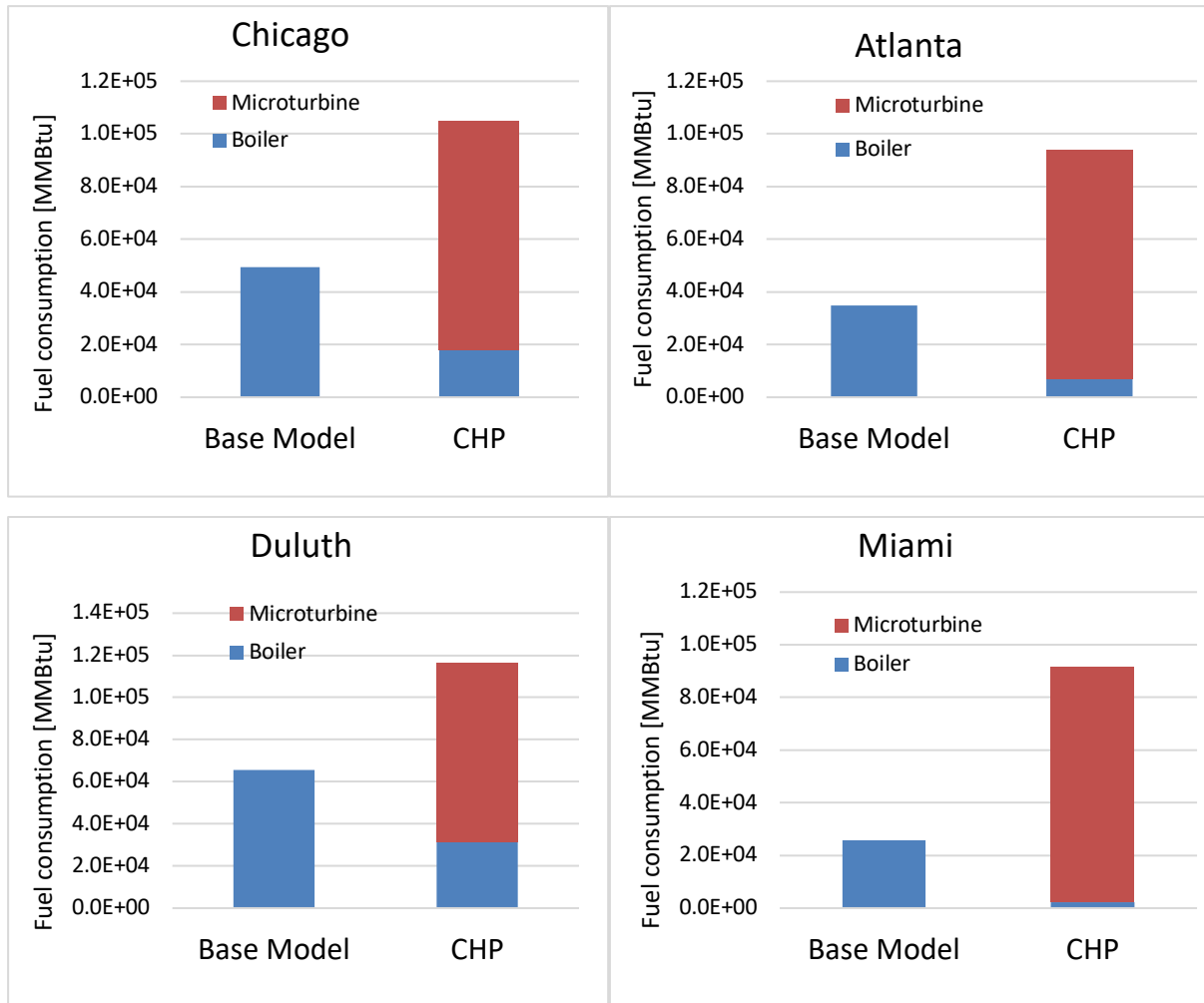


Figure 48: Annual fuel consumption, Base model vs CHP

### 6.3 CHP system coupled with TES

In the following paragraphs, for each location, are reported the graphs and results of the Excel models discussed in the previous chapter. As already mentioned, the tank volume has been varied between 0 [gal] and 60,000 [gal], in order to determine how the introduction of a TES system, and especially its size, influence a cogeneration and trigeneration plant.

By comparing hour-by-hour the heat recovered through the thermal storage and the heat stored in the tank, it's possible to study the storage operation. The charts provided are all related to the same volume equal to 20,000 [gal]. When the storage is charged and the boiler demand is not 0, the TES system provide energy and it empties. This happens mainly in autumn and spring when the amount of wasted heat is actually lower compared to the warmer months, but in

summer there is no request from the boilers. In fact, in this period, the tank is always full and remains unused, which from an energetic point of view is unprofitable, both because we have a large amount of available energy not exploited and because a large portion will be lost due to thermal losses. More are the fluctuations, better is exploited the storage. The only solution to this issue is to couple the storage with a CCHP system and to use the available heat also to satisfy the cooling demand; this option is analyzed in the next paragraph.

Between Chicago, Atlanta and Duluth, it's clear how in the second location the TES system is exploited in a better way, since it starts operating more often. As was shown in Figure 44 and 46, in Atlanta a considerable amount of heat is lost even in the months characterized by a higher demand from the boilers, instead in Miami even if there's a lot of wasted heat available, the boiler demand is so low that the storage is almost never used, which makes the trigeneration the only profitable solution. Certainly, in this case, a smaller storage would be more suitable, in fact the different volume will be compared. An intermediate volume, equal for all the locations, was chosen just to better show the heath fluctuations.

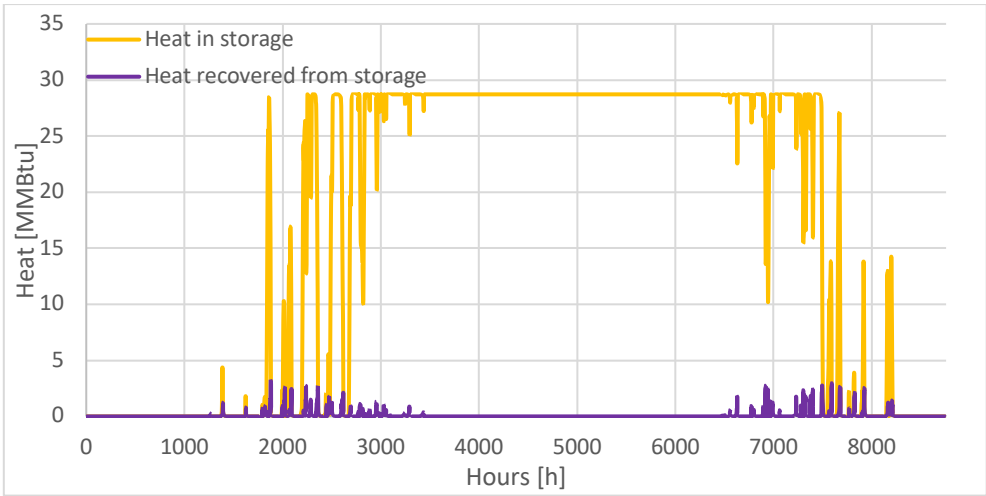


Figure 49: Storage operation, 20,000 [gal], *Chicago*

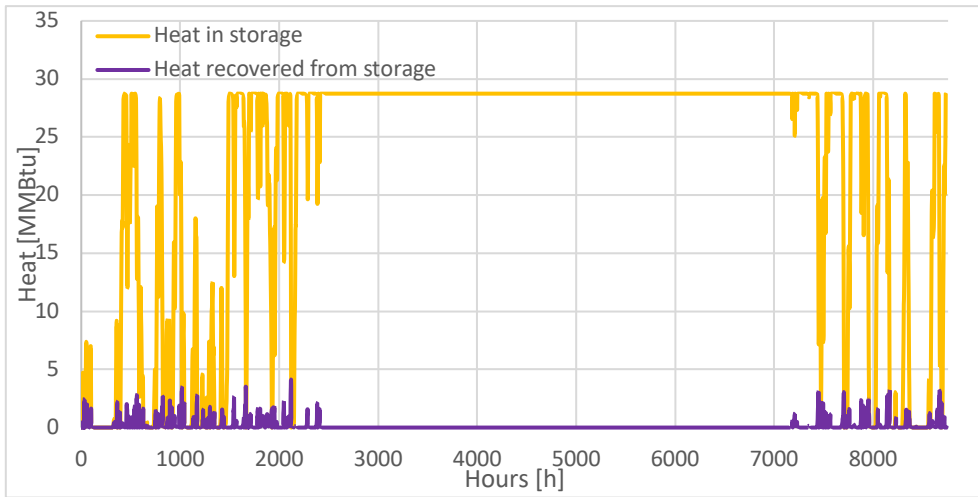


Figure 50: Storage operation, 20,000 [gal], *Atlanta*



Figure 51: Storage operation, 20,000 [gal], *Duluth*

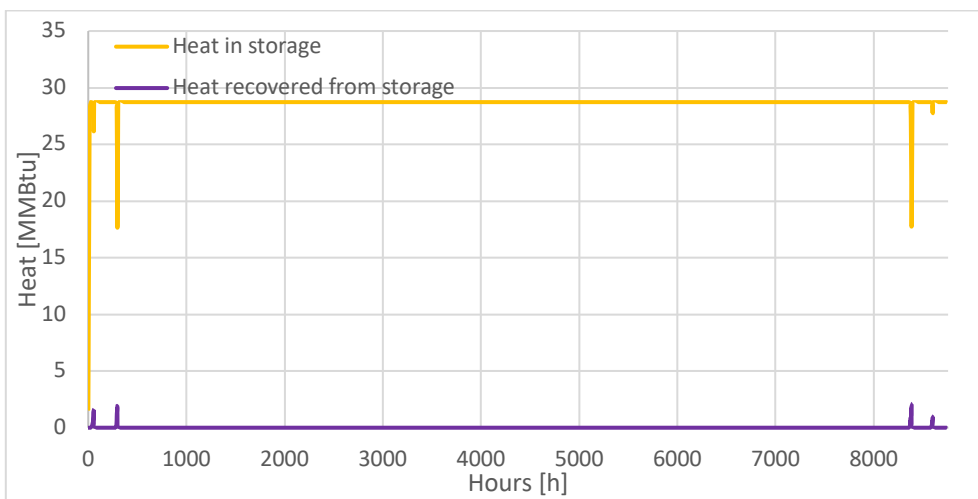


Figure 52: Storage operation, 20,000 [gal], *Miami*

To better show the improvements obtained in the different cogeneration plants, it helps to look at the boilers' operation and at the total heat recovered. For this analysis, the graphs provided were obtained considering the maximum volume of 60,000 [gal] in order to provide the best solution for each location. In this way it's possible to get an idea on the benefit of the thermal storage system. In Figure 53, 55, 57 and 59, the starting boiler demand of the CHP system is compared with the demand that would occur when the system is coupled with the storage. In the other graphs is provided the comparison between the hospital demand and the heat recovered in the two different layouts. From this, it's even more evident that warmer is the climate, more beneficial will be the introduction of such an equipment. As said before, Miami is excluded from these considerations, since its demand behavior is completely different from the other locations. In this case the facility heat demand is so low that even before the introduction of the thermal storage, the wasted heat was covering almost all of it. As a consequence, the improvements are minimal.

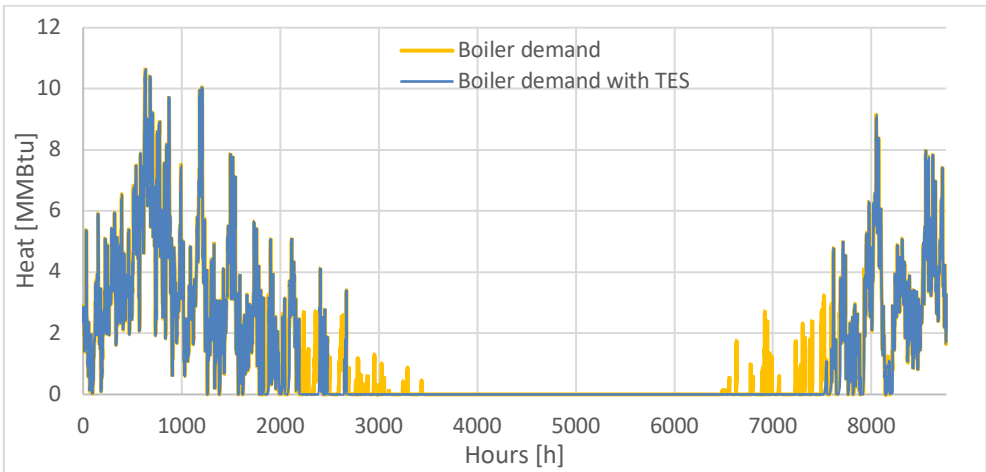


Figure 53: Boiler demand, 60,000 [gal], Chicago

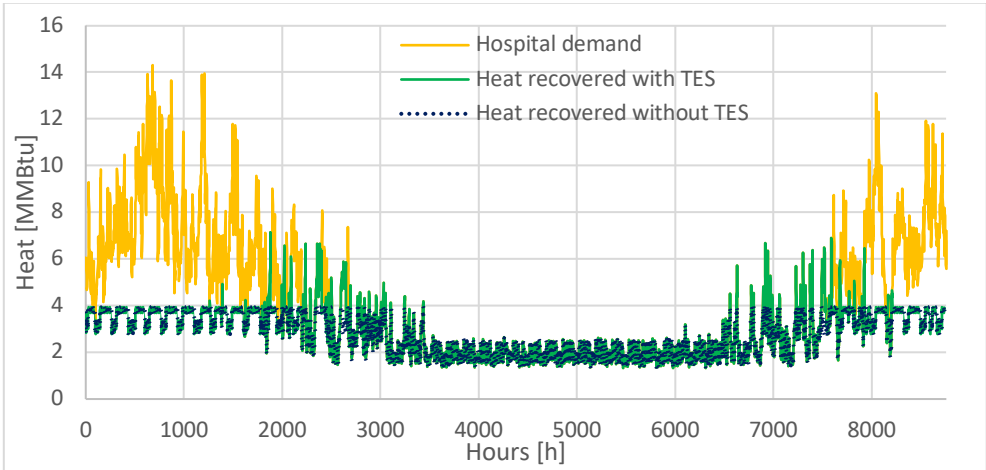


Figure 54: Recovered heat, 60,000 [gal], Chicago

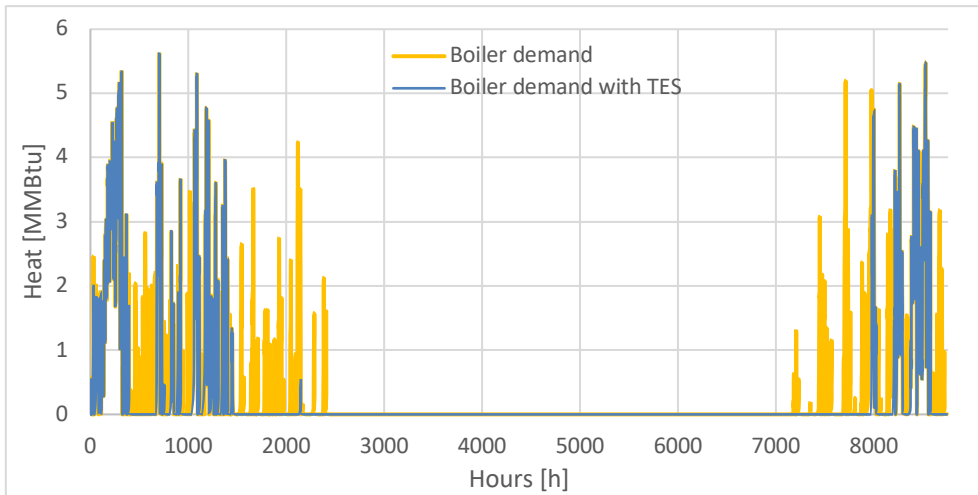


Figure 55: Boiler demand, 60,000 [gal], *Atlanta*

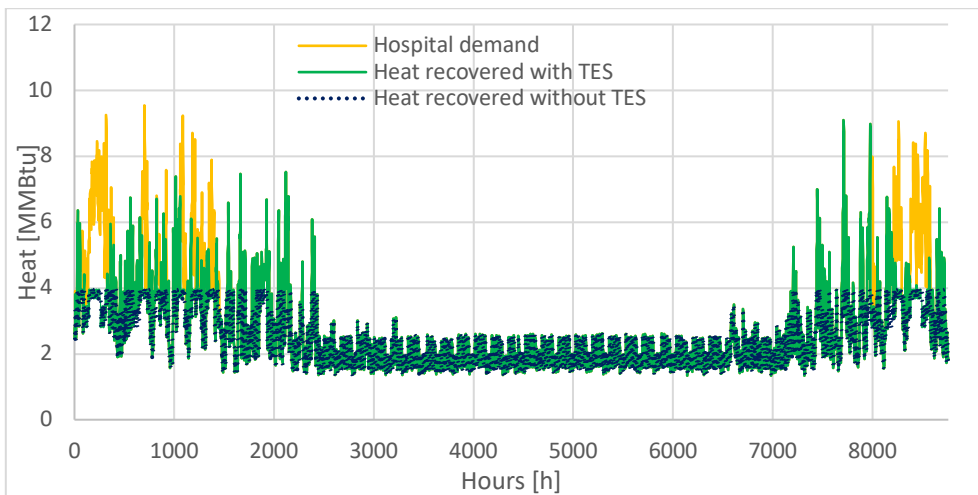


Figure 56: Recovered heat, 60,000 [gal], *Atlanta*

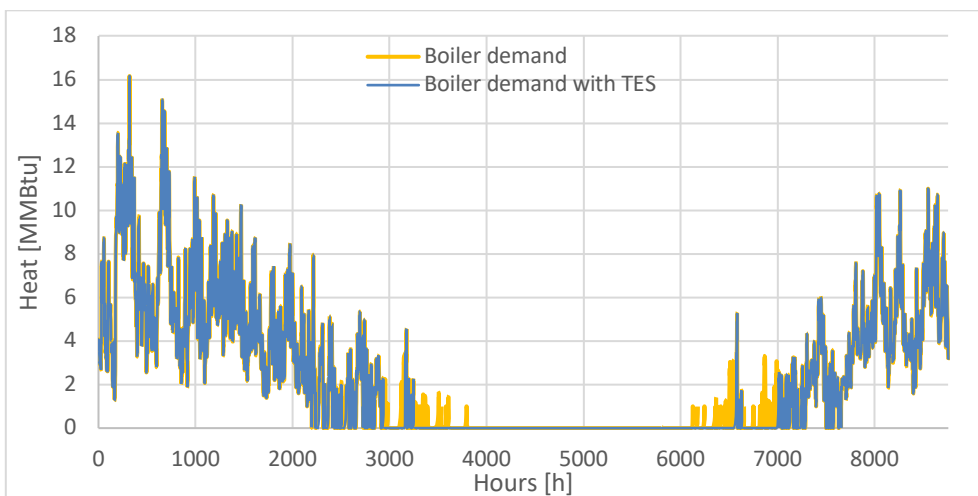


Figure 57: Boiler demand, 60,000 [gal], *Duluth*

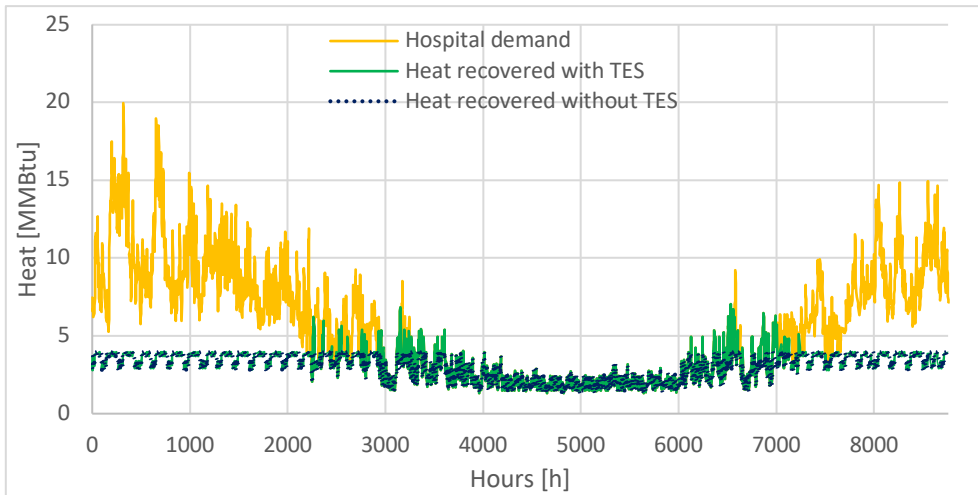


Figure 58: Recovered heat, 60,000 [gal], *Duluth*

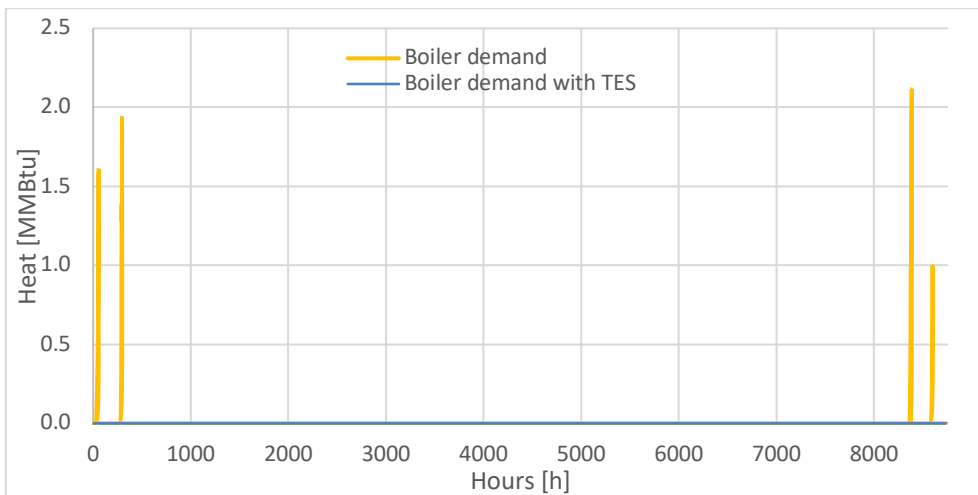


Figure 59: Boiler demand, 60,000 [gal], *Miami*

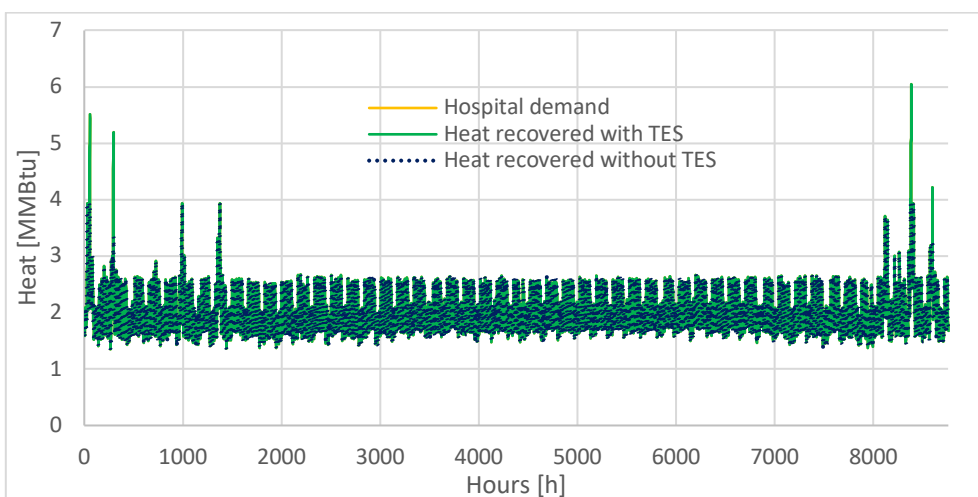


Figure 60: Recovered heat, 60,000 [gal], *Miami*

Lastly a study regarding the different tank size has been conducted. The results obtained for the different locations are represented in Figure 61 and listed in Table 7. It can be noticed how actually in the case of a hospital served by a CHP system, independently from the location of the facility, a TES system is not going to improve that much the operation of the plant. By looking at the curves' behavior, it makes no sense to work with very large sizes. In fact, with volumes greater than 20,000 or 30,000 [gal], the curves become almost constant and a large increase in size corresponds to a very small variation in recovered heat. In Miami there is almost no difference with or without storage: even if all the boiler demand is going to be satisfied through recovered heat, an increase of +0.1% is too low for the storage to make sense. The best percentage increase in recovered heat is measured in Atlanta, where the boiler demand is greatly reduced, meaning substantial savings. Obviously, a low ratio between recovered and recoverable heat means there is still a high amount of waste, so with a CCHP system it will be possible to exploit them and, maybe, to obtain a greater improvement of the whole plant.

	<b>Chicago</b>	<b>Atlanta</b>	<b>Duluth</b>	<b>Miami</b>
<b>Recovered heat vs Recoverable heat</b>	+1.3%	+2.3%	+1.1%	+0.1%
<b>Recovered heat vs Heat demand</b>	+1.2%	+3.1%	+0.7%	+0.1%
<b>Boiler demand</b>	-3.84%	-24.96%	-1.72%	-100%

Table 7: Comparison between the CHP system and the coupling between CHP and a 20,000 [gal] TES

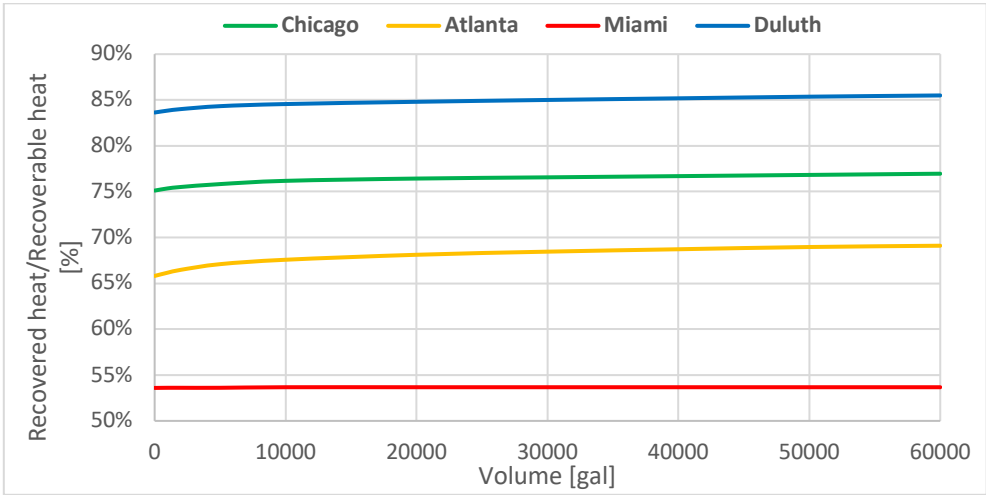


Figure 61: Comparison between Recovered Heat ratio for different TES volume

### 6.4 CCHP and TES systems

With same approach already used, the trigeneration system was analyzed by varying the size of the thermal storage and, in addition, also of the absorption chiller. For each location the different solutions have been compared in two figures. In the first graph, each curve shows the effect of a different cooling capacity of the absorption chiller in [MMBtu]; in the second one, the cooling capacity is on the x-axis and the different curves refer to different storage volumes in [gal]. The CHP caption stands for an absorption chiller characterized by a capacity equal to 0 [MMBtu]. As noticed before in the cogeneration analysis, above a certain value of TES volume, the variation in recovered heat become minimum and the curves start to overlap. The same behavior occurs with the absorption chiller cooling capacity. For both components there is a limit value related to the amount of wasted heat; above these thresholds all the available heat is recovered and the equipment starts to be oversized for the plant. Moreover, the graphs provided show how the same amount of recovered ratio can be reached by changing the dimension of both the components: it may be more convenient, depending on their prices, to work with a bigger storage and a smaller chiller or vice versa.

Regarding the absorption chiller size the behavior between the locations is similar. The best solution varies between 2 [MMBtu] for the warmer cities (Miami and Atlanta), to 2.5 [MMBtu] for Chicago and Duluth, where also a 3 [MMBtu] chiller could be accepted. Looking at Table 8, is evidenced how the best size for the chiller is in the range between 15 % and 25% of the maximum values of cooling demand requested by the facility. On the thermal storage size, the considerations made in the previous paragraph remain the same; the best solution for the first three locations is around 20,000 [gal]. From this condition on, the improvements are too small to justify a larger component. Regarding Miami, instead, the introduction of a tank to store the wasted heat is not so useful and a volume of 10,000 [gal] is enough. What really improves the operation of the plant in this case is the CCHP plant, since there is a lot of wasted heat and the cooling demand is almost constant during the whole year.

	<b>Chicago</b>	<b>Atlanta</b>	<b>Duluth</b>	<b>Miami</b>
<b>Max cooling capacity [MMBtu]</b>	12.43	15.86	11.29	14.45

Table 8: Maximum hospital cooling demand

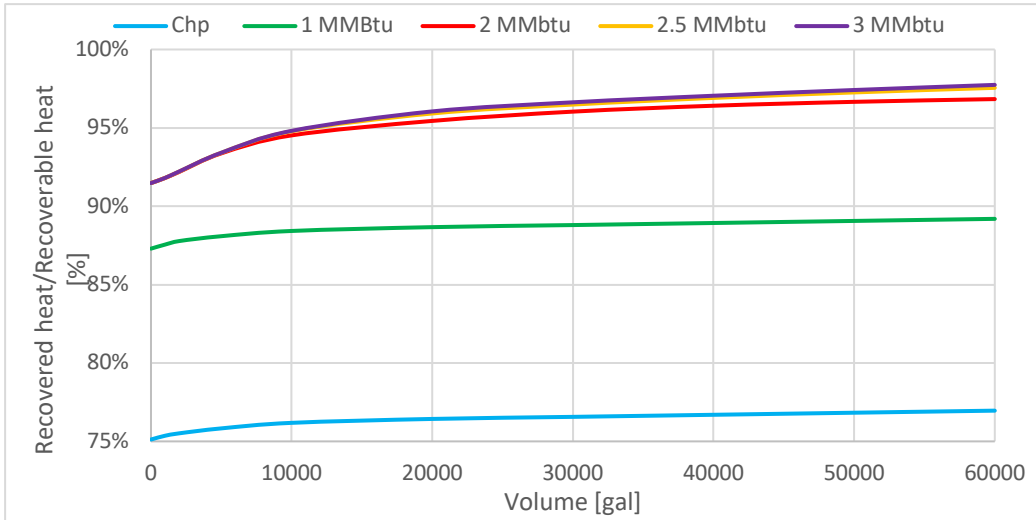


Figure 62: Recovered heat ratio for different chiller cooling capacity, *Chicago*

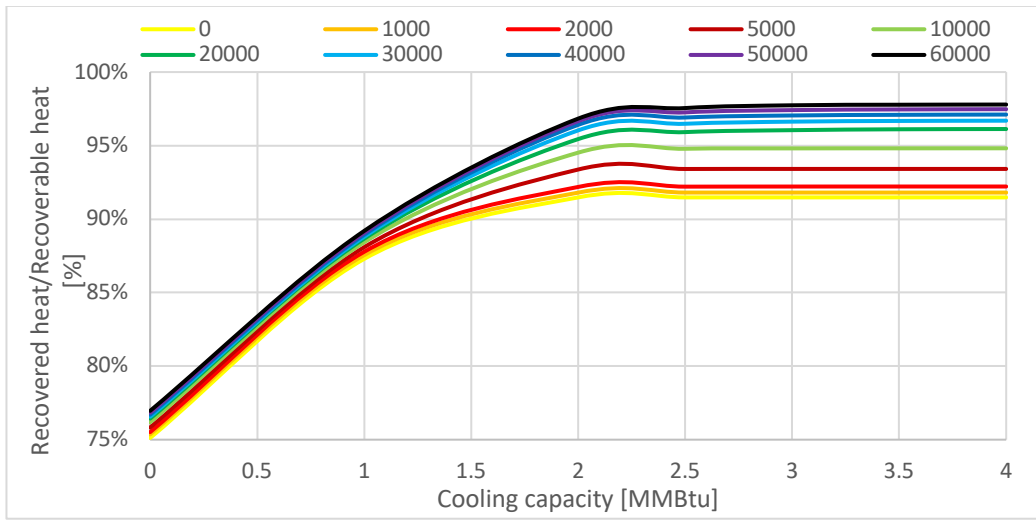


Figure 63: Recovered heat ratio for different TES volume, *Chicago*

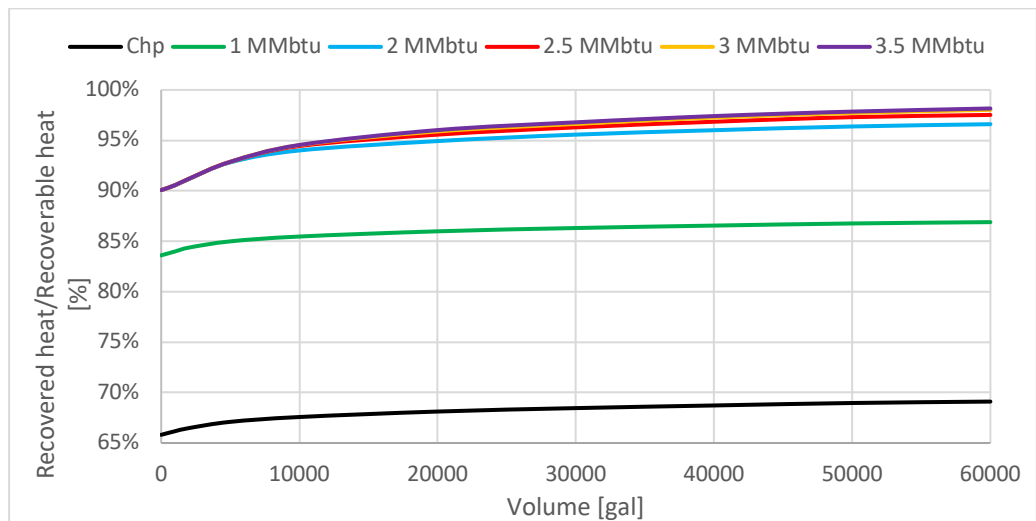


Figure 64: Recovered heat ratio for different chiller cooling capacity, *Atlanta*

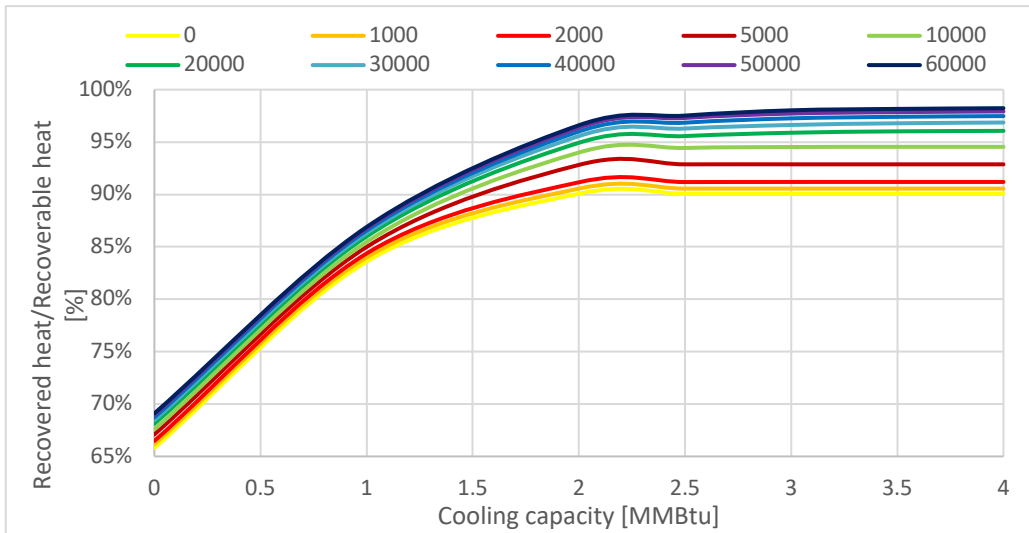


Figure 65: Recovered heat ratio for different TES volume, *Atlanta*

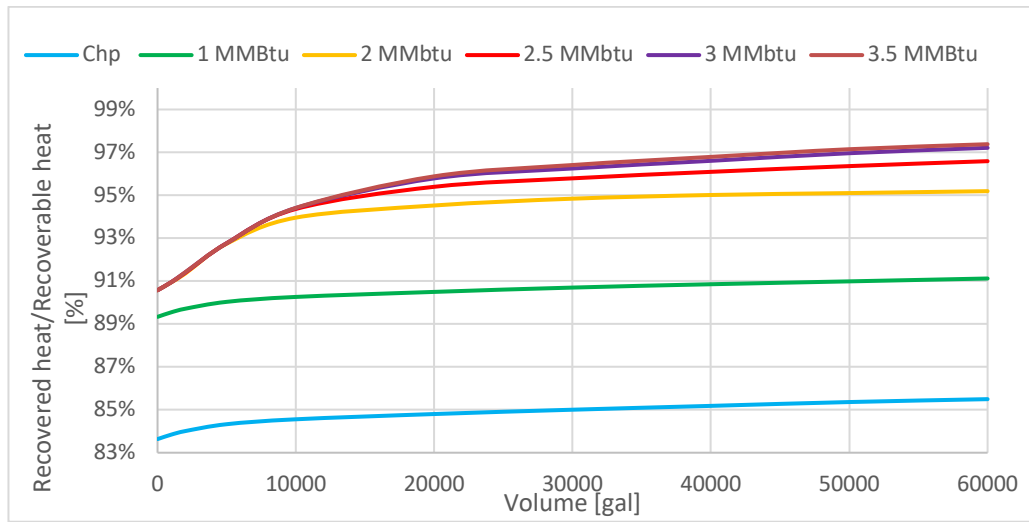


Figure 66: Recovered heat ratio for different chiller cooling capacity, *Duluth*

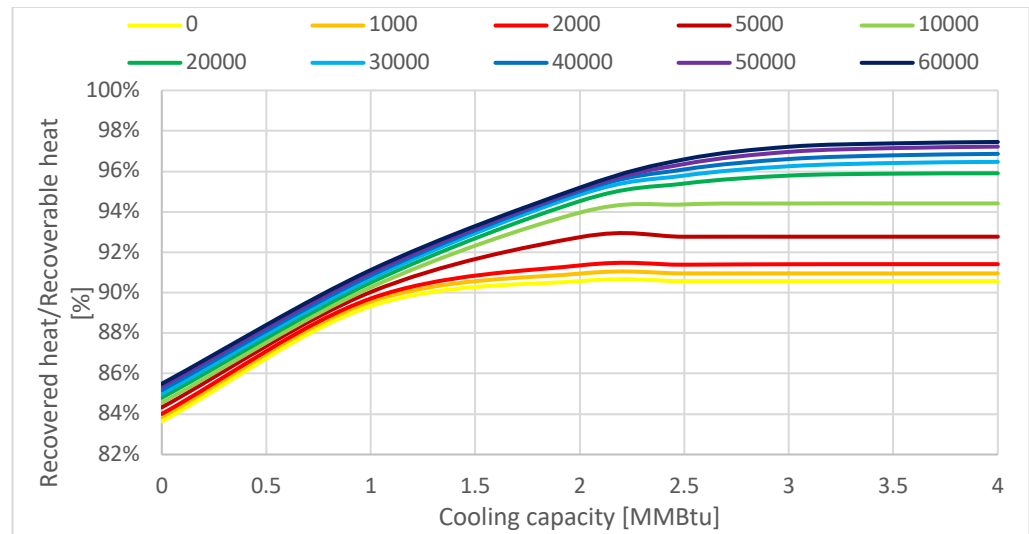


Figure 67: Recovered heat ratio for different TES volume, *Duluth*

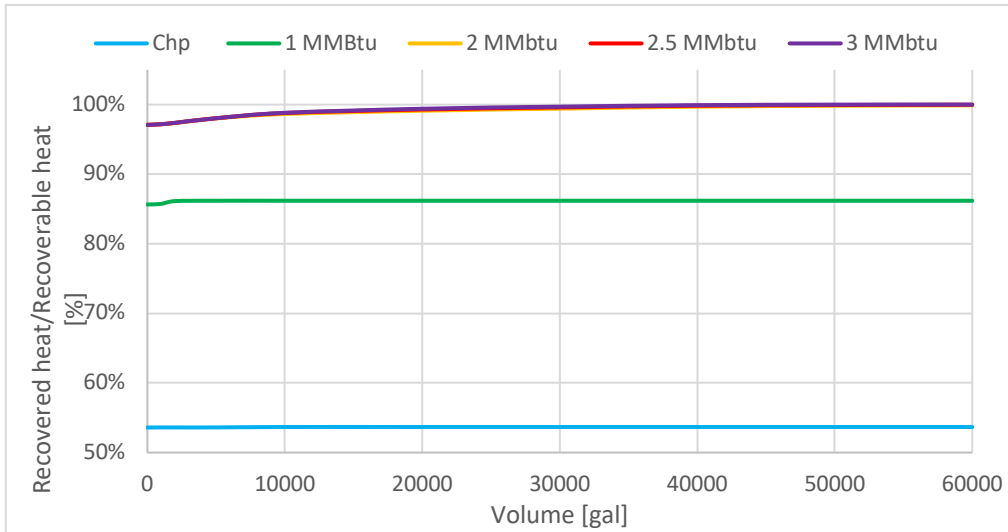


Figure 68: Recovered heat ratio for different chiller cooling capacity, *Miami*

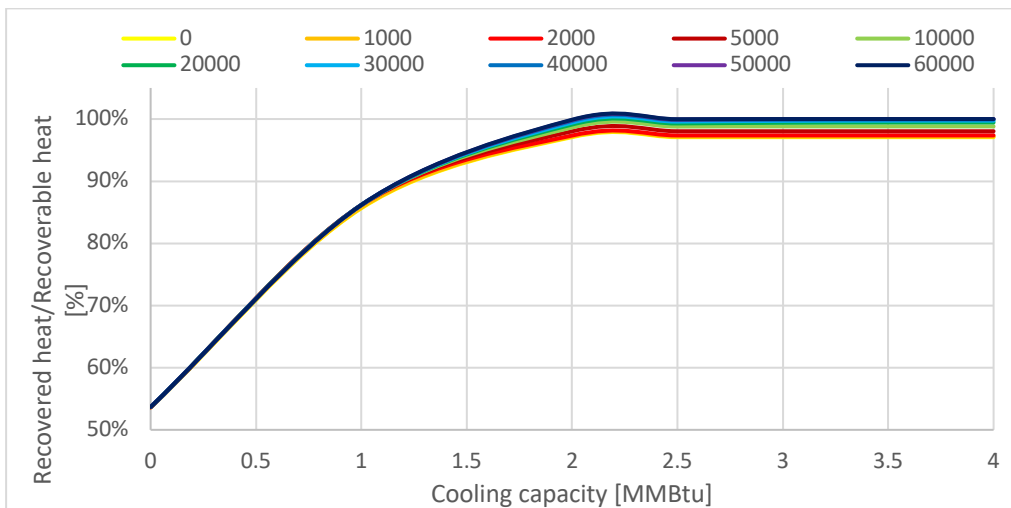


Figure 69: Recovered heat ratio for different TES volume, *Miami*

In Figure 70 is provided a comparison of recovered heat ratios to show how much is improving the system operation, by changing the plant from CHP to CCHP; so, no thermal storage is considered. As expected, and already analyzed, Miami, which is characterized by a steeper curve, is the city which benefit the most from this transaction, changing from a 53.6% ratio to a 97.1%, with a 2 [MMBtu] chiller. Clearly the other locations are in descending order, from the one with the highest cooling demand, Atlanta, followed by Chicago and Duluth. These three curves, after a certain value of chiller cooling capacity, reach a similar ratio. What happens in this graph, by increasing the storage volume, is that the Miami curve remains almost the same, while the limit value reached by the other cities comes closer to the Miami value.

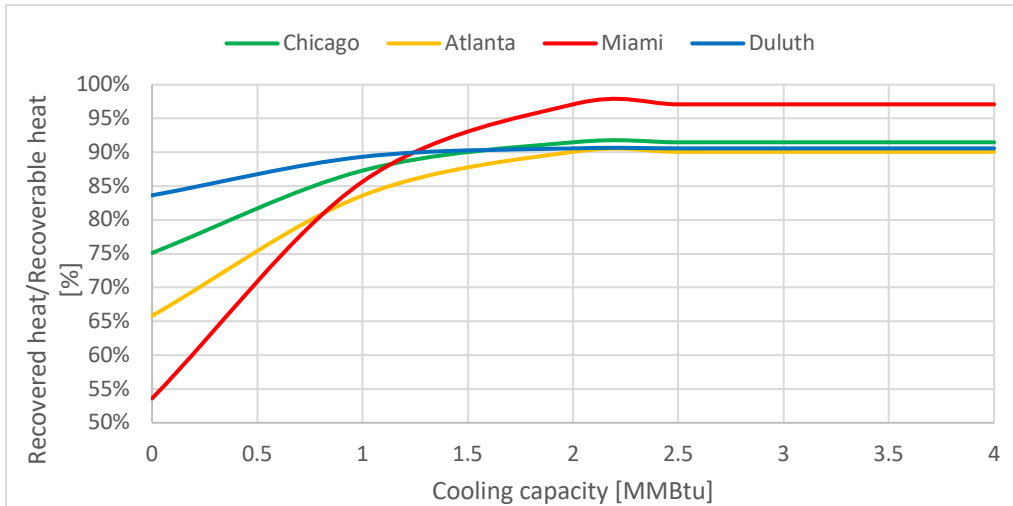


Figure 70: Comparison between recovered heat ratio without TES

Considering the best results obtained for thermal storage volume and absorption chiller capacity, which are resumed in Table 9, it is useful to take a further look to the storage operation, as done for the cogeneration plant, and to the cooling demand.

	<b>Chicago</b>	<b>Atlanta</b>	<b>Duluth</b>	<b>Miami</b>
<b>TES Volume [gal]</b>	20,000	20,000	20,000	10,000
<b>Absorption chiller capacity [MMBtu]</b>	2.5	2	2.5	2

Table 9: Best TES and Absorption Chiller sizes

It can be noticed how, thanks to the introduction of the absorption chiller, the operation of the TES is improved during the warmer months, since it's not unused anymore. In the warmer climates the cooling request in the summer will be obviously higher, so in these cases the tank is repeatedly emptied for a longer period. By looking at the cooling demand and at how much of this is covered by the absorption chiller and not by the electric chillers, it's understandable why in Miami the introduction of the storage is not that improving. While in the other climates, the cooling demand reaches a peak in the summer and then it decreases, becoming almost zero in the winter; in Miami, even if the maximum value reached is comparable with the others, the demand is high also during the rest of the year. Coupled with the fact that there is a lot of wasted heat always almost constant, a very large TES is of little use, since the absorption chiller can be fed with the heat available directly in that moment, without the need to store it and use it later. In Table 10, 11, 12 and 13 are provided the upgrades regarding the introduction of a

thermal storage in the trigeneration plant. In all cases, thanks to the coupling, we are able to recover almost all the recoverable heat, with an increase of around +4.5% thanks to the storage, expect Miami. The highest improvements regarding the satisfaction of the cooling demand through the absorption chiller and, as a consequence, the reduction in electric demand, due to the electric chillers, are measured in Duluth, explained by the lower cooling demand.

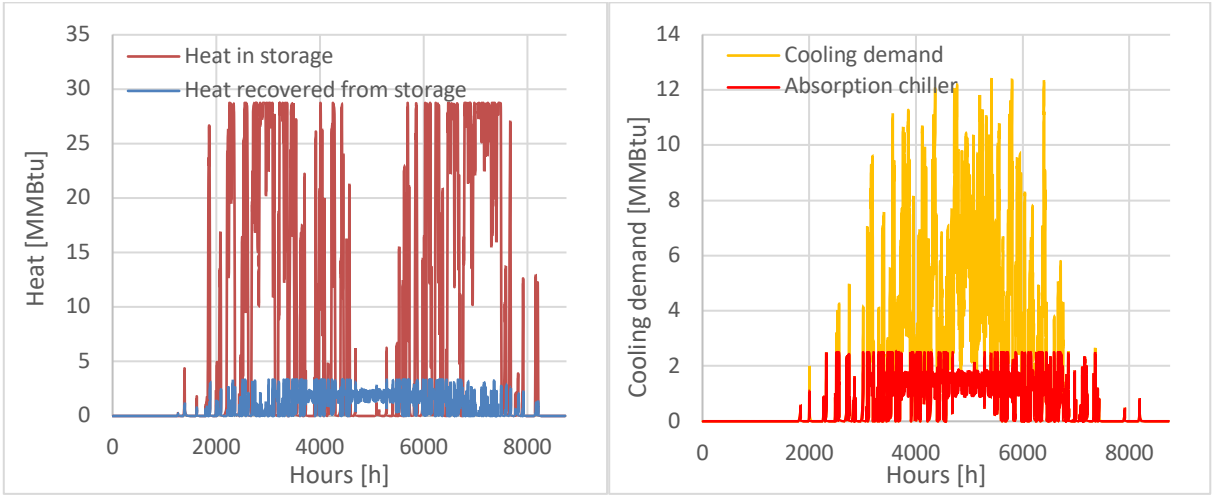


Figure 71: Storage operation and cooling demand covered by the absorption chiller, *Chicago*

	<b>CCHP</b>	<b>CCHP+TES</b>
<b>Recovered heat vs Recoverable heat</b>	91.5%	95.9%
<b>Absorption chiller vs Cooling demand</b>	28.4%	33.9%
<b>Electric reduction in demand</b>	-2.34%	-2.79%

Table 10: Comparison between the CCHP system and the coupling between CCHP and TES, *Chicago*

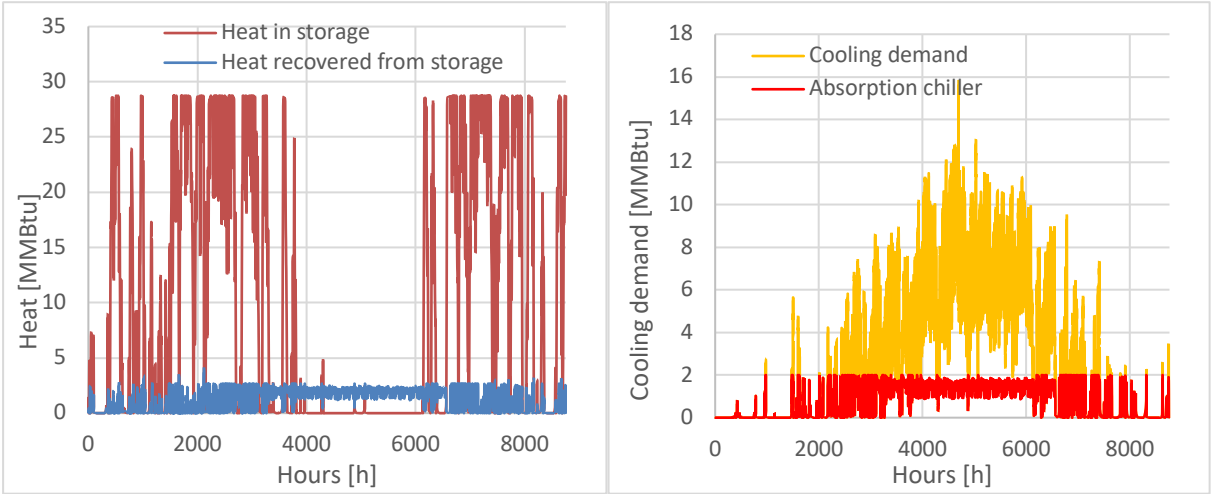


Figure 72: Storage operation and cooling demand covered by the absorption chiller, *Atlanta*

	<b>CCHP</b>	<b>CCHP+TES</b>
<b>Recovered heat vs Recoverable heat</b>	90.1%	94.9%
<b>Absorption chiller vs Cooling demand</b>	26.18%	29.03%
<b>Electric reduction in demand</b>	-3.32%	3.68%

Table 11: Comparison between the CCHP system and the coupling between CCHP and TES, *Atlanta*

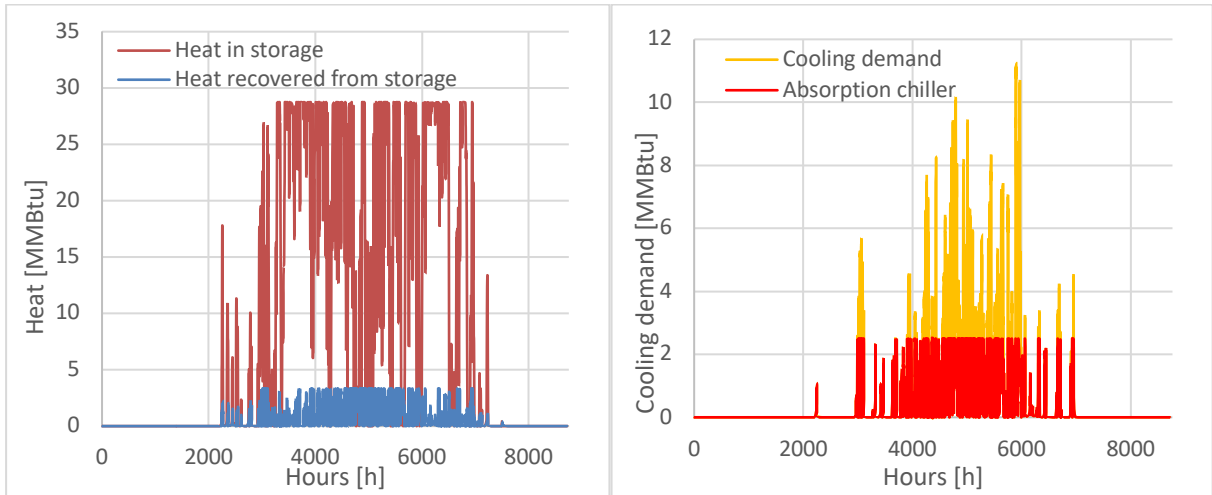


Figure 73: Storage operation and cooling demand covered by the absorption chiller, *Duluth*

	<b>CCHP</b>	<b>CCHP+TES</b>
<b>Recovered heat vs Recoverable heat</b>	90.6%	95.4%
<b>Absorption chiller vs Cooling demand</b>	38.24%	58.64%
<b>Electric reduction in demand</b>	-1.04%	-1.6%

Table 12: Comparison between the CCHP system and the coupling between CCHP and TES, *Duluth*

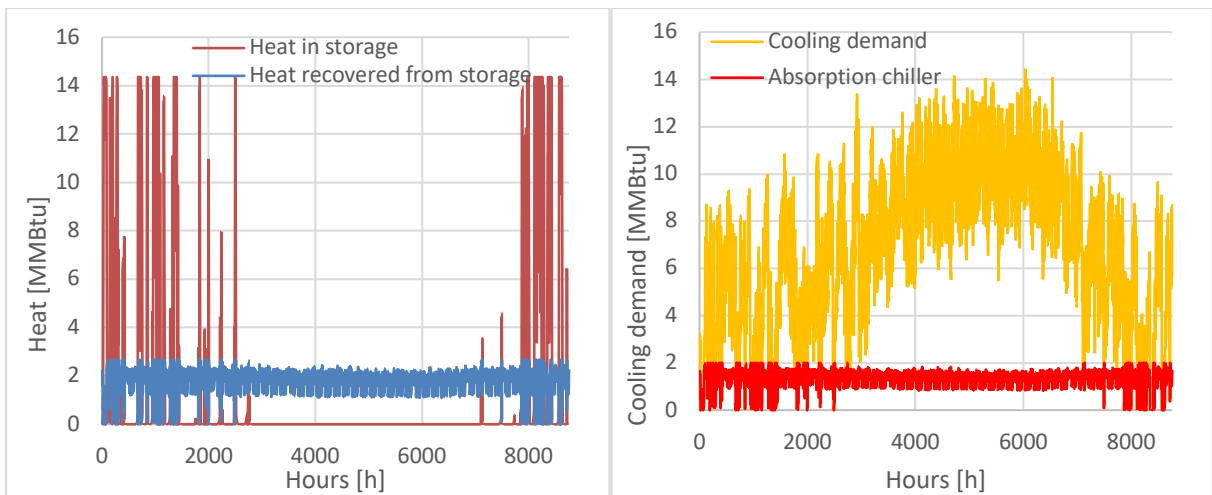


Figure 74: Storage operation and cooling demand covered by the absorption chiller, *Miami*

	<b>CCHP</b>	<b>CCHP+TES</b>
<b>Recovered heat vs Recoverable heat</b>	97.1%	98.6%
<b>Absorption chiller vs Cooling demand</b>	18.37%	18.99%
<b>Electric reduction in demand</b>	-4.96%	-5.13%

Table 13: Comparison between the CCHP system and the coupling between CCHP and TES, *Miami*

# 7 Emissions

As already stated, one of the benefits of cogeneration and trigeneration is the decrease in pollutant emissions, as shown in Figure 75. Thanks to the higher efficiencies, CHP and CCHP systems reduce the amount of total fuel required to provide the same energy demand to the user, and, moreover, they shift where that primary energy is used. The amount of fuel used at the site will generally increase, because an additional quantity is required to operate the CHP system compared to the previous equipment that would have been used to produce the thermal energy. Often project developers and policy makers need to quantify the fuel and CO<sub>2</sub> emissions savings of the new plants compared to the traditional separate heat and power production (SHP) [33].

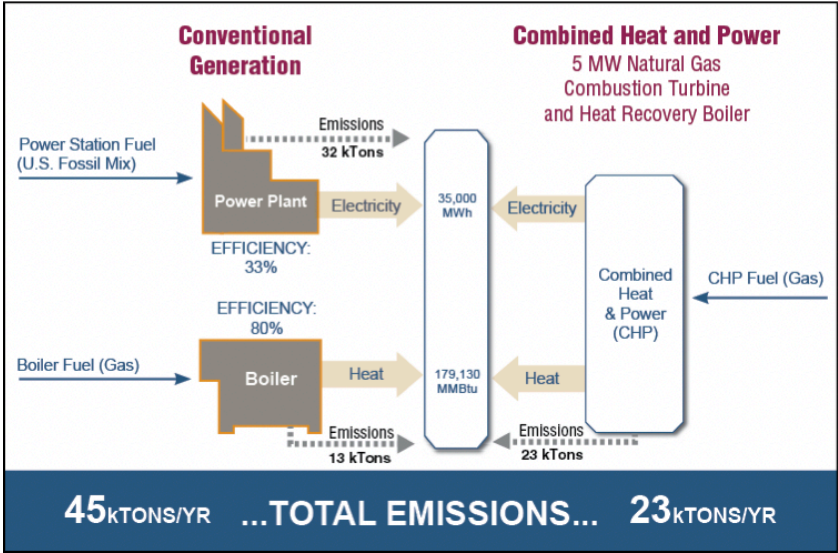


Figure 75: CO<sub>2</sub> emissions for SHP vs CHP [33]

The U.S. Environmental Protection Agency (EPA) lately has focused on how many states adopted and implemented energy efficiency (EE) and renewable energy (RE) programs, including energy storage policies which can lead to a reduction in greenhouse gases, especially on days characterized by high electric demand that typically coincide with poor air quality []. EPA’s *Roadmap for Incorporating Energy Efficiency / Renewable Energy Policies and Programs in State and Tribal Implementation Plans* [34] provides both basic and sophisticated methods, like the AVERT tool, to quantify the emissions changes resulting from such energy policies. While basic methods consist in a simple calculation, which is multiplying the electricity consumption by the emission rate of a specific pollutant in the region analyzed, the

AVERT system evaluates the magnitude and location of changes considering the hour-by-hour schedule of expected reductions in electricity demand for individual power plants, also known as electric generating units (EGUs) [34].

### 7.1 Average vs Marginal Carbon

The assessment of changes in generation and the consequent variations in emissions is characterized by several challenges. The balance between electricity supply, provided by several EGUs over a region, and demand varies hour by hour and seasonally.

When a customer is asking for more electricity, that doesn't cause all the power plants to evenly increase their production. In fact, within each region, system operators in each moment decide when and in what order to dispatch generation from the different EGUs and define the variable cost of production [34]. As power plants are dispatched by increasing cost, when the demand gets higher, the first plant to provide the electricity is the cheapest one that still has spare capacity, defined marginal power plant; as the load increases through peak hours, more expensive units are brought online [35], as described in the so-called "Bid Stack" represented in Figure 76.

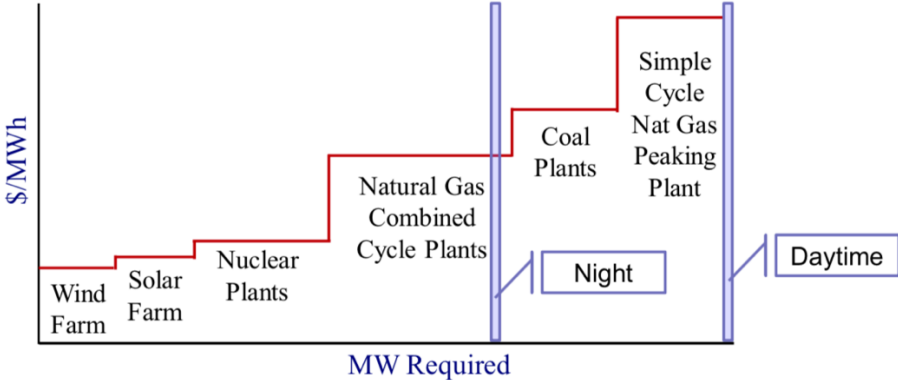


Figure 76: Bid Stack and marginal plants [35]

The lowest-cost generators, which constitute the baseload, are nuclear and hydroelectric plants; they operate continuously whenever they are available. Coal generation used to be the next operating source of power largely used for baseload plants; now efforts are being made to cut down on its application. Natural gas and oil-fired systems typically have the highest operating costs, so they are used to meet peaking loads, except natural gas combined cycle plants,

characterized by lower costs and exploited for intermediate loads. Usually the marginal plants consist of system capable to react fast to demand variations, such as gas turbine.

Where the grid is “on the margin” depends on the season, hour and circumstances This will define not only the hourly price, but also the marginal CO<sub>2</sub> intensity [35]. The marginal carbon defines how much added carbon is going to be put out in the next MWh of demand. A different generation in different times of the year affects the carbon output at the marginal carbon rate. To evaluate it are required hourly data, both regarding generation and emissions, for an entire year from every power plant in US or in the region considered. These details are provided by EPA AVERT system, which allows to enter an energy profile and comes up with the carbon savings.

Another factor influencing the margin is how the regional generation is subdivided. The grid generation and CO<sub>2</sub> emissions with the resource subdivision, for the four regions considered, are provided below. In general, the emissions follow the grid load behavior, but the region “Bid Stack” has a great impact on the magnitude of the marginal carbon. The peaks are usually satisfied with more expensive and polluting plants. Moreover, a higher nuclear percentage as baseload, as in Chicago or Atlanta regions, allows to keep down the emissions, while in Duluth the CO<sub>2</sub> almost overlap with the generation. In Florida the electric production is lower and more constant during the year due to the climate, as a consequence the natural gas plants are mainly for baseload and the emissions remain lower. The generation and emissions from the grid prove how important it is to consider the marginal carbon when we want to evaluate the real impact of a new plant on the environment. In fact, both the time of the day and the of the year affect the type of power plant in operation and, as a consequence, the CO<sub>2</sub> produced.

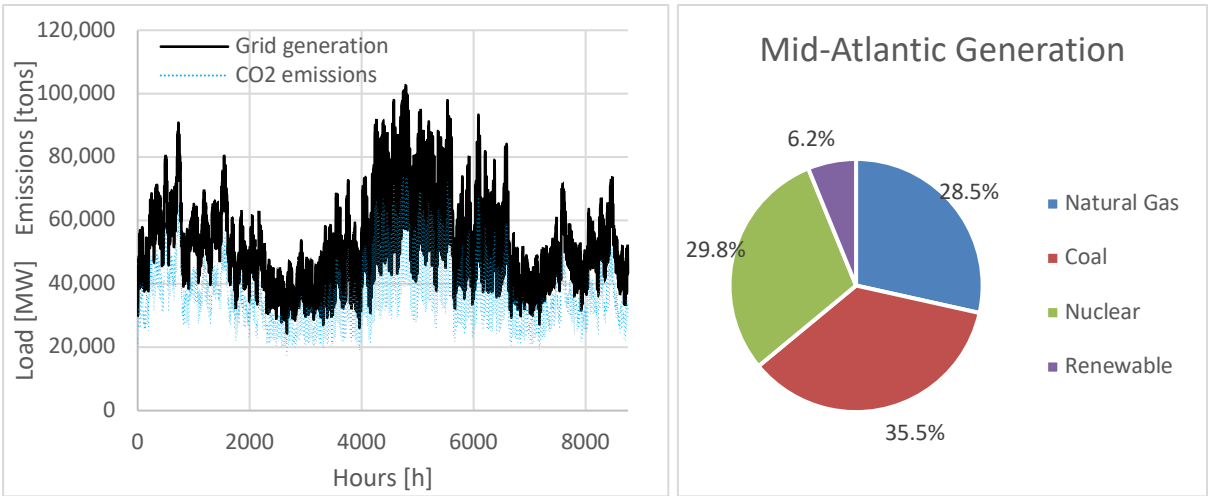


Figure 77: Mid-Atlantic grid generation and emissions

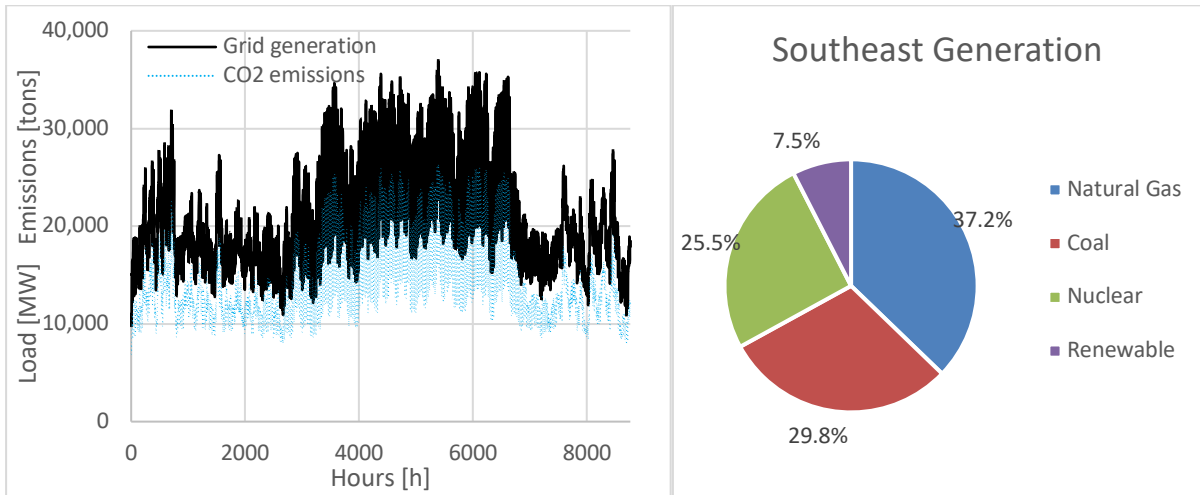


Figure 78: Southeast grid generation and emissions

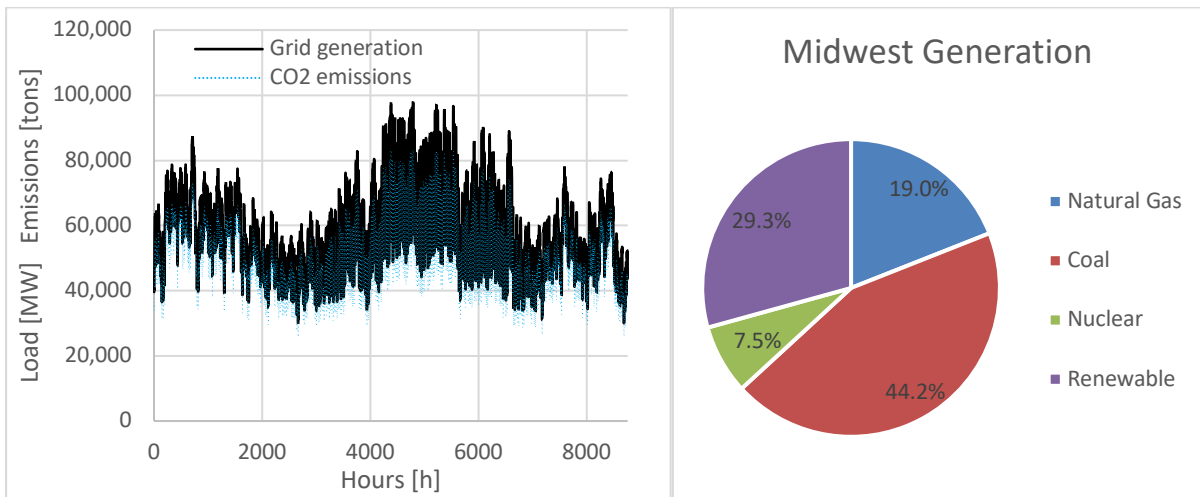


Figure 79: Midwest grid generation and emissions

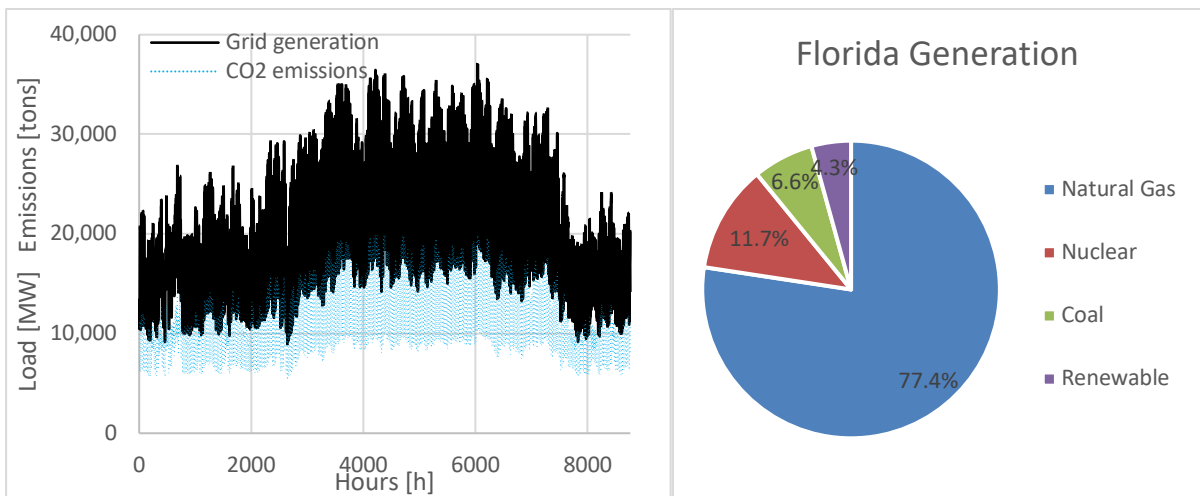


Figure 80: Florida grid generation and emissions

The other basic method mentioned above is based on the average emission factor. The average carbon is defined as the total CO<sub>2</sub> emissions of the grid load divided by the total electricity generation over a year [36]. Both national and regional factors are available. This evaluation makes the implicit assumption that each decrease in generation is evenly distributed over all the facilities, which is not in line with the actual operation of electricity markets.

The difference in the evaluation of emissions, by taking into account average or marginal carbon, is described by the Bid Stack, represented by the blue curve in Figure 81. Given a certain grid load, the marginal carbon curve it's much steeper than the average carbon line, meaning that the marginal carbon for the next MW added to the load is much more intense than the average one. As a consequence, the actual emission reduction is much higher than the value that would be incorrectly obtained by applying the average emission factor. This is why the marginal carbon is the only factor that should be used to review CO<sub>2</sub> intensity for energy use alterations, while the average factor should be just used to review national policies and overall progress [35].

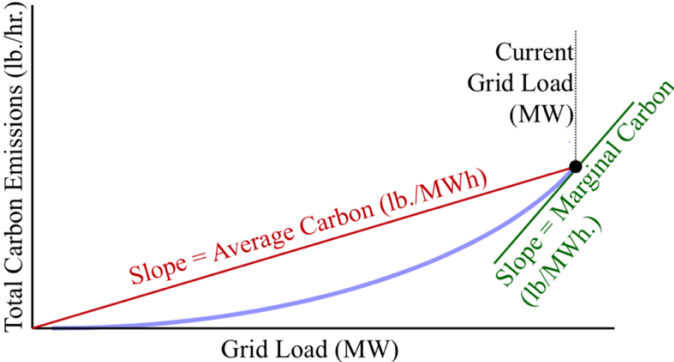


Figure 81: Bid Stack in term of carbon [35]

### 7.2 AVERT system

The AVOIDed Emissions and geneRATION Tool (AVERT), developed by Synapse Energy Economics Inc. under contract to EPA’s Climate Protection Partnerships Division and first released in 2014, is a free tool that allows to estimate the magnitude and location of emissions changes resulting from different types of energy policies within the United States, divided in 14 regions representing electricity markets. It is frequently used by quality planners to incorporate those impacts into National Ambient Air Quality Standards (NAAQS) State Implementation Plans (SIPs) [33]. Specifically, AVERT simulates hourly variations in sulfur

dioxide (SO<sub>2</sub>), nitrogen oxides (NO<sub>x</sub>), carbon dioxide (CO<sub>2</sub>), which this analysis is focused on, and particulate matter with diameter of 2.5 microns or less (PM<sub>2.5</sub>).

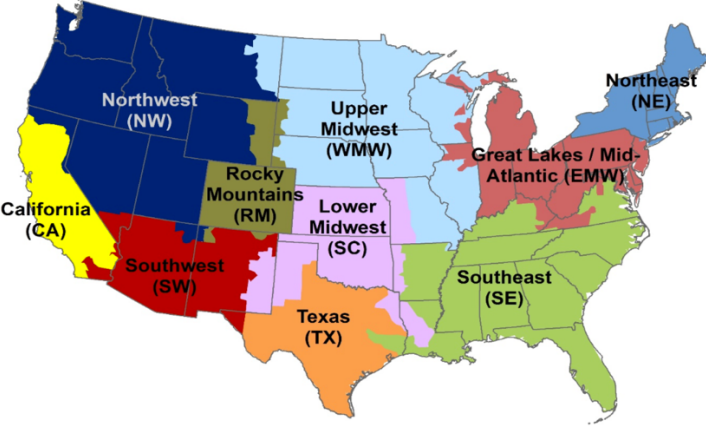


Figure 82: AVERT electricity market regions [33]

In AVERT’s Excel-based Main Module, users can manually enter hourly impact data consisting of 8760 values representing MWh saved from energy programs. Positive values represent displacements. Using these inputs, the system captures the actual historical behavior of EGUs’ operation to predict how much each plant will change its generation output and emissions as compared to the base year scenario without the program. The difference between the results obtained for the base year load and for the same year adjusted including the new energy profile is the change in emissions. The outputs are provided in tables, graphs and maps which show regional, state and county level variations. A brief procedure on how to set the AVERT Main Module can be found in Appendix A, while the methodology used for the different configurations is described in the next paragraph.

### 7.3 Emissions evaluation method

In order to quantify the fuel and carbon dioxide savings, both electric and thermal outputs must be taken into account. The CHP system’s thermal output is going to displace the fuel and the emissions related with the on-site fired boilers, and the microturbine power output displaces the

grid electricity. In addition, in the case of CCHP, the absorption chiller is going to replace the electric chillers and, thus, is going to further reduce the demand from the grid.

Starting from the eQuest<sup>®</sup> fuel consumption hourly data for the boilers and microturbine, in case of CHP and CCHP systems, it is possible to evaluate the corresponding CO<sub>2</sub> emissions for each configuration. Since the fuel used is natural gas the conversion emission factor is equal to 116.9 [lb/MMBtu]. When a thermal storage is added, the boiler consumption and, as a consequence, the emissions will decrease. Instead, for the CCHP system the microturbine consumption will be lower due to the lower demand.

Regarding the electric outputs two different analysis has been made to compare the results. In the first case the AVERT Main Module is used to obtain the marginal carbon emissions. The Regional Data Files uploaded for the four different regions, listed in Table 14, refers to 2019 data, the most recent year available. For the base hospital model, the electricity is totally delivered by the grid (SHP plant), so to get the emissions related to that production, the electric demand is set as input and compared to the case of no-load. In the other cases the input column is the microturbine production in [MW]: the Excel tool will return as output the variation in CO<sub>2</sub> compared to the Regional Fossil Load, which means the reduction obtained thanks to on-site production. To evaluate the marginal carbon, these values should be subtracted from the base hospital initial emissions. For the CCHP configuration, the new turbine production has to be considered, taking into account the different electric input required by the electric chillers. The second type of electric analysis is based on the concept of average carbon. The Main Module also provides the annual results with regional generation and total emissions, therefore the average emission rates in [tons/MWh], reported In Table 14. For this more basic evaluation, it is sufficient to multiply the factor of the region by the electricity bought from the grid. In the case of basic hospital, it will be the total demand, while in the other configurations it will be equal to the difference between the demand and the microturbine production.

	<b>Chicago</b>	<b>Atlanta</b>	<b>Duluth</b>	<b>Miami</b>
<b>Region</b>	Mid-Atlantic	Southeast	Midwest	Florida
<b>Average emission factor [tons CO<sub>2</sub>/MWh]</b>	0.691	0.682	0.863	0.545

Table 14: Average emission factor for analyzed regions

Finally, the two different total emissions are obtained as the sum hour-by-hour of the natural gas and of the electric contribution, one taking into account the marginal carbon and the other the average.

## **7.4 Results**

In this section are provided and compared the results obtained from AVERT system.

The CO<sub>2</sub> emitted due to the natural gas burnt for the boilers' and microturbine's operation is not reported since it follows exactly the fuel consumption behavior, expect for the conversion factor. In comparison with the base model, in the CHP and CCHP systems the CO<sub>2</sub> from the fuel is going to increase because of the prime mover. The addition of a thermal storage helps to decrease a little the fuel consumed by the boilers.

As explained above, the carbon emissions due to the electric load have been evaluated according both to marginal carbon and to average carbon. Then, starting from the value obtained, two total emissions graphs have been plotted. For each of the four locations are reported the graphs for both approaches to better understand the difference between the methods. While the basic hospital curve (SHP) is easily distinguishable, the other configurations tend to overlap; they were all reported anyway to show the improvements. Through such an hourly analysis, it's really clear how using the average carbon for an environmental impact assessment is going to provide unrealistic results. Obviously, the emissions curves due to electric production tend to be more uniform and this is going to impact the total emissions behavior. Not only are not taken into account the peak of generation, which can affect the electric purchase decision, but also the total annual CO<sub>2</sub> reduction is going to be influenced.

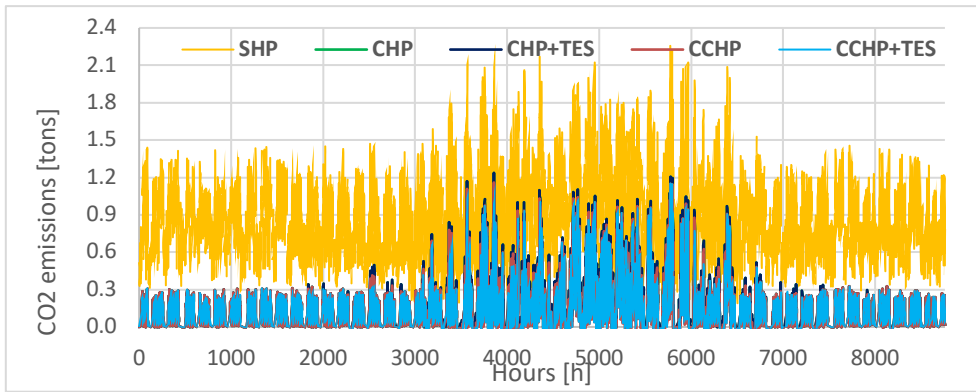


Figure 83: Marginal carbon due to electric production, *Chicago*

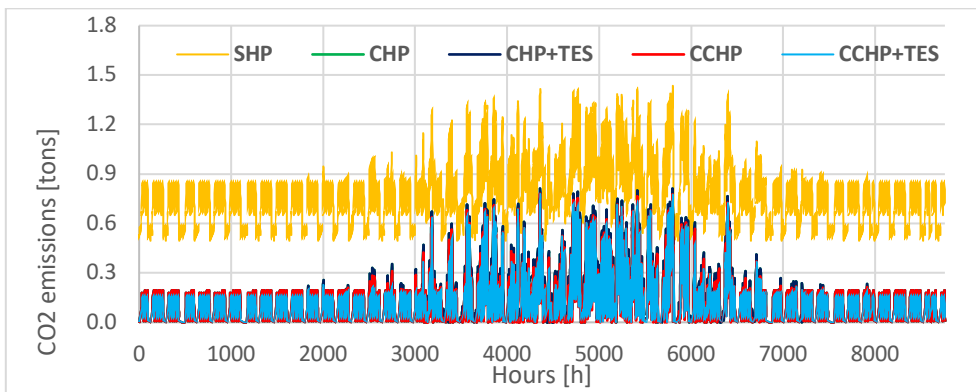


Figure 84: Average carbon due to electric production, *Chicago*

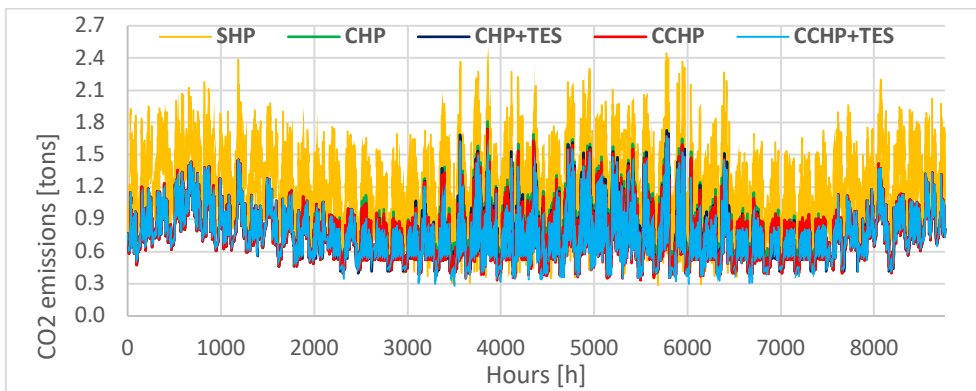


Figure 85: Total marginal emissions, *Chicago*

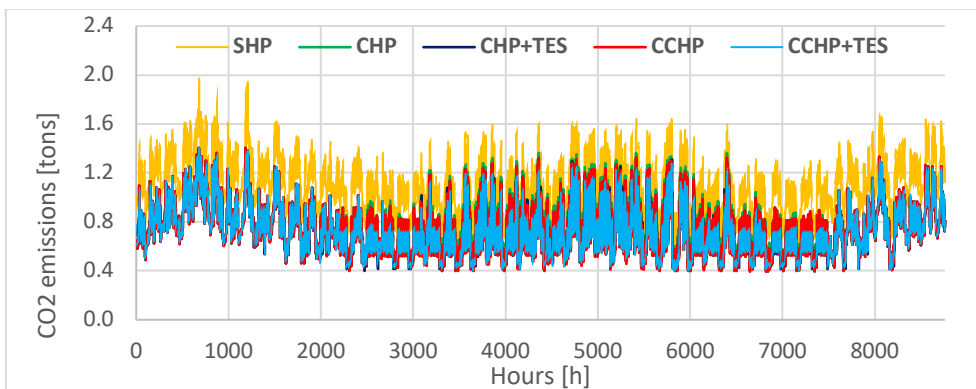


Figure 86: Total average emissions, *Chicago*

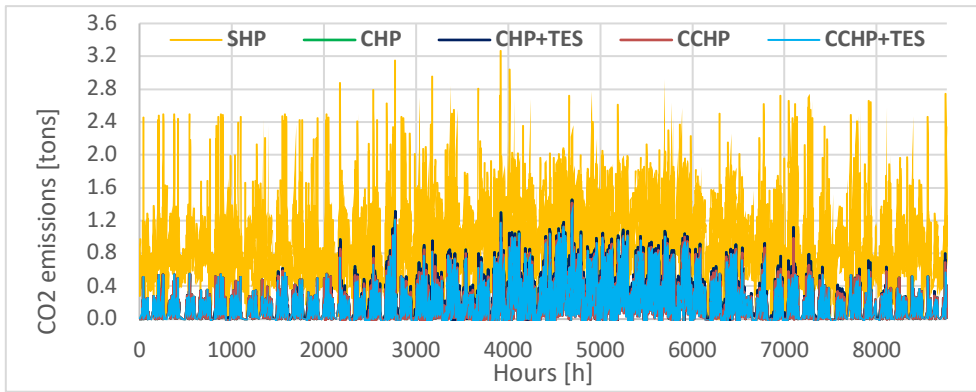


Figure 87: Marginal carbon due to electric production, *Atlanta*

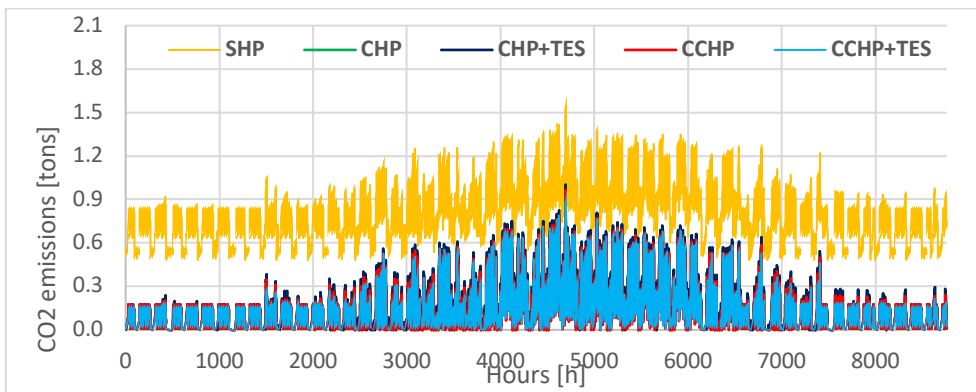


Figure 88: Average carbon due to electric production, *Atlanta*

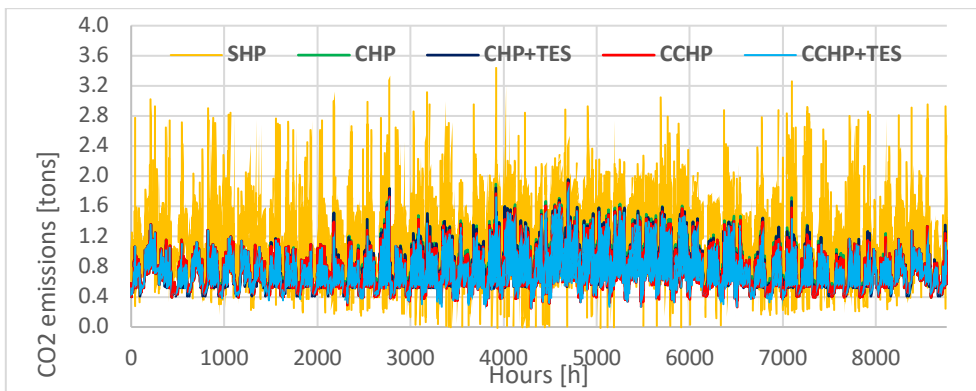


Figure 89: Total marginal emissions, *Atlanta*

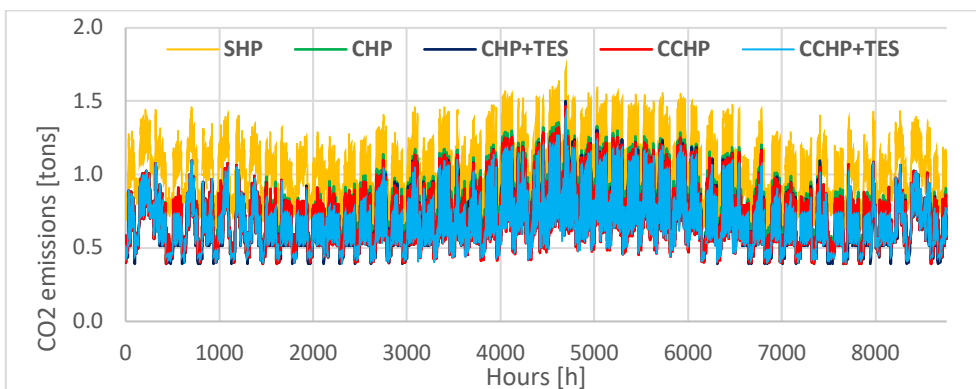


Figure 90: Total average emissions, *Atlanta*

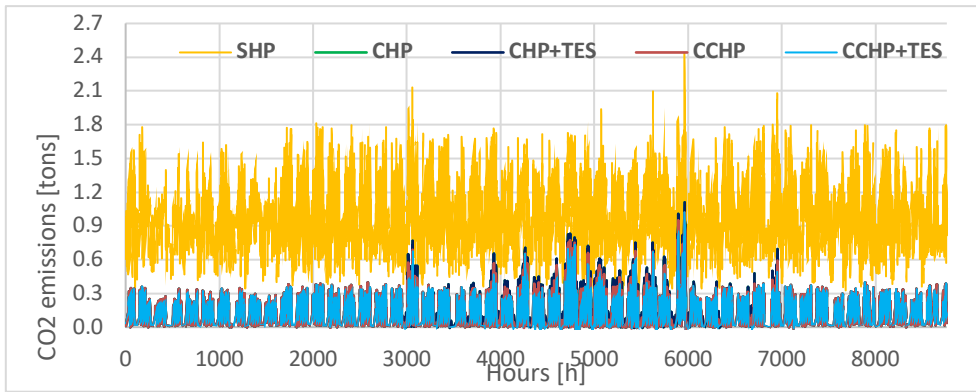


Figure 91: Marginal carbon due to electric production, *Duluth*

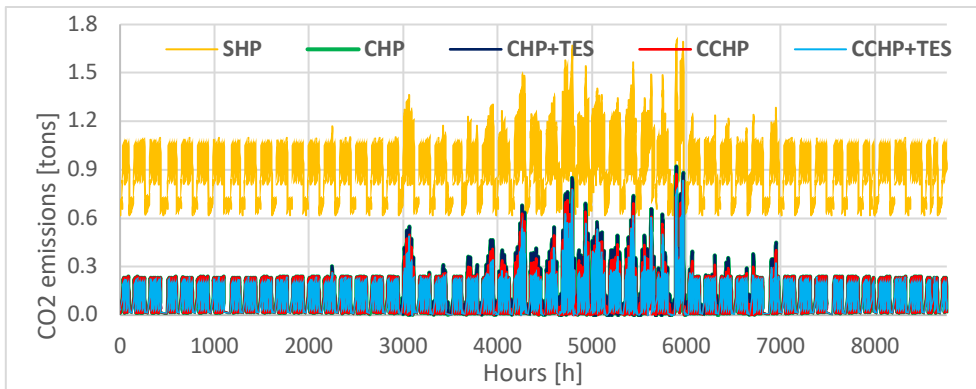


Figure 92: Average carbon due to electric production, *Duluth*

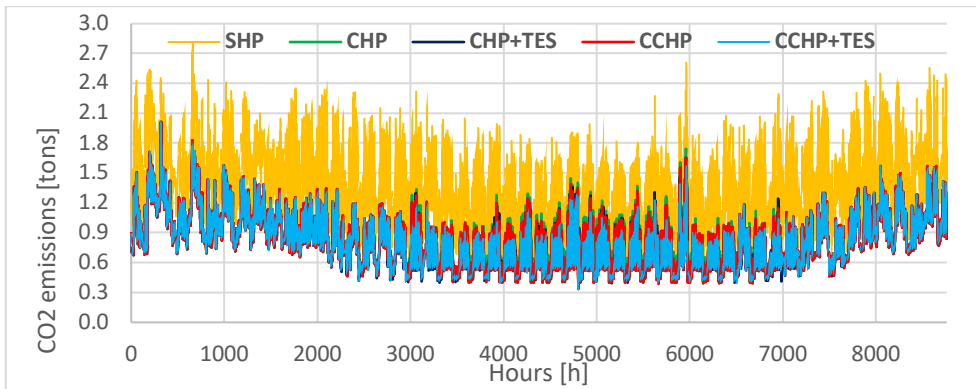


Figure 93: Total marginal emissions, *Duluth*

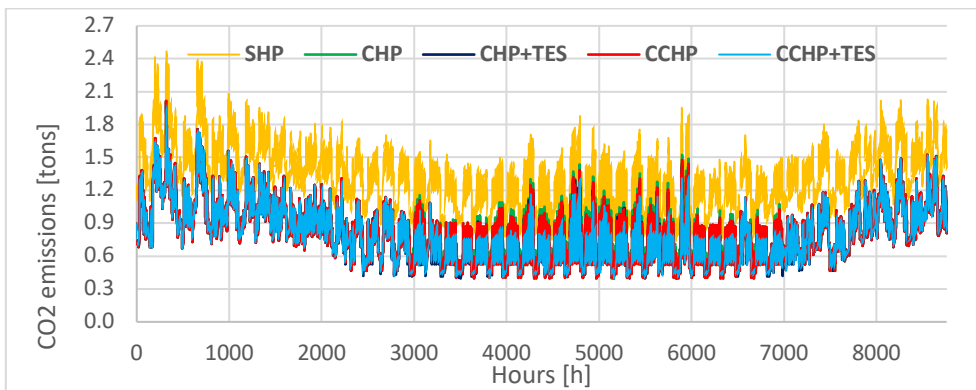


Figure 94: Total average emissions, *Duluth*

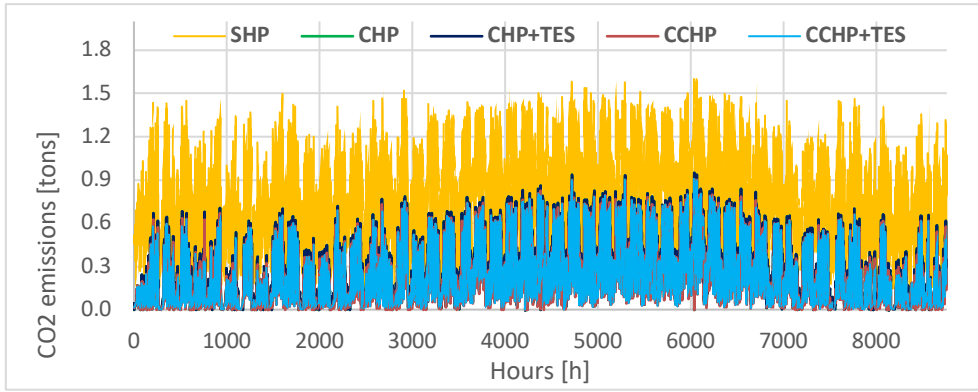


Figure 95: Marginal carbon due to electric production, *Miami*

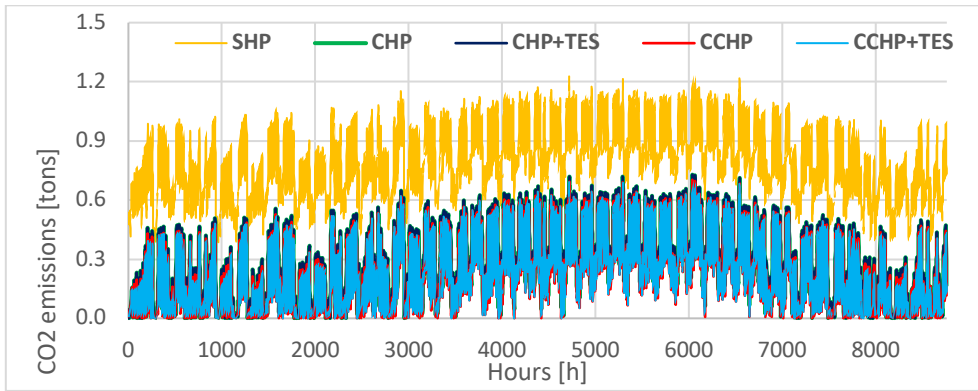


Figure 96: Average carbon due to electric production, *Miami*

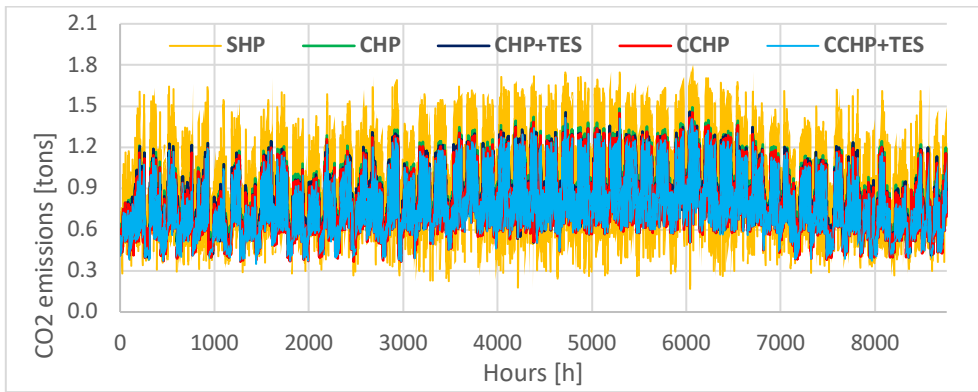


Figure 97: Total marginal emissions, *Miami*

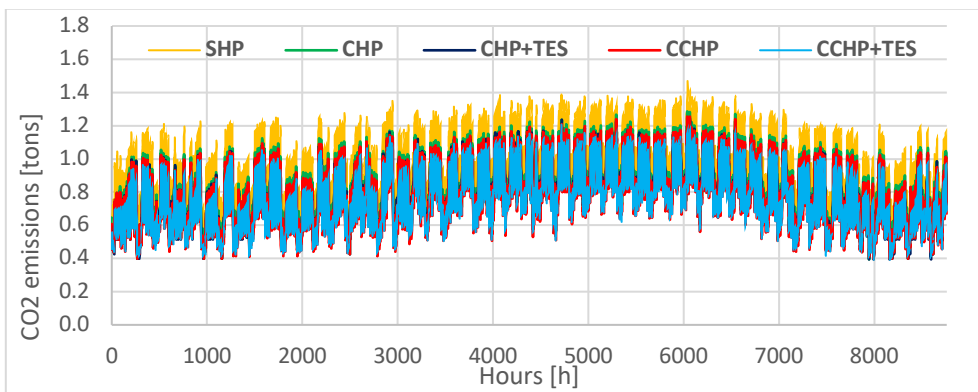


Figure 98: Total average emissions, *Miami*

Taking a look to the total annual emissions and the improvements obtained with the different methods, demonstrate even further what has been already mentioned. The CO<sub>2</sub> produced in any case studied reduces from the base model. For the separate generation plant, in fact, the emissions come almost all from the electricity purchased by the grid, while when a prime mover is installed, it leads to have more CO<sub>2</sub> from the fuel burnt to feed the microturbine. Using the average emission factor for the evaluation, underestimate the real CO<sub>2</sub> reduction, evaluated with the marginal carbon method, of a 4-5% in locations as Chicago and Atlanta, where the emissions due to the electric production show higher peaks in the middle of the year, due to the climate and the type of plant operating. Instead, more uniform is the grid load, lower will be the difference in total reduction between average and marginal carbon. In fact, in Miami the final results obtained are very similar; however, it is still important to consider the marginal carbon and not the average since, even if the annual results tend to be almost the same, if we take a look at the hourly emissions they are quite different.

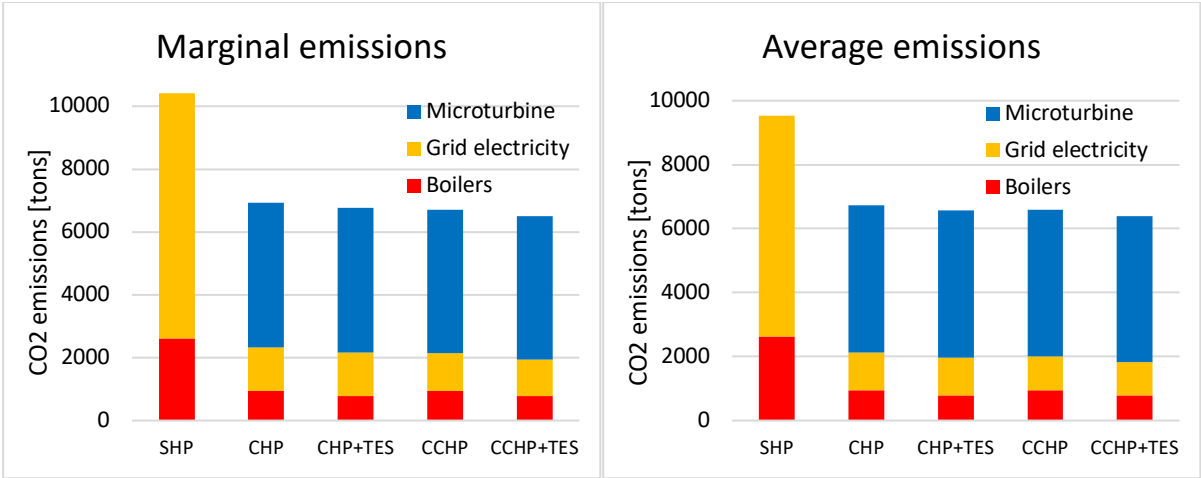


Figure 99: Total emissions comparison, Chicago

	Total marginal emissions [tons CO <sub>2</sub> /year]	Reduction [%]	Total average emissions [tons CO <sub>2</sub> /year]	Reduction [%]
<b>SHP</b>	10404.9		9538.0	
<b>CHP</b>	6930.4	-33.4%	6740.1	-29.3%
<b>CHP+TES</b>	6765.0	-35.0%	6574.7	-31.1%
<b>CCHP</b>	6716.5	-35.4%	6585.0	-31.0%
<b>CCHP+TES</b>	6509.0	-37.4%	6390.7	-33.0%

Table 15: Reduction in emissions, Chicago

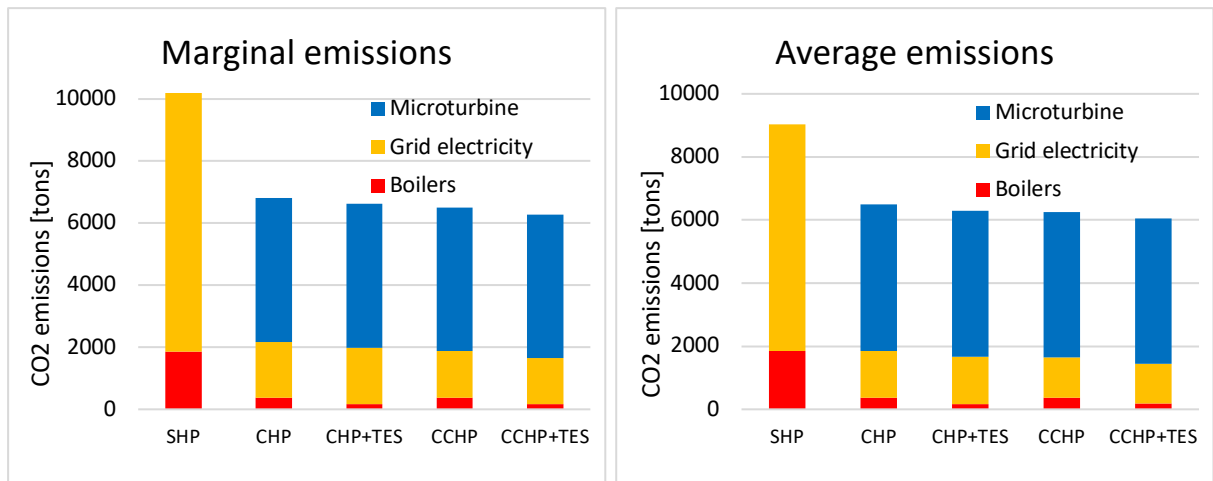


Figure 100: Total emissions comparison, *Atlanta*

	Total marginal emissions [tons CO <sub>2</sub> /year]	Reduction [%]	Total average emissions [tons CO <sub>2</sub> /year]	Reduction [%]
<b>SHP</b>	10193.6		9038.8	
<b>CHP</b>	6806.7	-33.2%	6491.2	-28.2%
<b>CHP+TES</b>	6616.7	-35.1%	6301.2	-30.3%
<b>CCHP</b>	6491.2	-36.3%	6259.5	-30.7%
<b>CCHP+TES</b>	6269.4	-38.5%	6046.7	-33.1%

Table 16: Reduction in emissions, *Atlanta*

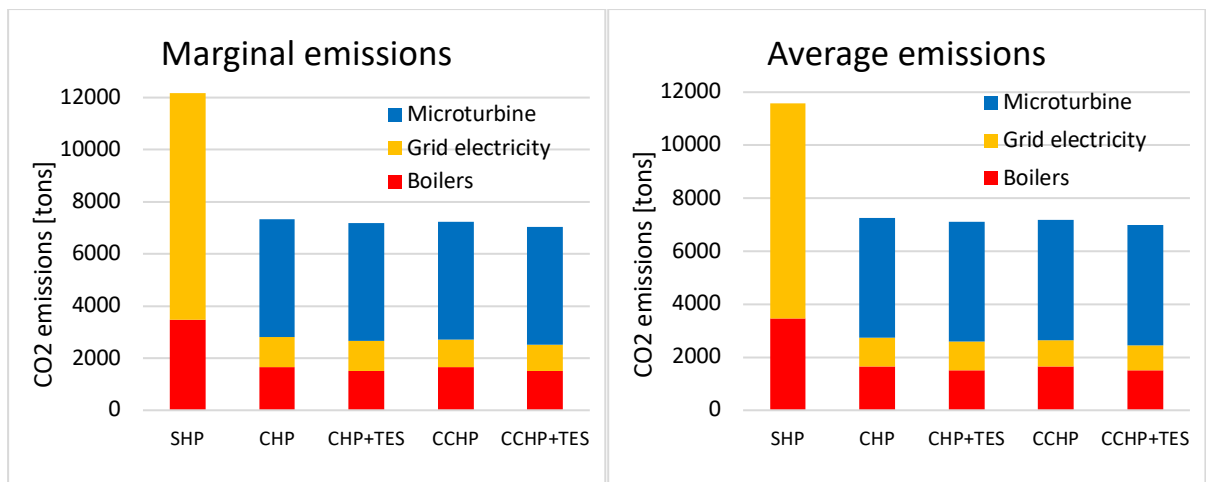


Figure 101: Total emissions comparison, *Duluth*

	Total marginal emissions [tons CO <sub>2</sub> /year]	Reduction [%]	Total average emissions [tons CO <sub>2</sub> /year]	Reduction [%]
<b>SHP</b>	12176.4		11586.32	
<b>CHP</b>	7328.6	-39.8%	7259.27	-37.35%
<b>CHP+TES</b>	7175.7	-41.1%	7106.41	-38.67%
<b>CCHP</b>	7238.8	-40.6%	7175.11	-38.07%
<b>CCHP+TES</b>	7037.9	-42.2%	6979.37	-39.76%

Table 17: Reduction in emissions, *Duluth*

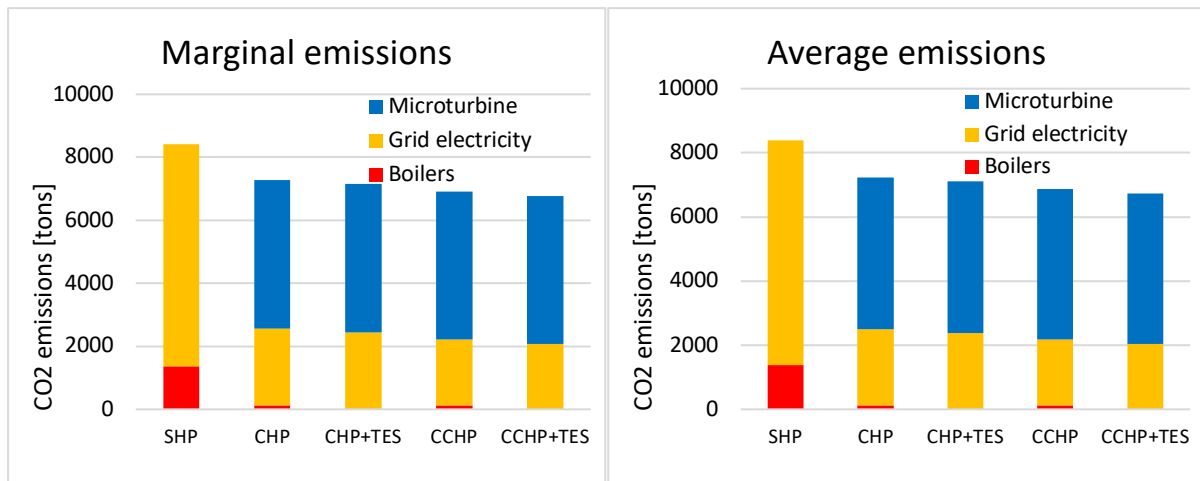


Figure 102: Total emissions comparison, *Miami*

	<b>Total marginal emissions [tons CO<sub>2</sub>/year]</b>	<b>Reduction [%]</b>	<b>Total average emissions [tons CO<sub>2</sub>/year]</b>	<b>Reduction [%]</b>
<b>SHP</b>	8408.4		8386.8	
<b>CHP</b>	7280.1	-13.4%	7223.4	-13.9%
<b>CHP+TES</b>	7157.6	-14.9%	7100.9	-15.3%
<b>CCHP</b>	6905.5	-17.9%	6875.0	-18.0%
<b>CCHP+TES</b>	6770.1	-19.5%	6740.6	-19.6%

Table 18: Reduction in emissions, *Miami*

The last figures reported shows how actually the electric grid will operate in case of a new CHP or CCHP plant in Chicago, Atlanta, Duluth and Miami and how these are going to affect all the electricity market region. The marked EGUs are the marginal plant operating at that time.

The diameter of each circle indicates the magnitude of a unit's change in generation / emissions. Circles are semi-transparent and darker areas occur in regions with overlapping units [34].

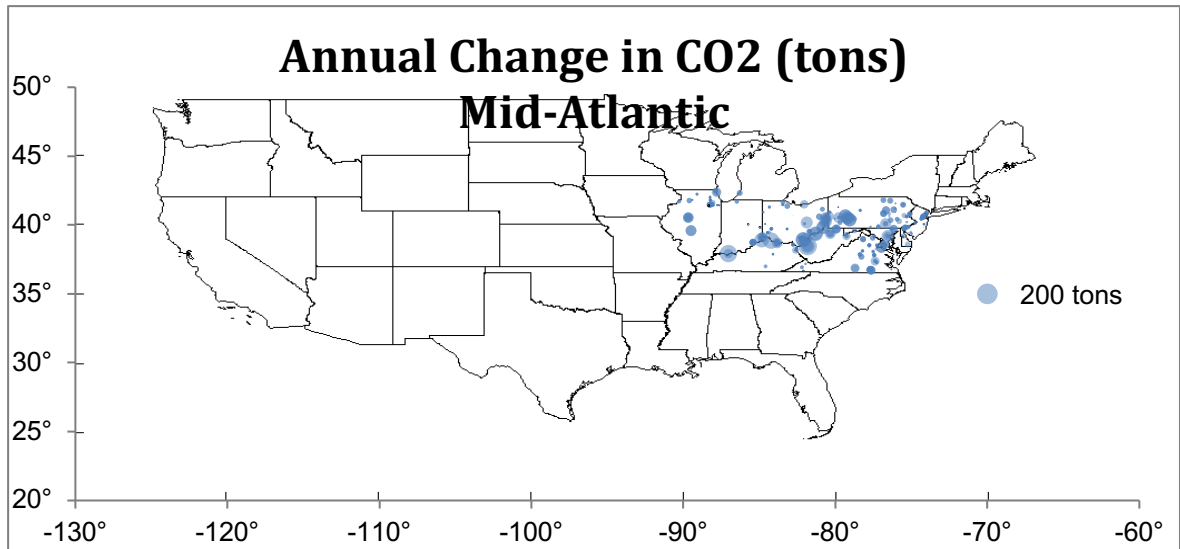


Figure 103: Map of generation and emission changes, *Mid-Atlantic region (Chicago)*

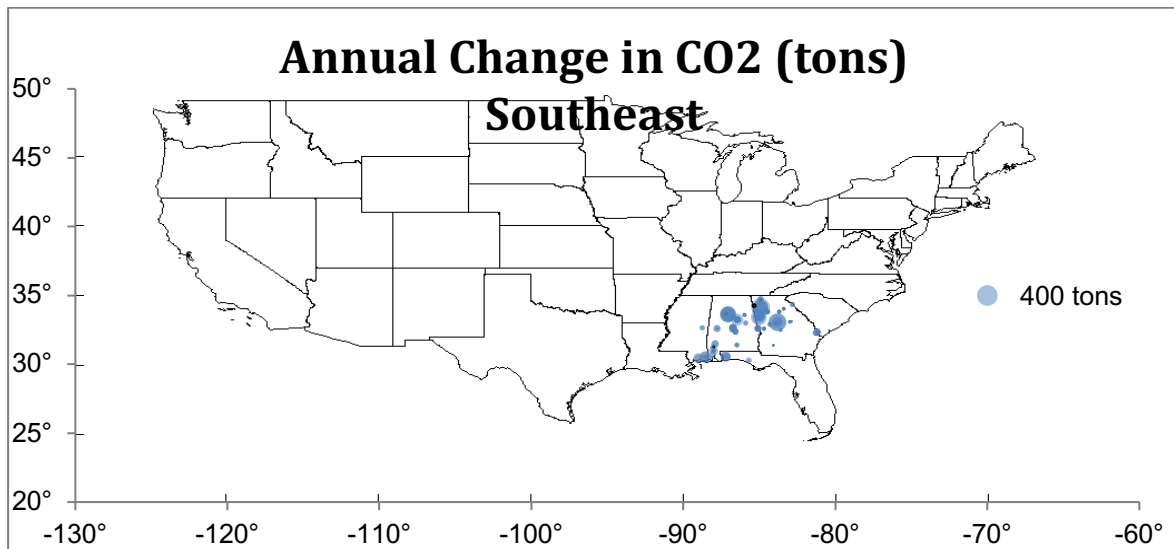


Figure 104: Map of generation and emission changes, *Southeast region (Atlanta)*

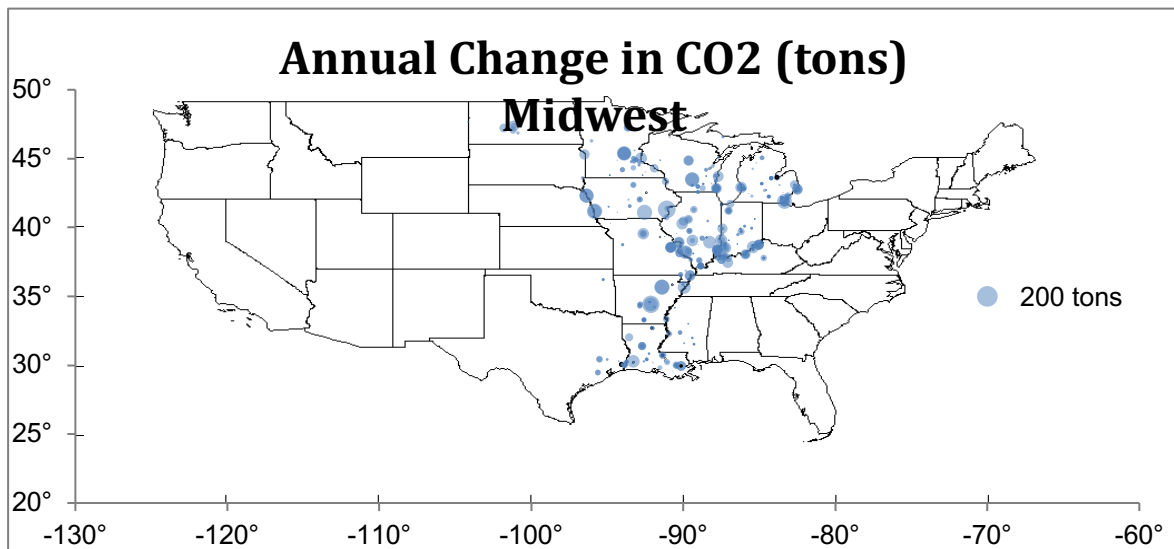


Figure 105: Map of generation and emission changes, *Midwest region (Duluth)*

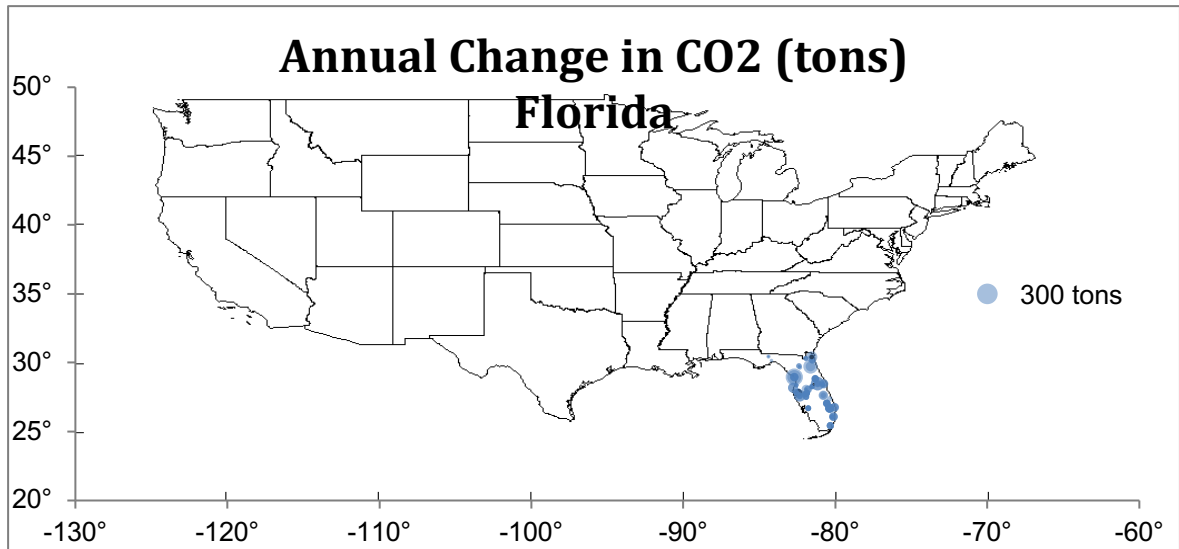


Figure 106: Map of generation and emission changes, *Florida (Miami)*

## 8 Conclusions

In this thesis a total of five plant layouts have been analyzed and compared:

- A separate heat and power production plant;
- A combined heat and power plant;
- A combined heat and power plant with hot thermal storage;
- A combined cooling, heating, and power plant;
- A combined cooling, heating, and power plant with hot thermal storage.

Each of the configuration has been studied in four locations: Chicago, Atlanta, Duluth and Miami. In this way it was possible to understand how different climates influence the facility demand. Considering the different peak in the electric load, the prime mover that has been chosen is a Capstone C1000 microturbine. After the analysis of the hospital facility, both the cogeneration and the trigeneration systems have been modeled on eQuest® and, due to inner limitation of the software, a more specific Excel model has been implemented. Lastly a hot temperature thermal storage was introduced to try to improve the wasted heat exploitation. With a single model it was possible to summarize all the different systems and to compare the different solutions. A detailed performance analysis was performed in each case, focusing especially on the amount of Recovered Heat exploited in comparison with the total available Recoverable Heat. One of the primary goals of this work was to determine if the introduction of a thermal storage was going to be actually useful in this kind of applications. By varying the tank size, it has been noticed how, independently from the location, a TES system is not going to improve that much the operation of the plant. A slightly better picture was observed in the case of CCHP layout, where the introduction of the absorption chiller permitted a significantly higher exploitation of the recoverable heat throughout the entire year, as listed in Table 19. In this circumstance the implementation of a TES facility had a bigger impact on the overall management of the system, especially during the warmer months, since it's not unused anymore.

	<b>CHP</b>	<b>CHP+TES</b>	<b>CCHP</b>	<b>CCHP+TES</b>
<b>Chicago</b>	75.1%	76.4%	91.5%	95.9%
<b>Atlanta</b>	65.8%	68.1%	90.1%	94.9%
<b>Duluth</b>	83.6%	84.8%	90.6%	95.4%
<b>Miami</b>	53.6%	53.7%	97.1%	98.6%

Table 19: Recovered heat vs Recoverable heat

With the same approach used for the tank, also the absorption chiller capacity has been varied in order to obtain the better solution. For both components, above a certain size the variation in recovered heat becomes minimum. This happens when all the available heat is recovered and the equipment starts to be oversized for the plant. On the thermal storage size, the best solution is around 20,000 [gal], except Miami where a volume of 10,000 [gal] is enough. Regarding the absorption chiller size the best solution varies between 2 [MMBtu] for the warmer cities (Miami and Atlanta), to 2.5 [MMBtu] for Chicago and Duluth. In this way, it has been proven that the best size for the chiller is in the range between 15 % and 25% of the maximum values of cooling demand requested by the facility.

Lastly, a study on CO<sub>2</sub> emissions has been conducted. The carbon dioxide emitted due to the electric production has been evaluated considering both the marginal carbon, using the hourly eQuest® data and the AVERT system, and the average emission factor. Through a comparison between the two methodologies, it has been demonstrated how using the average carbon for an environmental impact assessment is going to underestimate the annual CO<sub>2</sub> reduction, other than providing wrong hourly values. The biggest difference has been measured in Atlanta, where the marginal carbon was 5% more than the average one. Actually, the gap between the two approaches was expected to be even higher; presumably such high values have not been reached due to the nature of the facility studied. In fact, the hospitals' demand is almost constant also during the night and, as a consequence, the baseload units, as nuclear plants, which are characterized by lower emissions, have a greater effect on the final marginal emissions. A further improvement to this work might focus on another type of facility, for example an office building, where the electric demand is concentrated in the peak hours, to demonstrate if that is going to affect even more the average emissions.

## Appendix A

- Download Main Module and ensure that macros are enabled. For Windows go in the Options menu and select Trust Center Settings > Macro Settings > Enable all macros; for Mac OS select “enable macros” when opening the file.
- *Regional Data File*: Open Main Module, select a region for the analysis and load the Regional Data File, that can be downloaded on EPA website []. Click on the green button to save the file [37].
- *Set Energy*: Click on “Enter detailed data by hour”. The hourly profile in [MW] should be pasted in the “Manual Profile” column. The “Total Change” column shows the total aggregate hourly energy change from the programs input.
- Run Scenario
- To get the hourly values of emissions go to the first page of the Excel file and click on the grey button to restore default Excel. In the “CO<sub>2</sub>” section are provided the original tons and the post-change tons. The emissions reduction is equal to the difference between the two columns.

## Cited Literature

1. Haefke, C. & Cuttica 2013, *J. Market sector fact sheet: Combined heat and power in hospitals*, US DOE CHP Technical Assistance Partnership
2. Bourgeois T., Dillingham G., Panzarella I. & Hampson A., 2013, *Combined heat and power: Enabling resilient energy infrastructure for critical facilities*, ICF International Paper
3. Taddonio K., 2011, *Hospitals Discover Advantages to Using CHP Systems*, Building Technologies Program, U.S Department of Energy
4. Bonnema E., Studer D., Parker A., Pless S. & Torcellini P., 2010, *Large hospital 50% energy savings: Technical support document tech. rep.*, National Renewable Energy Lab. (NREL), Golden, CO (United States)
5. ANSI/ASHRAE Standard 90.1-2004, *Energy standard for buildings except low rise residential buildings*, American Society of Heating, Refrigerating and Air-Conditioning Engineers
6. Crinò A., 2014, *CHP Technologies in the Midwest of USA: Energy and Economic Evaluation of a CHP System*, Politecnico di Torino, University of Illinois at Chicago
7. Ciciarella F., 2015, *Simulation of Emerging Smaller-Scale Tri-Generation Systems*, Politecnico di Torino, University of Illinois at Chicago
8. ASHRAE Standard 169-2006, *Weather data for building design standards*, American Society of Heating, Refrigerating, and air-conditioning Engineers
9. Darrow K., Tidball R., Wang J., Hampson A., 2017, *Catalog of CHP Technologies*, U.S. Environmental Protection Agency Combined Heat and Power Partnership
10. Ho J.C., Chua K.J., 2004, *Performance study of a microturbine system for cogeneration application*
11. Capstone Turbine Corporation, 2009, *Capstone C1000 Microturbine Systems, Technical Reference*
12. Galli P., 2016, *Simulation of a Small-Scale Cogeneration System Using a Microturbine*, Politecnico di Torino, University of Illinois at Chicago
13. Leo G., 2017, *Simulation of a cogeneration system using microturbines and organic rankine cycle*, Politecnico di Torino, University of Illinois at Chicago

14. EPA, <https://www.epa.gov/chp>
15. U.S Department of Energy, 2016, *Combined Heat and Power Technology Fact Sheet Series*
16. EREC, *Creating Markets for Renewable Energy Technologies EU*, RES Technology Marketing Campaign
17. U.S Department of Energy, 2016, *Combined Heat and Power Technical Potential in the United States*
18. U.S. Department of Energy, *Combined Heat and Power Installation Database*, <https://doe.icfwebservices.com/chpdb/>
19. Otis P., 2015, *CHP Industrial Bottoming and Topping Cycle with Energy Information Administration Survey Data*
20. Al-Sulaiman F. A., Hamdullahpur F., and Dincer I., 2010, *Trigeneration: a comprehensive review based on prime movers*, International journal of energy research
21. <https://www.cogenlab.com/soluzione/trigenerazione-cchp/>
22. Standford III H.W., 2017, *HVAC Water Chillers and Cooling Towers: Fundamentals, Application, and Operation*, CRC Press
23. <https://www.araner.com>
24. Romano L., 2018, *Simulation Techniques for Thermal Storage Coupled to Cogeneration/Trigeneration Systems*, Politecnico di Milano, University of Illinois at Chicago
25. York, *MILLENIUM™ YIA Single-Effect Absorption Chillers, Technical Reference*
26. Standard A. 550/590, 2003, *Performance rating of water-chilling packages using the vapor compression cycle*, Air-conditioning & Refrigeration Institute
27. Cabeza L. F., 2014, *Advances in Thermal Energy Storage Systems, Methods and Applications*, Woodhead Publishing
28. Pagliarini G., and Rainieri S., 2010, *Modeling of a thermal energy storage system coupled with combined heat and power generation for the heating requirements of a university campus*, Applied Thermal Engineering

29. Haeseldonckx D., Peeters L., Helsen L., and D'haeseleer W., 2007, *The impact of thermal storage on the operational behavior of residential CHP facilities and the overall CO2 emissions*, Renewable and Sustainable Energy Reviews
30. A. Campos Celador, M. Odriozola, J.M. Sala, 2011, *Implications of the modelling of stratified hot water storage tanks in the simulation of CHP plants*, ENEDI Research-Group, University of the Basque Country
31. Guyer J. P., 2011, *Introduction to High Temperature Water Heating Plants*, Continuing Education and Development, Inc.
32. Highland Tank, 2019, *HighDRO® Water Tanks, Technical Reference*
33. U.S. Environmental Protection Agency, 2015, *Fuel and Carbon Dioxide Emissions Savings Calculation Methodology for Combined Heat and Power System*
34. U.S. Environmental Protection Agency, 2020, *AVoided Emissions and geneRation Tool (AVERT) User Manual*
35. W. Ryan, 2020, *The Electric Industry, Decarbonization, and the Role of Storage*
36. Schram W., Lampropoulos I., AlSkaif T., Van Sark W., 2019, *On the Use of Average versus Marginal Emission Factors*
37. <https://www.epa.gov/statelocalenergy/avert-tutorial-getting-started-identify-your-avert-regions>